International Scientific-Technical and Production Journal

The Paton WELDING JOURNAL

March
2006
3

English translation of the monthly «Avtomaticheskaya Svarka» (Automatic Welding) journal published in Russian since 1948

Founders: *E.O. Paton Electric Welding Institute of the NAS of Ukraine*
International Association «Welding»

Publisher: *International Association «Welding»*

Address:
E.O. Paton Electric Welding Institute,
International Association «Welding»,
11, Bozhenko str., 03680, Kyiv, Ukraine
Tel.: (38044) 287 67 57
Fax: (38044) 528 04 86
E-mail: journal@paton.kiev.ua
http://www.nas.gov.ua/pwj

State Registration Certificate
KV 4790 of 09.01.2001

Subscriptions:
$324, 12 issues per year,
postage and packaging included.
Back issues available.

CONTENTS

IMPROVEMENT OF WELDING CONSUMABLES AND TECHNOLOGIES FOR INCREASED SAFETY AND LIFE OF NPS WITH WWER REACTORS

I.V. GORYNIN, G.P. KARZOV, B.T. TIMOFEEV and **S.N. GALYATKIN**
Federal State Unitary Enterprise «TsNII KM Prometej», St.-Petersburg, RF

Results of the gained experience on improvement of steels and welding consumables used in fabrication of WWER reactors for nuclear power stations are presented. Special attention is given to the problems of radiation and thermal embrittlement of the joints, influencing the safety of reactors at long-term operation.

Keywords: arc welding, low-alloy steels, WWER reactors, nuclear power station, radiation and thermal embrittlement, weld metal, safety, service life, material improvement.

At present in Russia, Ukraine, Armenia and in other CIS countries, as well as in Finland, more than 50 WWER type reactors of power 440 and 1000 MW are in operation, including 9 WWER-440 reactors of the first generation (for four of them the design life of 30 years was extended for another 10–15 years), 18 reactors of the same type belong to the second generation and 24 reactors are of WWER-1000 type. All of them are designed from heat-resistant steels of grades 15Kh2MFÀ and 15Kh2NMFÀ with application of welding consumables designed at Central Research Institute of Structural Materials «Prometej» and TsNII-Òmash. Reactor bodies of both the types consist of seven shells from steels of the above-mentioned grades. Shells are connected to each other by automatic submerged-arc welding (ASAW) with application of different welding consumables (wires and fluxes).

In welding circumferential welds on WWER-440 reactors manufactured from 15Kh2MFÀ steel (thickness of shell core is 140 mm, thickness of shell branch pipe zone is 240 mm) using Sv-10Kh Ì FÒ welding wire and flux ÀN-42. Initially welding was performed at high (up to 350 °C) temperature of heating, then weld joint was subjected to immediate tempering. All bodies of the first generation WWER-440 / 230 reactors were manufactured by this technology. In 1975 when welding circumferential welds of core shell of WWER-440 / 213 reactor body, that belonged to the second generation, for NPS «Loveesa» (Finland), wire of grade Sv-10KhMFÒU with a lower content of harmful impurities and flux ÀN-42M were used (Table 1).

Application of the above-mentioned welding consumables allowed to produce the weld metal with phosphorus content of up to 0.012 wt.% and copper of up to 0.1 wt.%, that essentially increased its radiation resistance. From the moment of manufacturing WWER-440 reactor for NPS «Loveesa», higher demands began to be made of the weld metal as well as of base metal in terms of ensuring a high brittle fracture resistance. For this purpose, critical temperature of brittleness, T_{CB}, was determined, while using Charpy specimens instead of Mesnager specimens for impact bend testing.

Further improvement of the technology of welding circumferential welds on WWER-440 / 213 reactors bodies was directed to lowering the temperature of pre-heating and concurrent heating from 350 to 150–200 °C. The improved technology was widely used in manufacturing WWER-440 reactor bodies at Izhora

Table 1. Requirements to chemical composition (wt.%) of the base and weld metal of WWER-440 reactors in ASAW by different technological variants

Steel / wire, standard, flux	C	Si	Mn	Cr	Mo	V
15Kh2 Ì FÀ (ÒU 5.961.1106–77)	0.13–0.18	0.17–0.37	0.3–0.6	2.5–3.0	0.6–0.8	0.25–0.35
15Kh2 Ì FÀ-À (Notification No.4.80)	0.13–0.18	0.17–0.37	0.3–0.6	2.5–3.0	0.6–0.8	0.25–0.35
Sv-10Kh Ì FÒ (GOSÒ 2246–70), flux ÀN-42	0.07–0.12	≤ 0.35	0.4–0.7	1.4–1.8	0.4–0.6	0.20–0.35
Sv-10Kh Ì FÒU (ÒU 14-1-3034–80), flux ÀN-42 Ì	0.07–0.12	≤ 0.35	0.4–0.7	1.4–1.8	0.4–0.6	0.20–0.35

Table 1 (cont.)

Steel / wire, standard, flux	S	P	Cu	As	Ni	Other
	Not more than					
15Kh2 Ì FÀ (ÒU 5.961.1106–77)	0.025	0.025	0.30	0.08	0.4	0.025Co
15Kh2 Ì FÀ-À (Notification No.4.80)	0.015	0.012	0.10	0.01	0.4	0.025Co
Sv-10KhMFÒ (G Î SÒ 2246–70), flux ÀN-42	0.030	0.030	0.25	–	0.3	(0.05--0.12)Ti
Sv-10Kh Ì FÒU (ÒU 14-1-3034–80), flux ÀN-42 Ì	0.012	0.010	0.10	–	0.3	(0.05–0.12)Ti

plant in former USSR and at «Škoda» plant in Czechoslovakia.

Welding of circumferential welds on reactors of WWER-1000 type from steel 15Kh2N Ì FA-À (core shells of 190 mm thickness) and 15Kh2N Ì FÀ (branch pipe zone shells of 290 mm thickness) was initially performed by two technological versions, namely by ASAW using welding wire of Sv-10KhGN Ì À-À type and flux FTs-16 (or ÀN-17 Ì), or welding of Sv-08KhGN Ì ÒÀ wire and flux NF-18 Ì .

Both technological versions for a number of years were used for making circumferential welds of industrial reactors of this modification, as they provided the properties and stable level of impurity components (phosphorus, sulfur, copper) and safe operation during the design life. At the moment of reactor manufacturing the requirements to strength value of weld metal produced by ASAW method, were not less than 422 and 392 MPa (yield limit) at the temperature of 20 and 350 °C, respectively, with tensile strength — 539 and 490 MPa at the same temperatures, and critical temperature of brittleness should not be above zero. Initially the content of impurities in the weld metal was limited by the following values, wt.%: 0.15Cu, 0.02S, 0.025P.

When more than 20 circumferential welds were made by each technological version, statistic analysis of mechanical properties distribution was carried out [1]. Its results showed the advantages of Sv-08KhGN Ì ÒÀ welding wire both by strength and ductility characteristics and by critical characteristics of brittle temperature. It should be mentioned that in welding by this version, the content of nickel in weld metal did not exceed 1.5 wt.%, and when another version was used, it reached 1.8 wt.%. It is known [2, 3] that the higher content of this element has a negative influence on radiation resistance of the material and leads to decrease of reactor body operating life.

Keeping in mind that using Sv-10KhGN Ì À-À welding wire, the level of metal mechanical properties was low, TsNIITmash suggested welding wire of Sv-12Kh2N2 Ì À-À grade in combination with flux FTs-16À for welding circumferential welds (Table 2). Due to increase of carbon and nickel content in wire composition it was possible to provide the increase of strength properties of weld metal and to provide stable low value of T_{CB}. That permitted using the mentioned version of technological process in manufacturing reactors of WWER type at Izhora plant and at Atommash. The results of investigations at RSC «Kurchatovsky Institute» [4], NIIAR [5] and «Prometej» [6] during these reactors operation showed that the coefficient of radiation embrittlement of weld metal when using new welding consumables was much higher as compared with the base metal — $A_F = 23$ at temperature 290 °C. In the first versions, when Sv-10KhGN Ì À-À and Sv-08KhGN Ì ÒÀ wires were used in the same conditions and at the same temperature, $A_F = 20$ for weld metal. In this connection it was decided to refuse using Sv-12Kh2N2 Ì À-À wire when welding circumferential welds on core shells of reactor body.

A large amount of data [7] has been accumulated so far on the mechanical properties of weld metal, obtained at specimen testing in reactor body manufacturing. After proper statistic treatment of these data, it was possible to judge about the advantages of this or that combination of welding consumables, and on the basis of the obtained structural strength characteristics — about the workability and reliability of the equipment in general. In study [1] the statistic treatment of mechanical test results for the metal of welds, made by the first two technological versions, was given. To describe these results, the law of normal distribution of random variable was applied in this study, and the values of mathematical expectation and dispersion were given for each parameter of mechanical characteristic (σ_t, $\sigma_{0.2}$, δ, ψ) that were obtained at welding with different welding consumables at 20 and 350 °C. Statistic treatment of weld metal mechanical properties data at automatic welding with Sv-12Kh2N2 Ì À-À wire using flux FTs-16À was carried out in study [8].

Comparison of mathematical expectation by *t*-criterion (Student criterion) showed that in welding with Sv-08KhGN Ì ÒÀ wire using flux NF-18 Ì we observe an essentially higher estimated value of relative reduction in area at temperature 20 °C, and when using wire Sv-12Kh2N2 Ì À-À and flux FTs-16À — increase of σ_t and $\sigma_{0.2}$ values at 350 °C. The results of statistic treatment of weld metal mechanical properties, made by the three technological versions, are given in Figures 1 and 2.

Tensile testing of fivefold samples (see Figures 1 and 2) was conducted at 20 and 350 °C (required level of mechanical properties in accordance with PNAE G-7-010–89 [9] is shown by dashed lines). The advantage of welding with Sv-12Kh2N2 Ì À-À wire in comparison with two other versions is obvious, when comparing the impact strength values by the results of testing Mesnager (*KCU*) and Charpy (*KCV*) samples. Value of critical temperature of brittleness ($T_{CB} = 0$) specified [10] for weld metal is provided by the above technological version with an error of 0.95. Proceeding from such an important characteristic as material resistance to brittle fracture, it is obvious that welding by Sv-12Kh2N2 Ì À-À wire has an advantage. In accordance with data of studies [4, 6], however, the increased content of nickel in weld metal obtained in welding with this wire, leads to its more intensive embrittlement in the process of reactor operation under the influence of neutron irradiation.

In study [6] two groups of consumables were examined to investigate the influence of nickel on radiation embrittlement of weld metal. There consumables provide different content of nickel in weld metal — from 1.1 to 1.36 and from 1.6 to 1.8 %, respectively. The first group of welds [6] was made by automatic welding with wires Sv-08KhG Ì ÒÀ and Sv-09KhGN Ì ÒÀ-VI using flux of NF-18 Ì and KF-30 grades. Nickel content in the deposited metal insignificantly differed from the admissible value for steel of 15Kh2N Ì FÀ-À grade (1.0–1.3 wt.%) by ÒU 108.765–98, although in steel with a higher content of impurity elements, namely of 15Kh2N Ì FÀ grade, the content of nickel can vary in wider limits (1.0–1.5 wt.%). Welds of the second group were made

Table 2. Required chemical composition (wt.%) of steel and metal of welds for WWER-1000 reactor

Steel / welding wire	Flux	Standard	C	Si	Mn	Cr	Ni	Mo	V	Ti
15Kh2N Ì FÀ	–	ÒU 108.765–78	0.13–0.18	0.17–0.37	0.30–0.60	1.7–2.4	1.0–1.5	0.5–0.7	≤ 0.12 (calc.)	–
15Kh2N Ì FÀ			0.13–0.16	0.17–0.37	0.30–0.60	1.8–2.3	1.0–1.5	0.5–0.7	0.10–0.12	–
15Kh2N Ì FÀ-À			0.13–0.16	0.17–0.37	0.30–0.60	1.8–2.3	1.0–1.3	0.5–0.7	0.10–0.12	–
Sv-08KhGN Ì ÒÀ Sv-08KhGNMÒÀ-VI	NF-18 Ì	PNÀE G-7-010–89	0.06–0.10	0.15–0.45	0.45–1.10	1.2–2.0	1.0–1.5	0.4–0.7	–	0.01–0.06
Sv-10KhGN Ì À-À	FTs-16		0.06–0.12	0.15–0.45	0.65–1.10	1.2–2.0	1.2–1.8	0.4–0.7	–	–
Sv-12Kh2N2 Ì À			0.06–0.12	0.15–0.45	0.65–1.10	1.2–2.0	1.2–1.9	0.4–0.7	–	–
Sv-12Kh2N2 Ì À-À	FTs-16À		0.06–0.12	0.15–0.45	0.65–1.10	1.4–2.1	1.2–1.9	0.45–0.75	–	–
Sv-08KhGN Ì ÒÀ-À	–	TU 14-1-1275–75	0.05–0.10	0.22–0.37	0.70–1.10	1.55–1.85	1.1–1.4	0.5–0.7	0.03	0.03–0.10
Sv-09KhGN Ì ÒÀ	–	TU 14-1-3675–01	0.07–0.11	0.17–0.30	0.80–1.05	1.6–1.9	1.0–1.3	0.5–0.7	0.03	0.05–0.11
Sv-09KhGN Ì ÒÀ-VI	–	TU 14-1-3675–01	0.07–0.11	0.17–0.30	0.80–1.05	1.6–1.9	1.0–1.3	0.5–0.7	0.03	0.05–0.11
Sv-09KhGN Ì ÒÀ	48NF-18M	TU 5.965-11175–02	0.09	0.4	0.4–1.0	1.1–1.8	0.9–1.3	0.40–0.75	–	0.01–0.06

Table 2 (cont.)

Steel / welding wire	Flux	Standard	Cu	S	P	As	Co	Sb	Sn	P + Sb + Sn
			Not more than							
15Kh2N Ì FÀ	–	TU 108.765–78	0.30	0.020	0.020	0.040	0.03	–	–	–
15Kh2N Ì FÀ			0.08	0.012	0.010	0.010	0.03	0.005	0.005	0.015
15Kh2N Ì FÀ-À			0.08	0.012	0.010	0.010	0.03	0.005	0.005	0.015
Sv-08KhGN Ì ÒÀ Sv-08KhGNMÒÀ-VI	NF-18M	PNÀE G-7-010–89	0.15	0.020	0.025	–	–	–	–	–
Sv-10KhGN Ì À-À	FTs-16		0.15	0.020	0.025	–	–	–	–	–
Sv-12Kh2N2 Ì À			0.15	0.020	0.025	–	–	–	–	–
Sv-12Kh2N2 Ì À-À	FTs-16À		0.08	0.015	0.012	–	–	–	–	–
Sv-08KhGNMÒÀ-À	–	TU 14-1-1275–75	0.10	–	–	–	–	–	–	–
Sv- 09KhGN Ì ÒÀ	–	TU 14-1-3675–01	0.10	0.012	0.012	0.010	0.03	0.008	0.001	–
Ñv-09KhGN Ì ÒÀ-VI	–	TU 14-1-3675–01	0.06	0.006	0.006	0.010	0.02	–	–	–
Ñv-09KhGN Ì ÒÀ	48NF-18M	TU 5.965-11175–02	0.10	0.015	0.012	–	–	–	–	–

using welding consumables developed by TsNIITmash (wire Sv-10KhGN Ì À-À with flux FTs-16 and Sv-12Kh2N2 Ì À-À with flux FTs-16À). In both the cases radiation embrittlement of weld metal was evaluated by the change of critical temperature of brittleness and by the level of impact energy E = 47 J at testing Charpy standard specimens. Specimens irradiation was conducted in research and industrial reactors up to neutron fluence of $3{\cdot}10^{20}$ neutron / cm^2.

The results of investigation showed that the shift of critical temperature of brittleness due to irradiation for weld metal, in which nickel content is not more than 1.36 wt.%, and neutron fluence does not exceed the design value for the full 30 year service life ($4.7{\cdot}10^{19}$ neutron / cm^2), can be predicted quite accurately by dependence (1.1) that was suggested in «The Norms for Strength Calculation» [10], when the radiation embrittlement coefficient A_F = 20. At higher values of neutron fluence, the experimental values of ΔT_F are higher than the calculated values determined by the mentioned dependence. So, at neutron fluence of $1.7{\cdot}10^{20}$ neutron / cm^2, this difference reaches 90 °C in weld metal with rather low nickel content (up to 1.36 wt.%) [6]. In weld metal with higher nickel content (1.6–1.8 wt.%) the normative dependence turned to be true only up to fluence $2{\cdot}10^{19}$ neutron / cm^2. If neutron fluence is higher, the nature of dependence (1.1) from study [10] is greatly different from the one that was obtained by experimental data for the same materials [6], that is why the investigators found a way to correct it. Thus, in study [6] it is suggested to replace the exponent 1 / 3 by 1 / 2 in equation (1.1) and to introduce complementary parameters allowing for the content not only of nickel, but also impurity elements in the weld metal.

Thus, despite the strength being a little higher and the critical temperature of brittleness being a little lower in the initial state of weld metal made by ASAW with Sv-12Kh2N2 Ì À-À wire using flux FTs-16A, for circumferential welds joining the core shells of reactor body, it is preferable to use welding consumables designed by «Prometej». Weld metal made with Sv-08KhGN Ì ÒÀ wire with flux NF-18 Ì features an increased resistance to radiation embrittlement.

Despite the fact that at present time, when designing new power plants with reactors of WWER type, the tendency to decrease the maximum summary neutron flow to reactor wall during service life at the

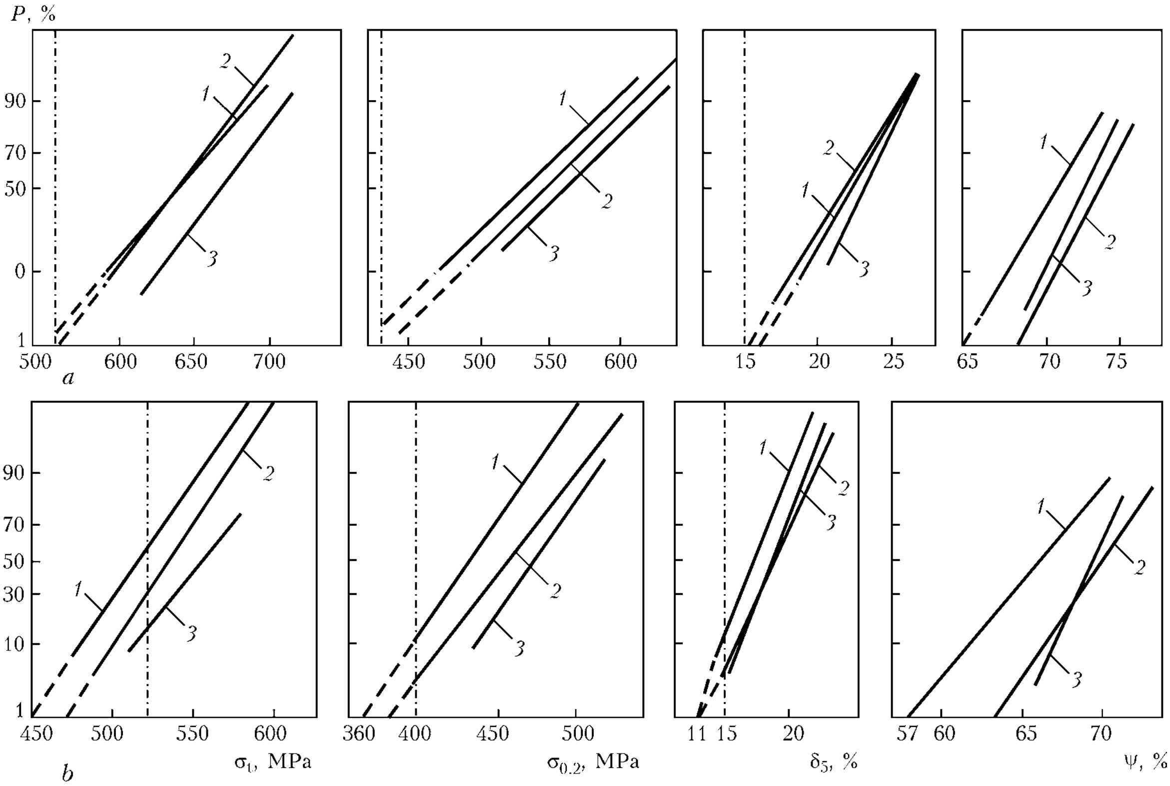

Figure 1. Integral curves of distribution of weld metal mechanical properties at 20 (*a*) and 350 (*b*) °C obtained in welding by different technological versions: *1* — Sv-10KhGN Ì À-À, fluxes ÀN-17 Ì and FTs-16; *2* — Sv-08KhGN Ì ÒÀ, flux NF-18 Ì ; *3* — Sv-12Kh2N2 Ì À-À, flux FTs-16À (*P* — integral probability of the event)

expense of applying progressive design solutions is observed, the problem of irradiation embrittlement of the metal is still urgent. This is connected with the information that appeared over the last years about the possibility of considerable lowering of resistance to brittle fracture of steels at irradiation by low-density neutron flows for a long time. Based on the experiments that were carried out in Russia and abroad, a detrimental influence of nickel on radiation resistance of the latter was established in the case when nickel content in metal is more than 1 wt.%.

Furthermore, in view of increase of the design life of reactor service from 30 to 60 years, ensuring of material thermal brittleness became one of the most important tasks. The gained experience showed that thermal brittleness even at rather low (up to 350 °C) temperature can essentially influence the security in long-term service. With the aim to prevent embrittlement of heat-resistant Cr–Mo steels at tempering and in operation, the amount of phosphorus, tin, antimony, silicon and manganese in material should be limited. Limitation of these impurities in the weld metal is taken into account by Bruscato criterion X:

$$X = (10\mathrm{P} + 4\mathrm{Sn} + 5\mathrm{Sb} + \mathrm{As}) / 100 \le 15{\cdot}10^{-6}$$

and for base metal — by Watanabe criterion I:

$$I = (\mathrm{Mn} + \mathrm{Si})\ (\mathrm{P} + \mathrm{Sn}){\cdot}10^{4} \le 150.$$

In order to produce weld metal that corresponds to all above mentioned requirements, it was necessary to develop new welding consumables. In this connec-

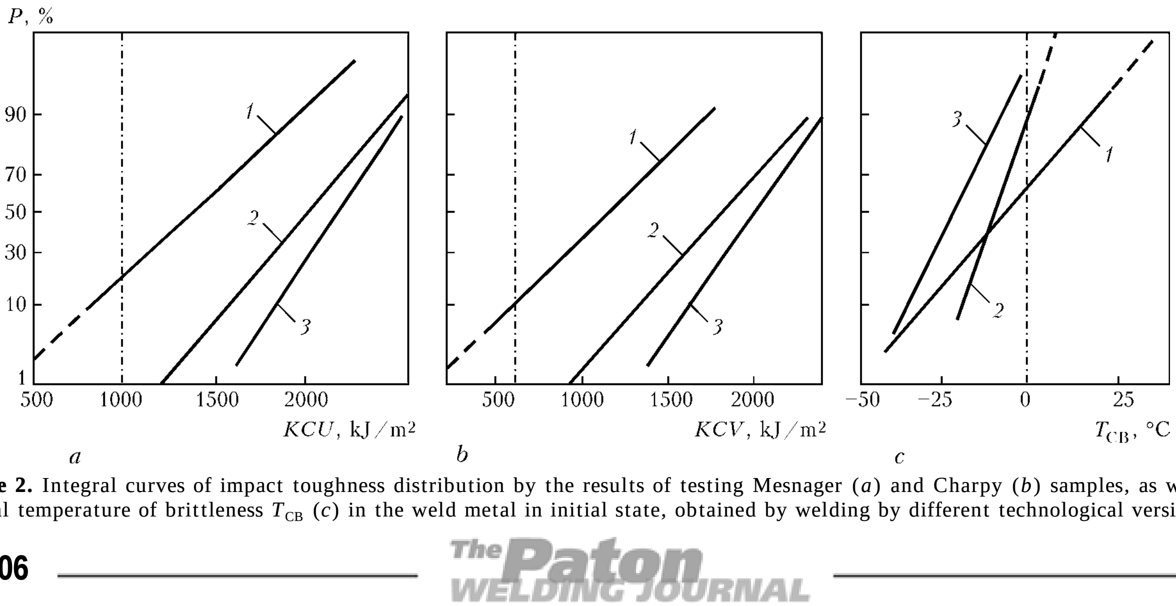

Figure 2. Integral curves of impact toughness distribution by the results of testing Mesnager (*a*) and Charpy (*b*) samples, as well as critical temperature of brittleness T_{CB} (*c*) in the weld metal in initial state, obtained by welding by different technological versions

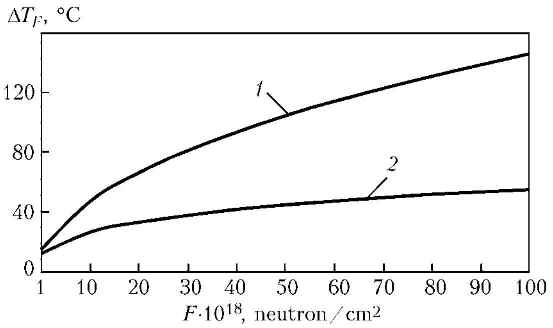

Figure 3. Change of calculated value of radiation embrittlement coefficient ΔT_F of weld metal with different alloying composition depending on neutron irradiation: *1* — Sv-09KhGNMTA-VI, flux NF-18M; *2* — Sv-10Kh3GMFTA-VP, flux FP-33

tion, «Prometej» at the end of 1990s developed welding wire of Sv-10Kh3G Ì FÒÀ-VP grade and flux FP-33 for automatic welding of steel 15Kh2MFÀ, and electrodes EP-35 (on the basis of Sv-10Kh3G Ì FÒÀ-VP wire) for manual arc welding of the same steel grades. Compared with Sv-10Kh Ì FTU wire that was used earlier, the content of molybdenum in the new wire was increased from 0.4–0.6 to 0.6–0.8 wt.%, that allowed producing weld metal of the strength equivalent that of the base metal. Increase of chromium content from 1.6–1.8 to 2.1–2.5 wt.% provided the cast metal weld with a tougher structure.

Besides, additional restrictions on elements that had a negative influence on thermal and neutron embrittlement were introduced for the new wire grade. This allowed producing weld metal with a limited content of impurity elements, namely, wt.%: S ≤ 0.01, P ≤ 0.01, Sb ≤ 0.008, Sn ≤ 0.001, As ≤ 0.001, Cu ≤ 0.08. Hence, the calculated value of irradiation embrittlement of weld metal at irradiation temperature of 270 °C does not exceed 12 (Figure 3).

Manufacturing of wire Sv-10Kh3GMFÒÀ-VP grade was mastered by industry, it is manufactured from super pure charge with application of vacuum-induction and vacuum-plasma remelting.

A distinctive feature of flux of FP-33 grade is its lower content of such active oxides as silicon dioxide and manganese monoxide, as well as presence of titanium dioxide. This allows reducing the intensity of silicon and manganese reduction from the flux in the weld metal in welding, that is favourable for increasing the resistance to thermal embrittlement. Flux of the above grade has also been mastered by industry, and is supplied in accordance with TU 5.965-11671–98. High welding and technological properties of the flux allow using it in narrow-gap welding with grove angle of 2°.

The results of investigation of welds that were made by the above-mentioned welding consumables in laboratory and industrial conditions showed that the weld metal after final heat treatment in the high tempering mode has a high level of strength and ductility characteristics. Guaranteed value of yield limit at the temperature of 350 °C is not less than 420 MPa, and critical temperature of brittleness does not exceed –20 °C. Investigation of thermal embrittlement susceptibility of weld metal of the given composition showed that the weld metal features a low sensitivity to thermal embrittlement in the case of long-term soaking at ageing temperature of 350–550 °C. This is indicative of a high margin of its stability at long-time influence of operating temperatures. Practically no change of the critical temperature of brittleness was observed after long-time heat soaking (up to 20,000 h) at the temperature of 350–450 °C.

From the above-stated it follows that welding circumferential welds that are located in WWER-1000 reactor body core, is recommended to be performed with wire of Sv-08KhGN Ì ÒÀ grade with flux NF-18 Ì , because this weld metal is characterized by the highest radiation resistance. With the aim to increase the design and real service life of WWER-1000 reactor body, additional limitations on the nickel content (1.3 wt.%) and the following impurities, wt.%: S ≤ 0.006, P ≤ 0.006, Sb ≤ 0.008, Sn ≤ 0.001, As ≤ 0.001, Cu ≤ 0.06, in Sv-09KhGN Ì ÒÀ-VI wire were set since 1995. Content of sulfur and phosphorus in flux NF-18 Ì is also lowered to 0.012 %. Furthermore, for welding core welds it was suggested applying wire of not more than 4 mm diameter at a narrow gap of the shells being welded.

For designing reactors bodies of advanced plants with higher indexes of operating safety and power and 1.5–2 times longer service life (up to 60 years and more), the most expedient is application of steel of 15Kh2NMFA grade, class 0 of improved composition and welding consumables Sv-10Kh3GMFTA-VP wire and flux FP-33, developed by the «Prometej» in cooperation with DB «Gidropress» and Izhora plant. This steel grade is the modification of steel 15Kh2MFA and contains in its composition not more than 0.8 wt.% Ni.

1. Gorynin, I.V., Ignatov, V.A., Timofeev, B.T. et al. (1983) Application of new welding consumables for circumferential welds on reactor bodies of nuclear power plant of increased capacity. *Avtomatich. Svarka*, **10**, 38–42.
2. Alekseenko, N.N., Amaev, A.D., Gorynin, I.V. et al. (1981) *Radiation damage of steel of WWER reactors*. Ed. by I.V. Gorynin. Moscow: Energoizdat.
3. Balandin, Yu.F., Gorynin, I.V., Zvezdin, Yu.I. et al. (1984) *Structural materials of nuclear power plant*. Moscow: Energoizdat.
4. (1997) *Radiation damageability and serviceability of structural materials*. Ed. by A.M. Parshin, P.A. Platonov. St.-Petersburg: Politekhnika.
5. Tsykanov, V.A., Shamardin, V.K., Pecherin, A.M. et al. (1998) Effect of nickel on radiation embrittlement of 15Kh2NMFA-A steel. In: *Problems of materials science in manufacturing and service of nuclear power plant equipment*: Call. of Abstr. of 5th Int. Conf. (St.-Petersburg-Pushkin, June 7–14, 1998). St.-Petersburg: TsNII KM «Prometej».
6. Morozov, A.M., Nikolaev, V.A., Yurchenko, E.V. et al. (2000) Effect of nickel on radiation embrittlement of base and weld metals of 15Kh2NMFA-A steel. In: *Problems of materials science in design, manufacturing and service of nuclear power plant equipment*: Transact. of 6th Int. Conf. (St.-Petersburg, June 19–23, 2000). St.-Petersburg: TsNII KM «Prometej».
7. Zherebenkov, A.S., Sobolev, Yu.V., Timofeev, B.T. et al. (1983) Analysis of mechanical properties of welded joints of WWER reactor bodies. *Voprosy Sudostroeniya*. Series Welding. Issue 35, 76–83.
8. Danausov, A.V., Timofeev, B.T. (2000) Comparison of mechanical properties of circumferential welds in operating WWER-1000 reactors made by different technological options. *Voprosy Materialovedeniya*, **3**, 96–103.
9. *PNAE G-7-010–89*: Equipment and tubing of nuclear power plants. Welded joints and deposits. Inspection code. Moscow: Energoatomizdat.
10. *PNAE G-7-002–86*: Calculation standard of strength of nuclear power plant equipment and tubing. Moscow: Energoatomizdat.

ACCELERATED INDUCTION HEAT TREATMENT OF WELDS ON PIPES FROM CONTROLLED-ROLLED STEELS

S.I. KUCHUK-YATSENKO, A.S. PISMENNY, M.E. SHINLOV, B.I. KAZYMOV and **V.F. ZAGADARCHUK**
E.O. Paton Electric Welding Institute, NASU, Kiev, Ukraine

Process of heat treatment (HT) at a comparatively short-term intensive action of the electromagnetic field on the welds made by flash-butt welding was studied. HT modes and mechanical properties of the treated and control welds are considered. It is established that application of accelerated intensive induction HT, envisaging a short-term increase in weld temperature above A_{c_3} point, leads to an increase in the index of weld impact toughness, narrowing of the heating zone, as well as saving of the energy consumed in HT. At weld HT duration of 90 to 180 s for steels of X65 and X80 grades, values of weld metal impact toughness are increased up to the required level, while the weld metal strength decreases by not more than 3.6 and 7.0 %, respectively. Accelerated induction HT can be used for improvement of impact toughness of weld metal in joints of large diameter pipes.

Keywords: induction heat treatment, line pipelines, controlled-rolled steels, weld, impact toughness, accelerated treatment

Higher requirements are made of the mechanical properties of pipe walls and butt welded joints of pipelines, particularly, if the pipelines are operated under extreme conditions (high pressure of the transported product, low operating temperature).

Pipes from sheet steels of a higher mechanical strength are now widely used in construction of line pipelines. These steels are manufactured using the controlled rolling technology [1]. Welding of butt welds in mounting of line pipelines is performed by highly mechanized and automated welding complexes, for instance of «Sever» type, designed for automatic flash-butt welding [2].

Requirements to weld impact toughness have a special role in the requirements made of the mechanical properties of material of pipelines operating at negative temperatures [3]. It is known [4] that heat treatment (HT) of the welds and HAZ is one of the methods to improve this characteristic.

Application of the traditional HT techniques (heating by electrical resistance belts due to Joule heat evolving in them [5, 6]; radiation heating by infrared heaters) and equipment for treatment of circumferential welds on large-diameter pipes is either impossible in site (furnace heating is required [7]), or is insufficiently effective. With these HT techniques, the heat propagates from the heat source to the pipe surface, and then inside the wall due to heat conductance. Heating zone is very wide in this case, which may lead to weld metal softening and damaging of the pipe external insulation. Considerable time is required to achieve sufficiently high HT temperature and specified uniform distribution of the temperature field across the weld thickness.

At welding in the field, heating time at HT has an essential influence both on the mechanical properties of the joints and on the productivity of the welding complex as a whole. It is known that at increase of HT duration, the heat source power is reduced, this being important in the case of HT, using a self-sufficient power source. Experience showed that increase of the heating duration leads to a greater degree of softening, which is manifested in welding higher strength pipes, made from steels of strength class X65–X80 and higher.

The aim of the conducted research was finding the possibility of intensifying the HT process with achievement of the effect of improvement of the strength properties of welds on the welded pipes.

The most effective possibilities for shortening the HT duration are provided by application of induction heating by HF currents. Heat evolves directly in the pipe wall being heated in a narrow zone, the formation of which is due to geometrical dimensions of the induction system and current frequency in the inductor. At a certain current frequency weld heating may proceed practically simultaneously across its entire thickness [8]. For instance, for the current range of wall thicknesses of large-diameter pipes (14–20 mm) applied in construction of line pipelines, the range of current frequency values acceptable for HT is equal to 1.0–2.5 kHz.

During investigations, also the influence of the intensity of induction HT and heating duration on impact toughness KCV and tensile strength σ_t of weld metal was evaluated at temperature T_{test} = –20 – +20 °C.

It is known that a feature of the technology of production of controlled-rolled steels is roll knobbing of the steel sheet at the heating temperature below that of transformation point A_{c_3}, which is similar to the process of work hardening (cold working). Therefore, for such steels it is particularly important to study HT influence near A_{c_3} point on the values of strength (especially, impact toughness).

Data on shifting of $\alpha \rightarrow \gamma$ transformation to a higher temperature region at accelerated heating [9] and lim-

Table 1. Composition of the studied steels, wt.%

Steel strength class	C	Si	Mn	S	P	Cr	Ti	Nb
Õ65	0.136	0.307	1.58	0.009	0.014	0.08	0.010	0.046
Õ80	0.062	0.461	2.04	0.004	0.016	0.05	0.027	0.042

Note. Nickel, vanadium and copper weight fraction is below 0.05 %, that of molybdenum — less than 0.03 %.

ited growth of austenite grains [10] were the prerequisite for application of HT with the short-time cycle of intensive induction heating, at which the temperature of weld heating is higher than that of transformation point A_{c_3}. This introduces the conditions under which just a slight lowering of weld metal strength can be found at a significant increase of impact toughness.

For controlled-rolled steels the yield point and ultimate strength are normed, while the composition is not specified. For instance, steels of the same strength class, but from different manufacturers, usually differ by their composition, the list of such steel grades being quite large.

In this work, the influence of HT of butt-welded joints was studied on pipes made of currently widely accepted pipe steels of X65 strength class 15.7 mm thick and X80 18.7 mm thick. Table 1 gives the results of spectral analysis of their composition.

As for each steel grade the value of temperature of point A_{c_3} is different, the differential vacuum dilatometer Shevenar, Switzerland, was used to conduct dylatometric investigations of samples of MI-102 type 1 (GOST 6996–66) made from steels of strength classes X65 and X80, for which A_{c_3} is equal to 850 and 880 °C, respectively.

Flash-butt welded joints were subjected to HT. Samples for welding were cut out of pipes of 1420 mm diameter in the form of sectors with welded pipe cross-section $s \times 200$ mm (here s is the wall thickness). Welding was performed in an all-purpose welding machine in keeping with VSN-006–89 requirements [11].

A laboratory unit, the elementary diagram of which is given in Figure 1, was developed to implement the induction HT.

Rotary converters of PVV-100-2.5 type of 100 kW power and 2.5 kHz current frequency were used as HF current sources. Power transformer of TZ-3-800 type was used for matching the power source and load. A bank of cosine capacitors was applied to compensate for the reactive power of the inductor. Heating of plates with the weld was performed from one side. This way, an inductor enclosing the pipe was used to simulate the conditions of heating a circumferential weld of large-diameter pipes in the route.

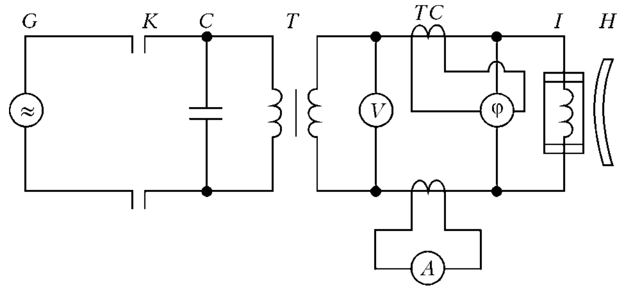

Figure 1. Elementary diagram of laboratory unit: G — power source (HF current converter); K — contactor; C — cosine capacitor bank; T — matching power transformer; V — voltmeter; A — ammeter; φ — phasometer; I — inductor; H — inductor load (sample being heated); TC — current transformer

The measuring components of the unit include sensors of electrical parameters and temperature. Voltage sensor is a standard measuring voltage transformer of VOS-8 type. Current sensor is made by Rogowski loop principle. Phasometer of F2-1 type was used to measure the angle of phase shift between inductor current and voltage. Electrical measurements were performed using electronic voltmeters of VU-15 and VK 7-9 type, this allowing determination of the power consumed in heating of welds on samples, and evaluation of the required power of the source to perform HT with a similar thermal cycle for large diameter pipes.

Samples of welded joints of steel of the considered strength classes were subjected to HT with three variants of heating duration, at which the weld metal was soaked at the temperature above point A_{c_3} for 90 to 180 s (Table 2). The Table gives the averaged values of temperature across the plate wall thickness achieved in the above HT modes. Used as temperature sensors were alumel-chromel thermocouples, the junctions of which were welded by capacitor-type welding at half-thickness of the plate in holes made in each butt welded joint. Thermal cycle was recorded by data recorder of KSP type. On-line monitoring of the pipe heating temperature was performed using an optical pyrometer of «Promin» type.

Procedure of evaluation of the influence of HT cycle parameters on the mechanical properties of weld metal consisted in comparison of the ultimate strength and impact toughness of welded samples subjected to HT with the basic ones, which were taken to be the

Table 2. HT mode parameters

Steel strength class	Mode No.	τ, s	T, °Ñ
Õ65	1	110	950
	2	130	980
	3	150	1030
Õ80	1	90	970
	2	135	1020
	3	180	1060

Note. τ — duration of weld metal staying at temperature above point A_{c_3}; T — HT temperature averaged by pipe wall thickness.

respective results of testing welded samples without HT. Samples to GOST 6996–66, cut out mechanically from flash-butt welds, were tested in PWI Mechanical Testing Laboratory.

Dependences were plotted by points, which are the mean arithmetic results of testing samples after HT by three variants of the modes (see Table 2). A notch was made in the weld center so that the direction of the pendulum hammer impact was tangential to the axis of the pipe, from which the plates were cut out for welding. The notch location was determined by chemical etching of a ground surface of the sample in 10 % solution of ammonium persulphate.

For steel of X65 strength class (Figure 2, *a*) an essential increase of impact toughness is noted in the entire range of testing temperatures. At –20 °C testing temperature of samples subjected to HT at temperature above A_{c_3} point with soaking for 100–150 s, impact toughness values rose 5.2 to 8.8 times; at T_{test} = 0 °C — 7.7–13 times, at T_{test} = 20 °C — 9.3–12.8 times.

For steel of X80 strength class (Figure 2, *b*) also an essential increase of impact toughness is found in the entire range of testing temperatures. At 20 °C temperature of testing samples subjected to HT at temperature above A_{c_3} point with soaking for 90–180 s, an increase of impact toughness 3.3–6.7 times is found; at T_{test} = 0 °C — 4–8.7 times; at T_{test} = = 20 °C — 5–9.6 times.

Thus, a tendency to increase of impact toughness of weld metal subjected to accelerated induction HT can be noted in the entire range of testing temperatures. A certain scatter of impact toughness values is observed, which is characteristic for joints made by pressure welding.

Metallographic investigations of welded joints before and after HT by the proposed technology confirmed the results of mechanical testing. No coarse grains causing the low impact toughness, were found in the structure of the metal of samples of welded joints from steels of both the grades. Metal structure in the zone of joint welding is more uniform and fine-grained after HT (Figure 3).

Figure 4 shows the results of tensile testing of full-thickness samples of a weld with removed reinforcement (flash) of MI-18 type to GOST 6996–66.

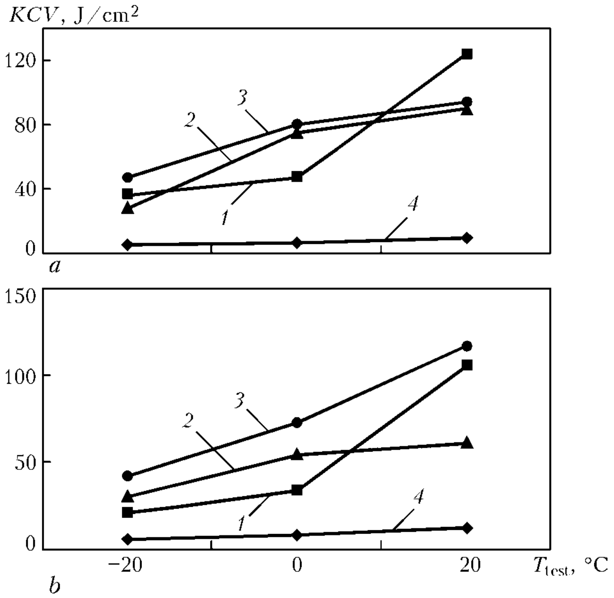

Figure 2. Change of impact toughness *KCV* of samples from steel of X65 (*a*) and X80 (*b*) strength classes depending on testing temperature T_{test} at different HT modes (*1–3*) and without HT (*4*)

Strength of welded joints after HT by the proposed technology, compared to the earlier applied one, has higher values in connection with a comparatively short duration of the thermal cycle. However, the strength values decrease in this case also.

Steels of X65 strength class are characterized by lowering of ultimate strength after intensive HT by not more than 3.6 % compared to the base metal (Figure 4, *a*), and for steels of X80 strength class, this value is equal to 7.0 % (Figure 4, *b*). The above strength values are underestimated, compared to the actual pipe joints, because tensile testing was performed on narrow samples. In view of manifestiation of contact strengthening effect, the actual values of ultimate strength of a welded joint of the full pipe cross-section will be higher [12], which is confirmed by experimental and calculated data [13].

Mechanical testing results showed that the highest values of welded joint impact toughness are reached at higher values of HT mode parameters. A reverse dependence is found at strength testing, it, however, being less pronounced for the above steels.

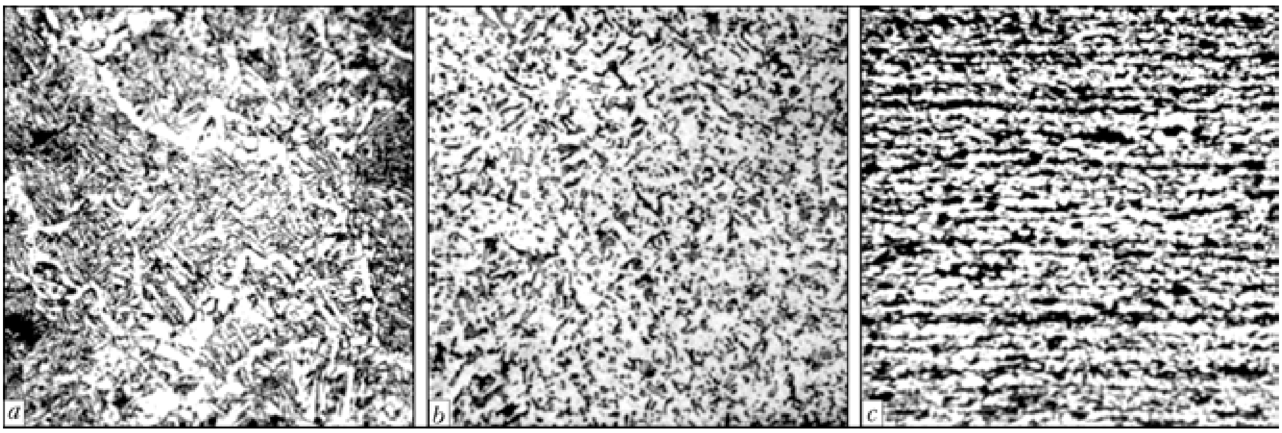

Figure 3. Characteristic microstructure of metal in the zone of butt joint of X65, X80 pipe steels in as-welded condition (*a*) and after HT (*b*), as well as base metal (*c*) (×100)

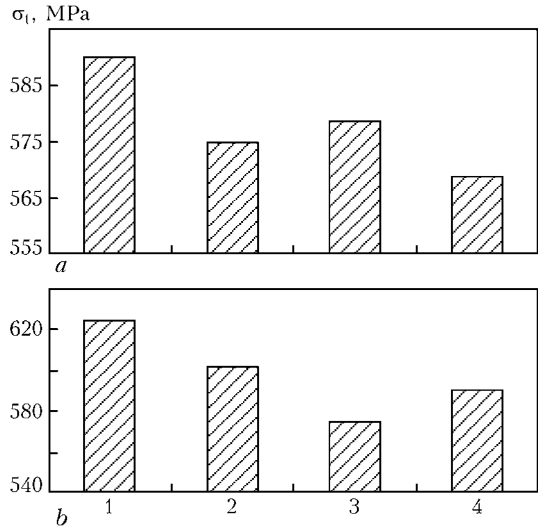

Figure 4. Tensile strength σ_t of samples of steels X65 (*a*) and X80 (*b*): *1* — without HT; *2–4* — with HT (modes *1–3* acc. to Table 2, respectively)

In development of equipment for this kind of HT of circumferential welds on large-diameter pipes, evaluation of power consumed in performance of induction HT of the considered type is of substantial interest.

As shown by measurements, values of the inductor active power should be about 85 kW per 1 m of linear length of a weld at pipe wall thickness of 16 to 19 mm.

Figure 5 (curve *1*) shows the dependence of specially developed inductor power on pipe diameter based on experimental data. For instance, at HT of pipes of 820, 1020, 1220 and 1420 mm diameter with 16 to 19 mm wall thickness, it is necessary to ensure the induction heating power of about 220, 280, 330 and 380 kW, respectively, this being lower than the power (Figure 5, curve *2*) consumed by the inductor at HT of large diameter pipes performed in the earlier proposed mode [14].

Power consumed at HT is a particularly important criterion in the case of work performance in the field conditions, with the limited power of the mobile power plant. One of the schematics of work performance envisages powering the HF converter from the power plant feeding the welding machine. HT is performed immediately after welding and cutting-off the inner and outer flash. In this case the inductor and outer flash remover can be combined into one unit, using one mechanism of displacement along the pipeline (either a pipe layer, or a self-sufficient displacement system). During the inductor operation the welding machine moves to the pipeline end, where preparatory operations are performed for welding the next pipe.

Depending on the construction conditions, the outer flash can be removed independently of welding. Such a sequence is used, if all the production facilities are to be concentrated on performance of the main technological operation, for instance, welding in the period of the most favourable climatic conditions. In this case a separate power plant is used for flash removal and HT.

In the interval between the welding operations, it is rational to use the power plant of the welding machine for performance of weld HT.

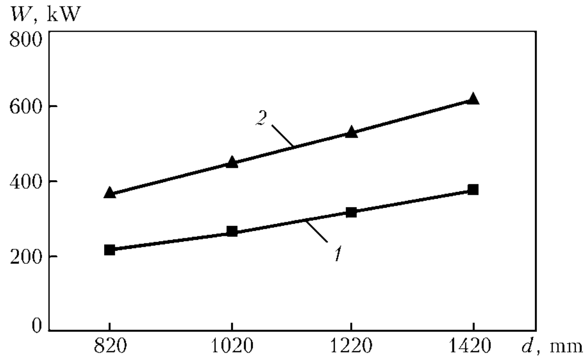

Figure 5. Dependence of inductor power on pipe diameter (for explanations see the text)

CONCLUSIONS

1. Application of accelerated intensive induction HT envisaging weld metal temperature briefly exceeding transformation point A_{c_3}, leads to an increase of weld impact toughness, narrowing of the heating zone and saving of power consumed at HT.

2. During performance of weld HT for 90 to 180 s for steels of strength classes X65 and X80 (of the respective compositions), the values of weld metal impact toughness are increased up to the required level, the strength of standard samples of the weld decreasing by not more than 3.6 and 7.0 %, respectively.

3. Proceeding from the results of mechanical testing of welds on pipes from steels of strength classes X65 and X80, an accelerated induction HT can be recommended for increasing the impact toughness of weld metal on large diameter pipes.

1. Pogorzhelsky, V.I. (1979) Technology of controlled rolling of low-alloy steels. In: *Production of high quality rolled metal*. Moscow: Metallurgiya.
2. Kuchuk-Yatsenko, S.I., Krivenko, V.G., Sakharnov, V.A. et al. (1986) *Resistance butt welding of pipelines*. Kiev: Naukova Dumka.
3. *SP 105-34--96*: Code of rules on construction of main gas pipelines. Introd. 01.10.96. Moscow: Gazprom.
4. Lebedev, V.K., Skulsky, Yu.V., Kuchuk-Yatsenko, S.I. et al. (1977) Local heat treatment of welded butt joints of 1420 mm diameter gas pipes. *Avtomatich. Svarka*, **10**, 38–40.
5. Korolkov, P.M. (1987) Local heat treatment of welded tee fittings and tee joints. *Stroitelstvo Truboprovodov*, **7**, 24–25.
6. Korolkov, P.M. (1996) Heat treatment of pipeline welded joints under field conditions. *Montazh. i Spets. Raboty v Stroitelstve*, **11 / 12**, 21–24.
7. Khromchenko, F.A., Korolkov, P.M. (1987) *Technology and equipment for heat treatment of welded joints*. Moscow: Energoatomizdat.
8. Babat, G.I. (1965) *Induction heating of metals and its industrial application*. Moscow-Leningrad: Energiya.
9. Gridnev, V.N., Oshkaderov, S.P., Televin, R.V. (1970) On the problem of $\alpha \rightarrow \gamma$ transformations in deformable carbon steels under rapid heating conditions. *Metallofizika*, Issue 9, 107–109.
10. Golovin, G.F., Zimin, N.V. (1979) *Technology of heat treatment of metals using the induction heating*. Leningrad: Mashinostroenie.
11. *VSN 006--89*: Instruction on the technology of flash-butt welding of main pipelines of steels with 60 kgf / mm^2 tensile strength. Moscow: VNIIST.
12. Bakshi, O.A. (1985) Allowing for the factor of mechanical heterogeneity of welded joints in tensile testing. *Svarochn. Proizvodstvo*, **7**, 20–21.
13. Kuchuk-Yatsenko, S.I., Makhnenko, V.I., Kazymov, B.I. et al. (1987) Resistance butt welding of large-diameter high-strength pipes. *Stroitelstvo Truboprovodov*, **7**, 21–25.
14. Shvartsman, A.G., Budkin, G.V., Brielkov, I.N. et al. (1990) Study of operation modes of inductors for heat treatment of pipe butt joints in construction of pipelines. *Svarochn. Proizvodstvo*, **6**, 20–21.

MATHEMATICAL MODEL FOR MAG WELDING IN A MANUFACTURING ENVIRONMENT

T. OHJI, F. MIYASAKA, T. YAMAMOTO and **Y. TSUJI**
Osaka University, Osaka, Japan

A feasibility study has been conducted to determine if mathematical models can be used for the numerical simulation of MAG welding in a manufacturing environment. In the present work, a 3D non-stationary thermal model for the welding is developed. The transient temperature distribution on the base metal is numerically analyzed to estimate the molten pool size by using a finite difference model based on the heat flow equation, and the theoretical configuration of molten pool is calculated, taking into account of the balance of gravity, surface tension and arc pressure. The developed model has been applied to the simulation of various welding processes, such as multi-pass welding, and fillet and butt welding with torch weaving. As the result, it is made clear that the model is shown to be capable of predicting the MAG welding and its weld profile in the manufacturing environment.

Keywords: *arc welding, mathematical model, thermal model, temperature distribution, molten pool size, process prediction, manufacturing*

One of the important problems in welding engineering is to construct a mathematical model for the computer simulation of the welding process in a manufacturing environment. Many attempts have been made to develop the numerical models for TIG [1--5] and MAG welding [6--8]. Dilthey and Roosen [6] have developed a 3D quasi-stationary thermal model for MAG welding. In the model, the influence of process parameters, such as the wire diameter and the composition of the shielding gas, on the weld profile have been taken into account. Kim and Na [7] have proposed a model of MAG welding including the effect of the weld pool convection. Pardo and Weckman [8] have developed a prediction model of weld pool and reinforcement dimensions of MAG welds using a finite element method, which has been formulated for a moving coordinate framework. In spite of these efforts, some problems remain to be solved because of the complexity of arc welding process. For example, those models are in quasi-stationary. In MAG welding, the electrode wire is melted and supplied into the molten pool intermittently and the welding process is quite dynamic and irregular. In other words, the model in quasi-stationary is of limited application and it can not be applied to the typical MAG welding process, such as undercutting, welding with torch weaving and multi-pass welding.

The objective of the present work is to develop a 3D non-stationary thermal model for MAG welding processes in the manufacturing environment.

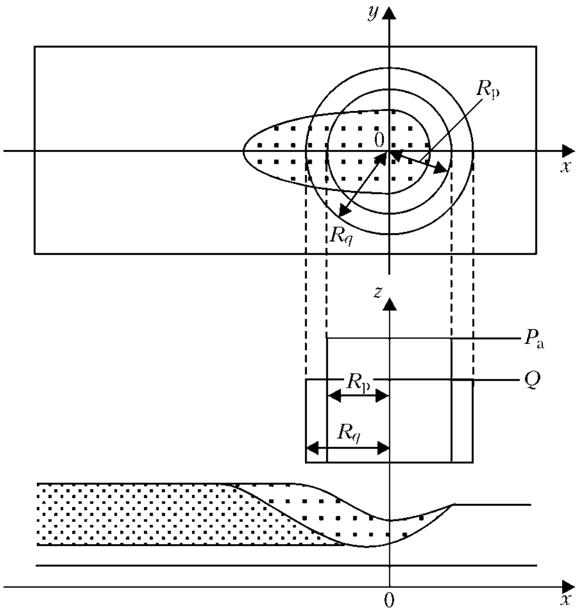

Figure 1. Heat input and arc pressure on molten pool (for designations see the text)

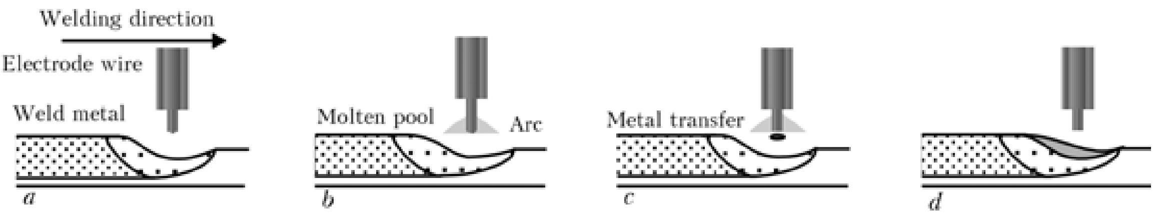

Figure 2. Model of MAG welding

---

*On the basis of materials of the Second International Conference «Mathematical Modelling and Information Technologies in Welding and Related Processes» (Katsiveli, Crimea, Ukraine, September 13–17, 2004).

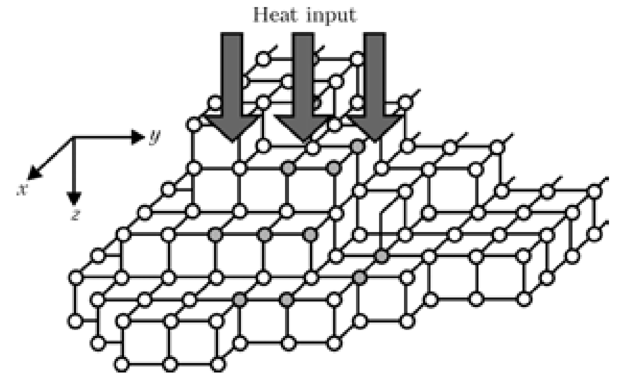

Figure 3. Schematic illustration of heat input on molten pool

Mathematical model. In order to simplify the numerical model for the MAG welding process, the following two fundamental assumptions have been introduced in the present work:

• heat flow in the weld pool is assumed to be conductive, i.e. the influence of the metal flow in the weld pool on the heat flow is neglected;

• weld pool is assumed to be in a static equilibrium under the gravity, surface tension and arc pressure.

Based on the above assumptions, the governing equations are given below [1, 9--12]:

$$\rho(T)\,\frac{\partial H}{\partial T} = \frac{\partial}{\partial X}\left\{K(T)\,\frac{\partial T}{\partial X}\right\} + \frac{\partial}{\partial Y}\left\{K(T)\,\frac{\partial T}{\partial Y}\right\} + \frac{\partial}{\partial Z}\left\{K(T)\,\frac{\partial T}{\partial Z}\right\}; \tag{1}$$

$$\sigma\left[\frac{(1+\varphi_y^2)\varphi_{xx} - 2\varphi_x\varphi_y\varphi_{xy} + (1+\varphi_x^2)\varphi_{yy}}{(1+\varphi_x^2+\varphi_y^2)^2}\right] = \rho g\varphi + P_a - \lambda, \tag{2}$$

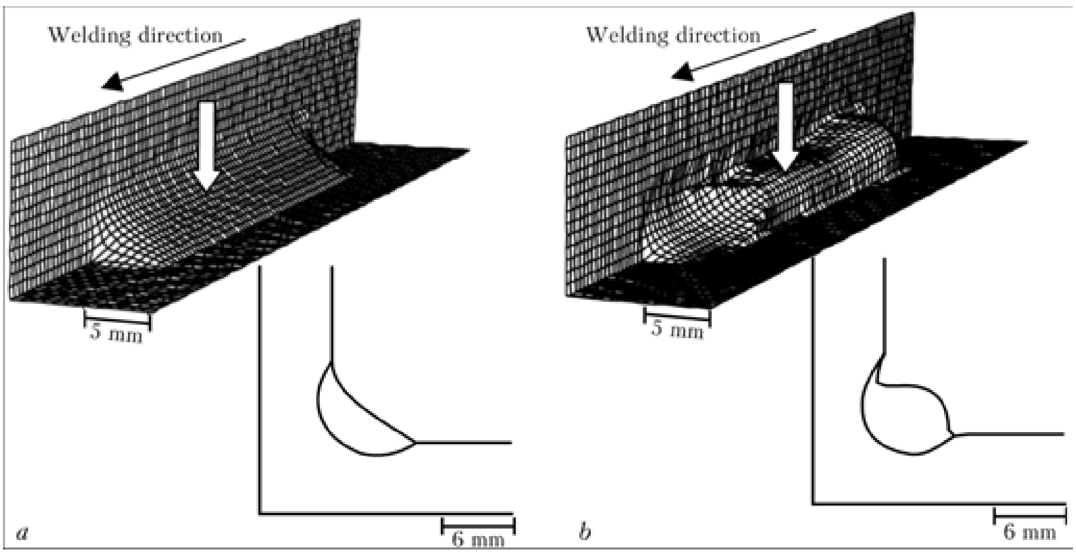

Figure 4. Influence of arc pressure (P_a = 0 (*a*) and 1000 (*b*) Pa) on welding profile in horizontal fillet welding at I = 230 A, U = = 25 V, v = 40 cm / min, R_q = 4 mm, R_p = 9 mm

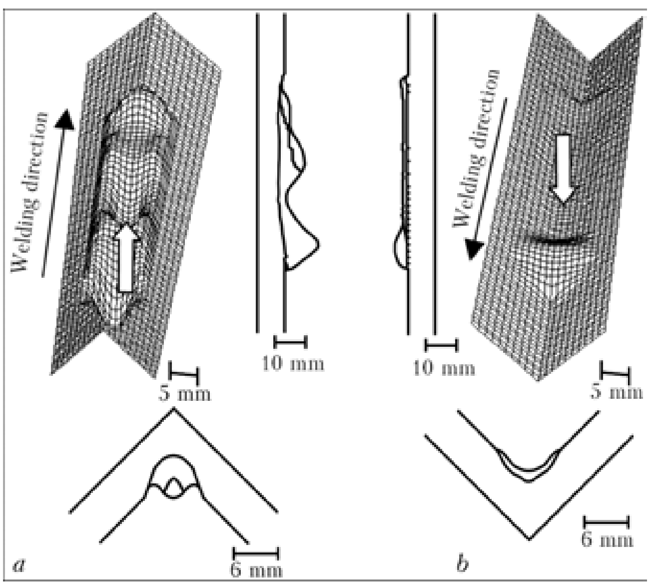

Figure 5. Calculated results in vertical up (*a*) and down (*b*) position of welding at I = 200 A, U = 30 V, v = 80 cm / min, P_a = 500 Pa, R_q = 4 mm, R_p = 4 mm

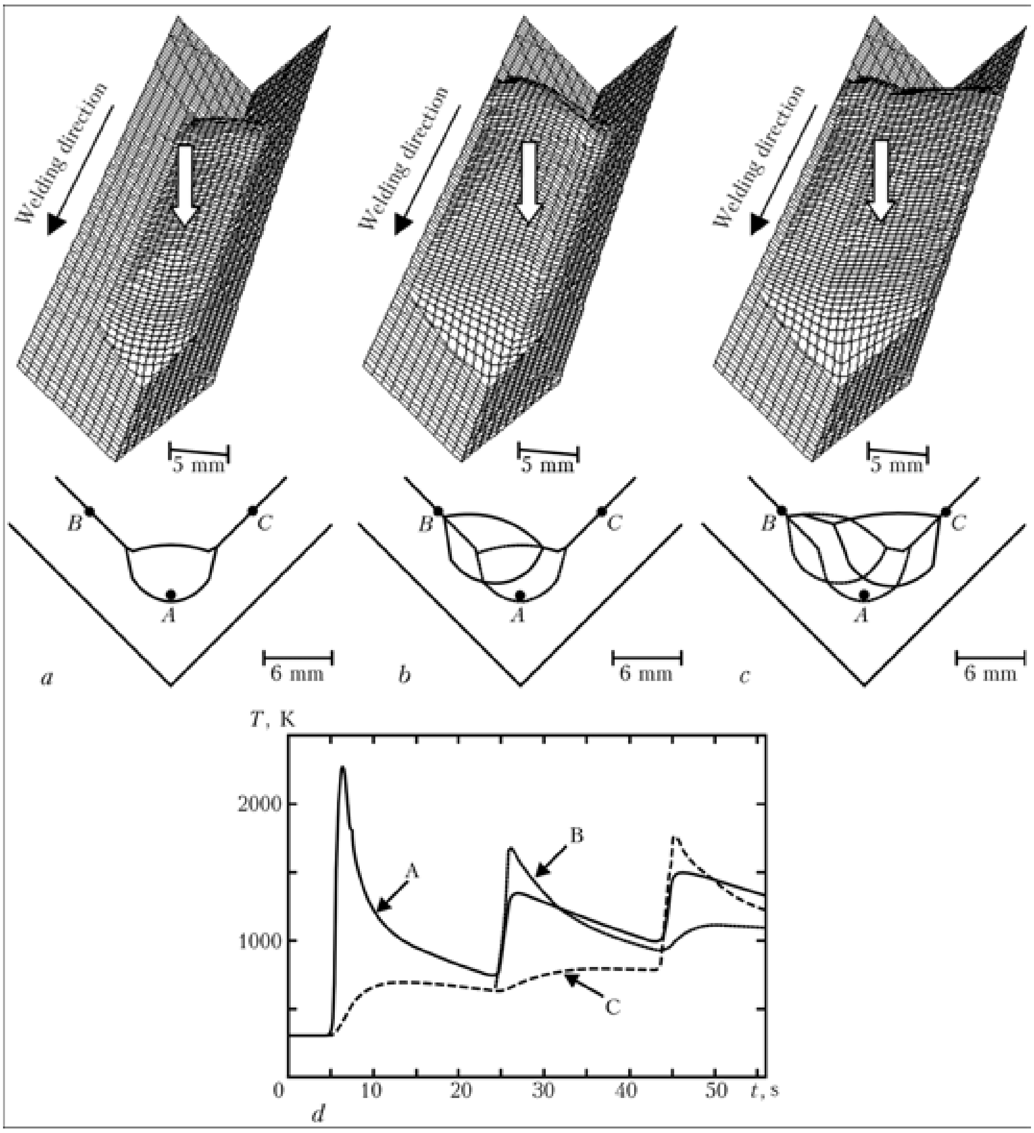

Figure 6. Calculated example of three-pass welding for the first (a), second (b) and third (c) pass, and calculated temperature history (d) at I = 230 A, U = 25 V, v = 40 cm / min, P_a = 800 Pa, R_q = 4 mm, R_p = 4 mm

where ρ is the density; H is the enthalpy; K is the thermal conductivity; T is the temperature; φ is the surface displacement; σ is the surface tension; g is the gravity; P_a is the arc pressure; λ is the Lagrange multiplier.

In the developed model, the arc is situated on the molten pool surface, numerically estimated by the molten pool balance equation (2), and the heat input from arc is assumed to be distributed in a circular zone with radius R_q on the molten pool surface as a boundary condition for the heat flow equation (1) as shown in Figure 1.

Accordingly, the heat input from arc is expressed by the equation (3):

$$q = \frac{Q}{S} = -K\,\frac{\partial T}{\partial Z}, \tag{3}$$

where Q is the total thermal energy inputted on the base metal per unit time; S is the area of heat source;

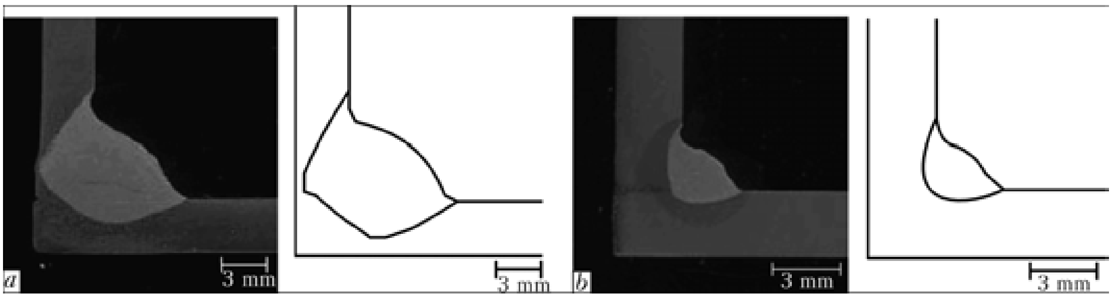

Figure 7. Comparison between calculation and experiment for plate thickness of 3 (a) and 6 (b) mm at I = 230 A, U = 24 V, v = = 40 cm / min

q is the thermal energy inputted on the base metal per unit time and per unit area.

The flow of the calculation during a unit time step in the model is shown in Figure 2 [10, 11]. As shown in Figure 2, *a*, the torch is fixed during the time step, and then the thermal energy is transferred into the base metal from the arc (Figure 2, *b*). In the final stage of the time step (Figure 2, *c* and *d*), the amount of the wire melted for this time step is transferred onto the molten pool and the surface profile is calculated by using the equation (2). Once the calculation during the time step is finished in the method, the torch is moved and the calculation in the next time step is repeated. And the next thermal energy is inputted on the calculated bead surface as shown in Figure 3, where the black lattice points indicate the positions of heat input.

Results and discussion. *Numerical result.* Figure 4, *a* shows a calculated bead surface profile in horizontal fillet MAG welding under the conditions of arc current I = 230 A, arc voltage U = 25 V, welding speed v = 40 cm / min, heat input radius R_q = 4 mm, arc pressure radius R_p = 9 mm and arc pressure P_a = = 0. In Figure 4, the attached figure is the bead cross section at the position indicated by the arrow on the profile. Figure 4, *b* shows the numerical result for arc pressure P_a = 1000 Pa while other process parameters are same as the case of Figure 4, *a*. The influence of the arc pressure on the weld bead formation is clearly observed from the Figure 4, *b*, where a weld bead of deep penetration with undercut is formed as a result of the digging action by the arc pressure.

Figure 5 shows another calculated example of the vertical fillet welding, where the longitudinal section along the centerline, as well as the bead cross section is attached. It is shown that the molten pool is hung down by the influence of the gravity in the vertical welding, so that the deep penetration is formed in Figure 5, *a*, and the shallow penetration is formed in Figure 5, *b*.

Figure 6 is a calculated example of the multi-pass welding. In this calculation, the cooling time between passes was set to 10 s. As a result of the heat input in the first and second pass welding, the penetration of third pass becomes deeper and wider than that of first pass. Figure 6, *d* shows the calculated temperature history in the three-pass welding, where the curves *A*, *B*, *C* correspond to the temperature histories at points *A*, *B*, *C* on the cross section in Figure 6, *a*–*c*. The influence of three heats on the temperature history is clearly observed in the Figure, while the temperature history depends strongly on the position in the workpiece.

Comparison between calculation and experiment. In order to evaluate the validity of the numerical model, the calculated result has been compared with the experimental MAG (Ar + 20 % CO_2) weld on mild steel plates.

Figure 7, *a* and *b* shows bead profiles of horizontal fillet welding for plate thickness of 3 and 6 mm, respectively. Figure 8 is another example of the comparison on bead profiles of three-pass butt welding on steel plates of 12 mm thickness. As is seen in these Figures, a good agreement between the experiment and calculation has been obtained.

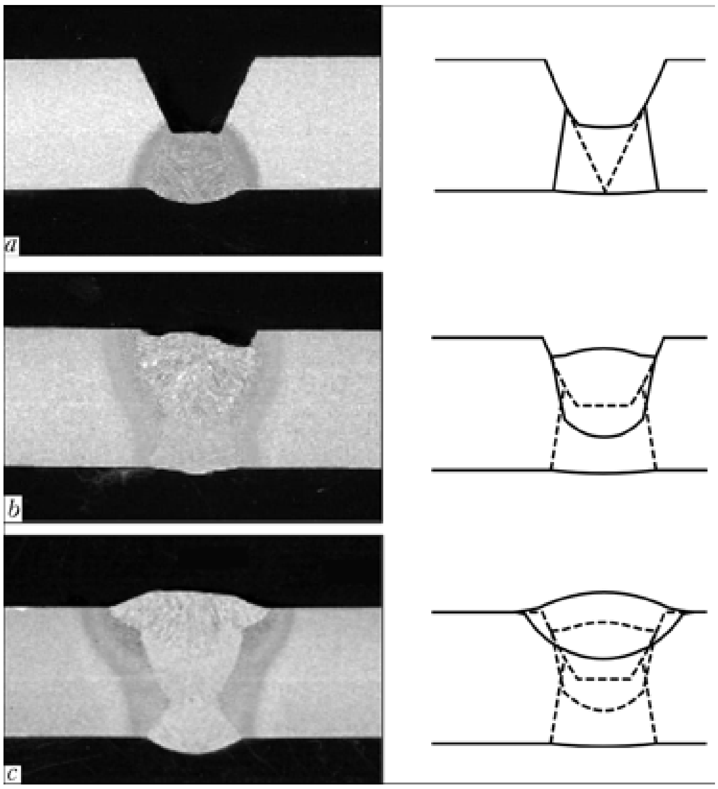

Figure 8. Comparison between experimental and calculated cross-sections of the first (*a*), second (*b*) and third (*c*) pass: *a* — I = 210 A, U = 26 V, v = 40 cm / min; *b* — I = 195 A, U = 26 V, v = 22 cm / min; *c* — I = 190 A, U = 26.5 V, v = 25 cm / min

Development of model-coupling system. In the present work, it is scheduled to develop a model-coupling system, where the process model, previously described, is linked to a metallurgical and / or mechanical model for simulating the arc welding comprehensively.

Figure 9, *a* is an example of the model-coupling, where the process model is linked a mechanical model. In the Figure, the original shape of workpieces is indicated by solid lines. The Figure shows that the workpiece of T-joint is deformed complicatedly as a result of the thermal stress due to MAG welding. In other words, the system indicates that a longitudinal bending seems to be severe in addition to the angular deformation under the input process condition.

Figure 9, *b* is another example, obtained by the model-coupling system, which shows the weld deformation in a butt welding of steel plates of 6 mm thickness. The original shape of work-pieces is indicated by solid lines in this case also. It is found that a remarkable shrinkage of workpiece in transverse direction takes place as a result of the welding.

These Figures suggest that the model-coupling system under development is useful as an engineering tool for optimizing process conditions in MAG welding.

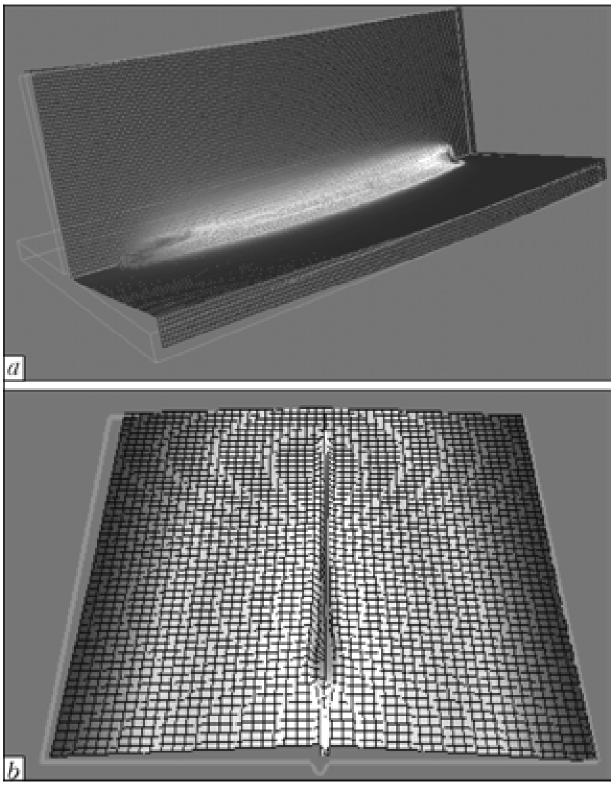

Figure 9. Calculated deformation in T- (*a*) and butt-joint (*b*) of MAG welded thin plate

CONCLUSION

A simulation model for MAG welding process has been developed in the present work. The model can be easily applied to the multi-pass welding and the arc welding with torch weaving, widely used in the manufacturing spot.

The weld profile, estimated by using the model, was compared with the experimental one in T- or butt-joint welding, and a good agreement was demonstrated between the calculation and experiment.

Accordingly, it is concluded that the model developed in the present work is useful as an engineering tool for the simulation of the welding in the manufacturing environment.

Acknowledgements. This work is the result of «Development of Highly Efficient and Reliable Welding Technology», which is supported by the New Energy and Industrial Technology Development Organization through the Japan Space Utilization Promotion Center within the program of the Ministry of Economy, Trade and Industry. The authors appreciate Prof. Murakawa and Dr. Serizawa in the Joining and Welding Research Institute, Osaka University, for contribution of the welding deformation model.

1. Ohji, T., Nishiguchi, K. (1983) *Technol. Rep. of Osaka Univ.*, **33**, 35–43.
2. Zacharia, T., Eraslan, A.H., Aidun, D.A. (1988) *Welding J.*, 67, 18–27.
3. Zacharia, T., David, S.A., Vitek, J.M. et al. (1995) *Ibid.*, 74, 353–362.
4. Nishiguchi, K., Ohji, T., Yoshida, H. et al. (1986) *Q. J. JWS*, 4(**4**), 673–677.
5. Kondoh, K., Ohji, T. (1998) *Sci. and Technology of Welding and Joining*, 3(**3**), 127–134.
6. Dilthey, U., Roosen, S. (1996) In: Proc. of Int. Symp. on Theoretical Prediction in Joining & Welding. *J. JWRI*, 133--154.
7. Kim, J.W., Na, S.J. (1994) In: Transact. of ASME. *J. Eng. for Industry*, 166, 78–85.
8. Pardo, E., Weckman, D.C. (1989) *Metallurg. Transact. B*, **20**, 937–947.
9. Ohji, T. (1978) Ph. D. Thesis. Osaka Univ.
10. Tsuji, Y., Yamamoto, T., Miyasaka, F. et al. (2000) *Q. J. JWS*, 18(**4**), 527--533.
11. Ohji, T., Tsuji, Y., Miyasaka, F. et al. (2001) *J. Materials Sci. & Technology*, **17**, 167–168.
12. Yamamoto, T., Ohji, T., Miyasaka, F. et al. (2002) *Sci. and Technology of Welding and Joining*, **7**, 260–264.

SENSITIVITY OF δ-FERRITE FORMATION TO FCAW PROCESS PARAMETERS IN STAINLESS STEEL CLADDINGS

P.K. PALANI[1] and **N. MURUGAN**[2]
[1]Government College of Technology, Coimbatore, India
[2]Institute of Technology, Coimbatore, India

The quality of clad components depends on the quantity of residual δ-ferrite formed during cladding, which in turn is controlled by the process parameters. The objective of controlling ferrite formed during cladding can easily be achieved by developing equations to predict ferrite number in terms of the process parameters, such as welding current, welding speed and nozzle-to-plate distance. Sensitivity analysis was performed for identifying the process parameters, which exert the most influence on the δ-ferrite formation and to know the parameters, which must be most carefully controlled. Studies reveal that change of nozzle-to-plate distance affects the formation of ferrite more strongly than the other process parameters.

K e y w o r d s : cladding, process parameters, δ-ferrite, sensitivity analysis, response surface methodology

Corrosion is a problem which weakens the structure causing its failure. Though corrosion can not be eliminated fully, it can be reduced to certain extent. To improve corrosion resistance, a protective layer is formed over the less corrosion-resistant substrate by a process called cladding [1–5]. Cladding is a surfacing process of depositing a relatively thick layer of corrosion-resistant material on a carbon or low alloy steel base metal [6–10]. Among various methods employed for protecting the surfaces, welding is the most popular technique when the thickness of the coating needed exceeds 3 mm. Cladding is extensively applied in power, nuclear and process industries [11]. The quality of these clad components depends on metallurgical characteristics such as δ-ferrite formed during cladding.

Austenitic stainless steel weld metal typically contains 2 to 7 % ferrite in an austenitic matrix, which improves weldability and strength of the welds [12–23]. Preserving these prescribed ferrite-austenite contents in the finished weld is essential to have desired corrosion resistance properties and service life of the clad structures [24].

Investigations have shown that small amounts of primary ferrite retained in the weld metal at room temperature reduce the hot cracking tendencies of 300 series stainless steel, which are fully austenitic in the as-formed condition [14–18]. However, too much ferrite reduces mechanical strength and corrosion resistance. Hence, a critical percentage of ferrite is desirable, which is about 3–8 vol.% depending on the application [19–25]. Higher this amount would mean the possibility of conversion to brittle phases such as σ-phase, when the material is in service at high temperature [26–34]. Another situation where it becomes necessary to restrict the presence of ferrite in welds is when the components or structure have to be non-magnetic.

The residual δ-ferrite formed in cladding is largely affected by the process parameters such as welding current, wire feed rate, welding speed and nozzle-to-plate distance. Consequently, there is a need to develop a methodology to control and optimize the amount of δ-ferrite formed during cladding of austenitic stainless steel.

Taking the above into consideration, the present study aims to develop a regression equation relating the cladding process parameters to the amount of δ-ferrite formed. Using this equation, sensitivity analysis has been carried out to know which parameters have more influence on the ferrite formation and how much.

The study was carried out in two steps: in the first step, experiments were conducted with different process parameters using design of experiments, to develop statistical models for the prediction of ferrite formed, and in the second step, sensitivity analysis was carried out based on the empirical equations so developed.

The study was carried out for the flux-cored wire arc welding (FCAW) process using 1.2 mm diameter

Table 1. Chemical composition of filler and base materials used, wt.%

Material	C	Si	Mn	P	S	Cr	Mo	Ni	N_2	Cu
Flux-cored wire 317L	0.021	0.89	1.38	0.016	0.007	18.46	3.18	13.1	0.057	0.007
IS:2062	0.180	0.18	0.98	0.016	0.016	--	--	--	--	--

317L austenitic stainless steel flux-cored wire (AWS: A5-22-95; EN 12073) with substrate as IS:2062 structural steel plate. Chemical compositions of base and filler materials used in this investigation are given in Table 1.

Experimental procedure. The independently controllable process parameters were identified; they are welding current, welding speed and nozzle-to-plate distance. The working range was decided by conducting trial runs and by inspecting the bead for smooth appearance and absence of any visible defects. It was found that the wire feed rate is directly proportional to the welding current and the relation is found to be $W_f = -6.92 + 0.086I$ [35], where I is the welding current, A; W_f is the wire feed rate, m / min; and hence it was treated as dependent variable.

After determining the working range of the process parameters, the upper limit was coded as +1.682 and the lower limit as –1.682, the coded values of the intermediate levels being calculated from the relationship $X_i = 1.682[2X - (X_{max} + X_{min})] / (X_{max} - X_{min})$, where X_i is the required coded value of variable X; X is any value of the variable from X_{min} to X_{max}; X_{min} is the lower level of the variable; X_{max} is the upper level of the variable. The selected values of the process parameters together with their units and notations are given in Table 2.

Table 2. Process variables and its bounds

Process variables	Factor levels				
	–1.682	–1	0	+1	+1.682
Welding current I, A	176	190	210	230	244
Welding speed S, cm / min	26	29	34	39	42
Nozzle-to- plate distance N, mm	15	17	20	23	25

Experiments were carried out using the Unimacro Esseti 501 Synergic MIG welding machine available at the Coimbatore Institute of Technology, India. Twenty experimental runs were conducted as per the central composite rotatable design matrix at random to avoid any systematic error creeping into the system, by laying a single bead of 150 mm length on structural steel plates using 317L stainless steel flux-cored wire of 1.2 mm diameter, under the shield of gas mixture Ar + 5 % CO_2 supplied at the rate of 16 l / min. DCEP with electrode to work angle of 90° was maintained throughout the study.

Table 3. Design matrix and results of experiments

Process parameters			FN_{meas}	Curvilinear model		Polynomial model	
I, À	S, cm / min	N, mm		FN_{pred}	Error, %	FN_{pred}	Error, %
190	29	17	7.28	6.441868	13.05727	7.27302	0.137219
230	29	17	5.80	5.602188	3.530984	5.53902	4.711664
190	39	17	6.48	5.848796	10.84332	6.08182	6.596381
230	39	17	4.12	5.086421	–19.059	4.34782	–5.30887
190	29	23	5.62	6.539970	–14.1128	5.67252	–0.97875
230	29	23	5.67	5.687502	–0.36048	5.89452	–3.85986
190	39	23	5.70	5.937867	–4.00593	5.78632	–1.49179
230	39	23	5.72	5.163882	10.71129	6.00832	–4.84861
176	34	20	5.75	6.521081	–11.8244	6.10514	–5.81707
244	34	20	4.75	5.135792	–7.51183	4.81994	–1.45106
210	26	20	6.17	6.255008	–1.407	6.44838	–4.36358
210	42	20	5.43	5.349706	1.55698	5.58646	–2.747
210	34	15	5.55	5.649371	–1.75898	5.99242	–7.38299
210	34	25	6.23	5.795522	7.54855	6.04242	3.154034
210	34	20	5.88	5.731220	2.613408	6.01742	–2.26708
210	34	20	6.283	5.731220	9.627621	6.01742	4.413519
210	34	20	6.101	5.731220	6.452032	6.01742	1.388967
210	34	20	5.704	5.731220	–0.47494	6.01742	–5.20854
210	34	20	6.09	5.731220	6.260101	6.01742	1.206165
210	34	20	5.301	5.731220	–7.5066	6.01742	–11.9058
Coefficient of determination R^2				0.387		0.823	
Pearson's correlation coefficient P				0.600		0.933	
Root mean squared error				0.112		0.052	
Absolute error				0.406		0.190	

In this study, the ferrite content was measured using FERITSCOPE® MP30 (Fischer Instruments Ltd., England). The feritscope was calibrated according to WRC standards. It is tuned to specimen shape by performing a corrective calibration with user standards in accordance with procedures specified in ANSI / AWS A 4.2, before taking the measurements.

Six readings were taken on the ground flat top clad surface of each specimen along the longitudinal axis of the clad (linear survey). The measured values (average) of ferrite content in terms of ferrite number (FN) are given in Table 3.

Development of mathematical models. *Curvilinear model*. Considering the ferrite content FN as a dependent parameter and process parameters including welding current *I*, welding speed S and nozzle-to-plate distance N as independent parameters. The relation between them can be expressed by the following equation [36]:

$$\mathrm{FN} = AI^b\mathrm{S}^c\mathrm{N}^d, \tag{1}$$

where *A*, *b*, *c* and *d* are the constants to be determined.

This equation can be written as

$$\log(\mathrm{FN}) = \log(A) + b\log(I) + c\log(\mathrm{S}) + d\log(\mathrm{N}). \tag{2}$$

The above the equation can be expressed in the following linear mathematical form:

$$K = \beta_0x_0 + \beta_1x_1 + \beta_2x_2 + \beta_3x_3, \tag{3}$$

where *K* is the logarithmic value of the experimentally measured response FN; β_0, β_1, β_2 and β_3 are the constants to be estimated; x_0 is the unit column vector; and x_1, x_2, x_3 are the logarithmic values of welding current, welding speed and nozzle-to-plate distance.

The above constants were determined for the experimental data given in Table 3, using a statistical software Systat® V11.

The curvilinear equation so developed is given below:

$$\mathrm{FN} = 10^{2.89}I^{-0.731}\mathrm{S}^{-0.326}\mathrm{N}^{0.050}. \tag{4}$$

Polynomial regression modeling of ferrite number. The second-order polynomial (regression) equation used to represent the response surface for *K* factors is given in [1, 37—44]:

$$Y = b_0 + \sum_{i=1}^{K} b_iX_i + \sum_{\substack{i,\, j=1 \\ i \neq j}}^{K} b_{ij}X_iX_j + \sum_{i=1}^{K} b_{ii}X_i^2, \tag{5}$$

where *Y* is the response; b_0 is the free term of the regression equation; the coefficients b_1, b_2..., b_k are the linear terms; the coefficients b_{11}, b_{22}..., b_{kk} are the quadratic terms; and the coefficients b_{12}, b_{13}..., b_{k-1k} are the interaction terms.

Evaluation of coefficients of model. The values of the coefficients of the above polynomial were determined with the help of statistical software Systat®, v. 11. The estimated model (full) with parameters in the natural form is given by the following equation:

$$\begin{aligned}\mathrm{FN} = {} & 33.58 + 0.0548I - 0.2646\mathrm{S} - 2.5999\mathrm{N} - \\ & - 0.00047I^2 + 0.00022\mathrm{S}^2 + 0.00384\mathrm{N}^2 - \\ & - 0.00114\mathrm{S}I + 0.00815\mathrm{N}I + 0.02175\mathrm{SN}.\end{aligned} \tag{6}$$

Development of final regression model. Insignificant coefficients (Eq. 6) can be eliminated without sacrificing much of the accuracy to avoid cumbersome mathematical labor. To achieve this, *t*-test and *F*-tests are used. Using the stepwise evaluation procedure available in Systat® software, the variables with *F* values greater than or equal to 4.0 are entered into the model, and the variables with *F* values less than 4.0 are removed from the model, one at a time automatically. After determining the significant coefficients, the final model was constructed by using only these coefficients.

The final mathematical model with parameters in the natural form, as determined by the above procedure, is presented below:

Table 4. Results of confirmation experiments

Exp. No	Process parameters			FN_{meas}	Curvilinear model		Polynomial model	
	I, A	S, cm / min	N, mm		FN_{pred}	Error, %	FN_{pred}	Error, %
1	200	32	21	5.730	6.072662	–5.64271	6.051	–5.305
2	210	29	23	5.700	6.078583	–6.22814	5.875	–2.978
3	210	39	20	5.790	5.480525	5.64682	5.643	2.605
4	230	34	23	5.610	5.400093	3.887105	5.831	–3.790
5	220	45	18	4.499	5.029275	–10.54380	4.362	3.141
6	190	34	20	6.399	6.166241	3.774732	6.130	4.388
7	230	29	20	5.430	5.647896	–3.85801	5.610	–3.208
Coefficient of determination R^2					0.599		1	
Pearson's correlation coefficient P					0.798		0.920	
Root mean squared error					0.126		0.099	
Absolute error					0.406		0.228	

Table 5. Analysis of variance for curvilinear and polynomial models

Source	Curvilinear model					Polynomial model				
	Sum-of-squares	df	Mean-square	F-ratio	P	Sum-of-squares	df	Mean-square	F-ratio	P
Regression	0.019	3	0.006	3.370	0.045	6.454	6	1.076	10.137	0
Residual	0.030	16	0.002	–	–	1.379	13	0.106	–	–

$$FN = 39.57 + 0.0197I - 0.4889S - 2.446N - 0.00048II + 0.00815NI + 0.02175SN. \quad (7)$$

Selecting the most accurate model. Of the two models so developed, the most accurate model was selected based on certain criteria such as ANOVA, coefficient of determination R^2, Pearson's correlation coefficient P, degree of accuracy and root mean squared error (RSME). The details of comparisons are presented in Tables 3–5.

The adequacies of the models so developed were tested by using the analysis of variance technique ANOVA [32–40] (see Table 5). As per this technique, it was found that the calculated F-ratio for curvilinear model is 3.37, whereas it is 10.13 for polynomial model. Similarly, R^2 and adjusted R^2 values for the curvilinear model are 0.39 and 0.27, whereas they are 0.82 and 0.74, respectively, for polynomial model.

Figure 1 shows a plot of the measured versus predicted values of FN for both models developed. It can be observed that the points are closer to 45° line for polynomial model than those of curvilinear model.

To ensure the accuracy of the developed models, additional experiments were also conducted (for process parameters and measured FN for the additional experiments see Table 4). The values of R^2, P, RMSE for curvilinear and polynomial models are 0.599, 0.79, 0.126 and 1, 0.92, 0.099, respectively.

It is evident from the foregoing discussions that reasonable agreement between experimental and predicted values occurs while using polynomial regression equation. Hence, polynomial equation was selected as the most accurate model for this study.

Sensitivity analysis. The qualitative and quantitative effectiveness of process parameters can be determined using sensitivity analysis. By this analysis, critical parameters can be identified and ranked by their order of importance [37]. This will help the plant engineers to select the process parameters efficiently and control the ferrite content effectively without much trial and error, resulting in saving of time and materials.

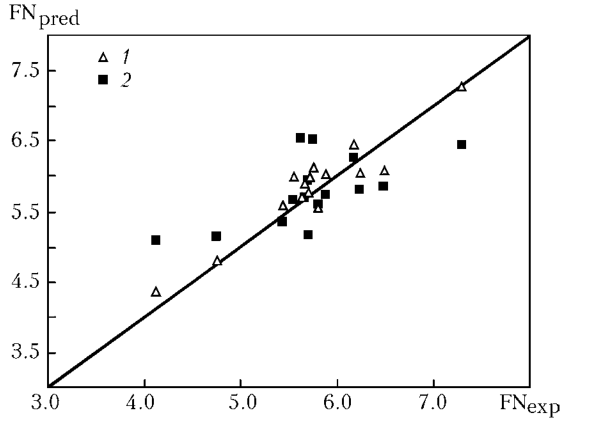

Figure 1. Scatter plot for polynomial (Δ) and curvilinear (■) models

The sensitivity equations for the ferrite content were obtained by differentiating Eq. 6 with respect to welding current, welding speed and nozzle-to-plate distance are given below [37]:

sensitivity of welding current I is

$$d(FN) / d(I) = 0.0197 - 2\cdot 0.00048I + 0.00815N; \quad (8)$$

sensitivity of welding speed S is

$$d(FN) / d(S) = -0.4889 + 0.02175N; \quad (9)$$

sensitivity of nozzle-to-plate distance N is

$$d(FN) / d(N) = -2.446 + 0.00815I + 0.02175S. \quad (10)$$

The calculated values of sensitivities of I, S and N using the above equations are presented in Table 6. Positive values of sensitivities mean that the amount of residual ferrite formed increases with the corresponding increase in the values of process parameters, and negative values mean that FN decreases with the corresponding increase in the values of process parameters. Figures 2–6 depict the results of sensitivity analysis.

From Figure 2, it can be observed that ferrite formed during cladding is more sensitive to welding current in higher current regions. It is interesting to note that the sensitivity is positive when the current is below 190 A, and it changes its sign to negative when the current level is above 190 A, which means that the effect of welding current is to increase the ferrite formation in lower regions of current and decrease the rate of ferrite formation in higher regions of current.

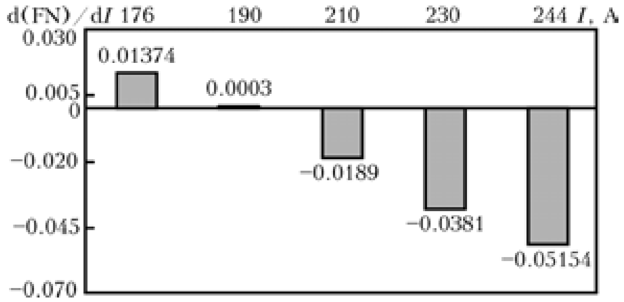

Figure 2. Sensitivity analysis results of welding current on FN at S = 34 cm / min and N = 20 mm

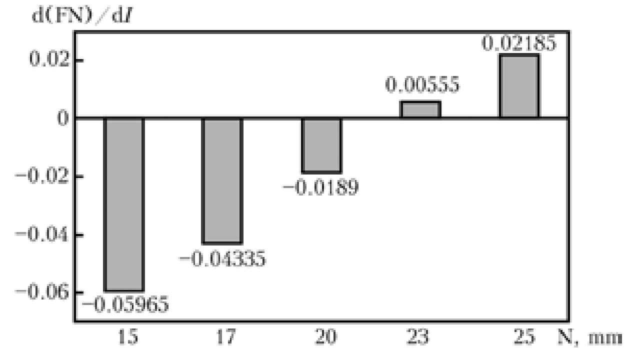

Figure 3. Sensitivity analysis results of welding current on FN at I = 210 A and S = 34 cm / min

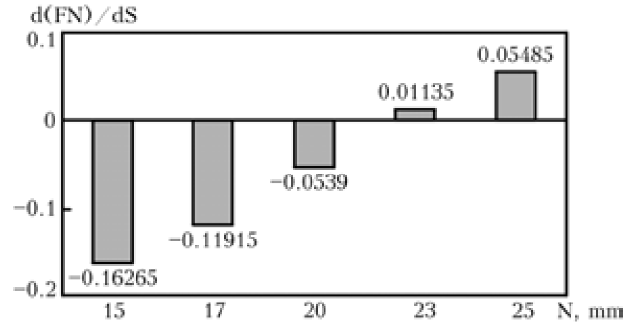

Figure 4. Sensitivity analysis results of welding speed on FN at I = = 210 A and S = 34 cm / min

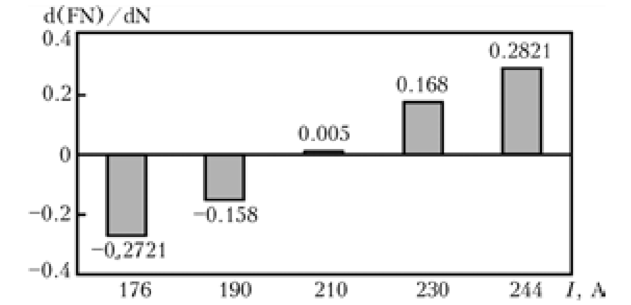

Figure 5. Sensitivity analysis results of nozzle-to-plate distance on FN at S = 34 cm / min and N = 20 mm

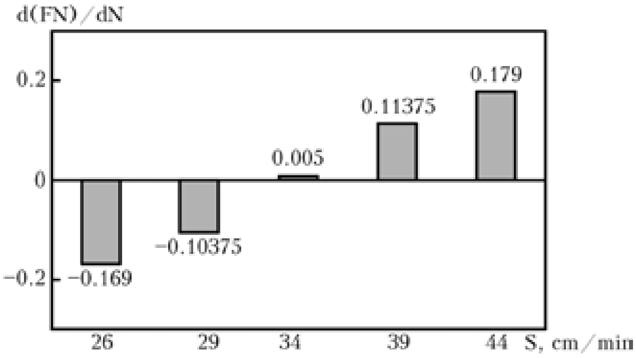

Figure 6. Sensitivity analysis results of nozzle-to-plate distance on FN at I = 210 A and N = 20 mm

Table 6. Ferrite content sensitivity to process parameters

Process parameter			Sensitivity		
I, À	S, cm / min	N, mm	d(FN) / dI	d(FN) / dN	d(FN) / dS
176	34	20	0.01374	–0.2721	–0.0539
190	34	20	0.0003	--0.158	–0.0539
210	34	20	–0.0189	0.005	–0.0539
230	34	20	–0.0381	0.168	–0.0539
244	34	20	–0.05154	0.2821	–0.0539
210	26	20	–0.0189	--0.169	–0.0539
210	29	20	–0.0189	–0.1038	–0.0539
210	34	20	–0.0189	0.005	–0.0539
210	39	20	–0.0189	0.11375	–0.0539
210	42	20	–0.0189	0.179	–0.0539
210	34	15	–0.05965	0.005	–0.1627
210	34	17	–0.04335	0.005	–0.1192
210	34	20	–0.0189	0.005	–0.0539
210	34	23	0.00555	0.005	0.01135
210	34	25	0.02185	0.005	0.05485

It is evident from Figure 3 that the sensitivity of welding current to FN is higher in lower regions of N. Also it can be observed that increase in I causes decrease in FN, however, when the value of N is in its higher region, say beyond 22 mm, the value of FN starts increasing with increasing the value of I.

It is evident from Table 6 that the sensitivity of welding current remains constant for all values of S, i.e. the change in FN can not be achieved by changing S alone.

The sensitivities of welding speed are represented in Figure 4. This Figure reveals that the formation of δ-ferrite is more sensitive to S in lower regions of N, and the sensitivity attains zero value when N is at its middle level. The sensitivities of S are positive in higher regions of N, meaning that the effect of change in S is to decrease the ferrite content when N is kept below, say 22 mm, whereas the effect of S is to increase the ferrite formation when the values of N are above 22 mm.

Figures 5 and 6 depict the sensitivities of N to ferrite formation for different values of S and I. It is evident that in both cases the sensitivities are positive in lower regions and negative in higher regions of S and I. Also, the magnitude of sensitivity of N is maximum when I is at 176 A and 244 A, which means that even small changes in N cause higher changes in the value of FN when the current levels are kept either in lower or higher regions.

CONCLUSIONS

1. The relationships between the process parameters and δ-ferrite formed during cladding for FCAW of 317L flux-cored wire on structural steel plate have been established. The response surface methodology was adopted to develop two regression equations, viz., curvilinear and polynomial models, which were checked for their accuracy, and the model developed using polynomial equation was found to be satisfactory.

2. Sensitivity analysis was performed to identify those process parameters that exert the most influence

on the δ-ferrite formation. Sensitivity analyses have indicated that ferrite formed during cladding is affected by change of process parameters.

3. Changes in nozzle-to-plate distance have a more significant effect on FN, compared to welding current and speed.

4. Though the effect of all the three variables are significant, the sensitivities of nozzle-to-plate distance and welding speed are more significant, therefore, controlling of nozzle-to-plate distance and welding speed are more useful in controlling the formation of residual ferrite.

Acknowledgements. The authors wish to thank the All India Council for Technical Education, New Delhi, and University Grant Commission, New Delhi, India, for their financial support for procuring the equipment and materials. The authors also wish to thank M/S.Böhler Thyssen Welding, Austria, for sponsoring the 317L flux-cored wire to carry out this investigation. The authors wish to thank the management of the Coimbatore Institute of Technology, India, for according permission to utilize the facilities available in their Welding Research Cell.

1. Murugan, N., Parmer, R.S. (1995) Mathematical models for bead geometry prediction in austenitic stainless steel surfacing by MIG welding. *Int. J. Joining of Materials*, 7(**2/3**), 71–80.
2. Murugan, N., Parmer, R.S. (1997) Stainless steel cladding deposited by automatic gas metal arc welding. *Welding J.*, 76(**10**), 391–402.
3. Khodadad Motarjemi, A., Kocak, M. (2001) Fracture assessment of weld repaired clad steel wide plates by SINTAP defect assessment procedure. *Welding in the World*, Special Issue, 45(July), 27–33.
4. Davis, J.R. (1996) *ASM specialty handbook on stainless steel*. 2nd ed. ASM Int., 107–119.
5. Alam, N., Jarvis, L., Harris, D. et al. (2002) Laser cladding for repair of engineering components. *Australian Welding J.*, 47, 38–47.
6. Heston, T. (2000) Cladding operations doubles life of boiler tubing. *Welding J.*, 79(**7**), 45–47.
7. Lee, J.S., Kim, I., Kimura, A. (2003) Application of small punch test to evaluate sigma-phase embrittlement of pressure vessel cladding material. *J. Neuclear Sci. and Technol.*, 40(**9**), 664–671.
8. Missori, S., Murdolo, F., Sili, A. (2004) Single-pass laser beam welding of clad steel plate. *Welding J.*, 83(**2**), 65–71.
9. Rajasekaran, S. (2000) Surface topography of pulsed current gas metal arc clads. *Surface Eng.*, 16(**6**), 495–500.
10. Nishimoto, K., Ogawa, K. (1999) Corrosion properties in weldments of stainless steels. Part 1: Metallurgical factors affecting corrosion properties. *Welding J.*, 13(**11**), 2–11.
11. Buvanasekaram, G., Venkateswara Prasad, N. (2001) Effect of cladding parameters on intergranular corrosion and bonding properties of cladding stainless steel layers. In: *Proc. of Nat. Conf. on Recent Advances in Materials Processing*. Annamalai Univ., 136–147.
12. Dhanuka, M.P. (2003) Measurement of delta ferrite content in austenitic stainless steel weld metals using WRC-92 diagram. In: *Proc. of Int. Welding Symp*. Mumbai, 219–222.
13. Smith, D.V. (1988) A practical approach to ferrite in stainless steel weld metal. *Welding J.*, 67(**6**), 57–69.
14. Nazir Ahmad, Wojciezh Mazur (2003) Confid. techn. report CMIT(C)-2-3-155: Assessment of the repair strategy and the effects of the repair on the reactor pool liner. *CSIRO Manufact. and Infrastructure Techn.*, August.
15. Kane, S.F., Farland, A.L., Siewert, T.A. et al. (1999) Welding consumable development for a cryogenic (4 K) application. *Welding J.*, 78(**8**), 292–300.
16. Saito, M., Yamamoto, A., Iida, T. et al. (1996) The effect of delta-ferrite phase in weld metal of stainless steel on the mechanical properties at cryogenic temperature. Mater. and Welding Res. Lab., Nagasaki-R7d Centre. *Japan.http://www.enaa.or.jp/we-net/ronbun/1996/e16/naga1996.html*
17. Delong, W.T. (1974) Ferrite in austenitic stainless steel weld metal. *Welding J.*, 53(**7**), 273–286.
18. Prasad Rao, K., Prasanna Kumar, S. (1984) Assessment criterion for variability of delta ferrite in austenitic weld and clad metals. *Ibid.*, 63(**7**), 231–239.
19. Olson, D.L. (1985) Prediction of austenitic weld metal microstructure and properties. *Ibid.*, 64(**10**), 281–295.
20. Kotecki, D.J. (1988) Standards and industrial methods for ferrite measurement. *Ibid.*, *77(***5**), 49–52.
21. Kotecki, D.J., Siewert, T.A. (1992) WRC-1992 constitution diagram for stainless steel weld metals: A modification of the WRC-1988 diagram. *Ibid.*, 71(**5**), 171–178.
22. Kotecki, D.J. (1997) Ferrite determination in stainless steel welds — advances since 1974. *Ibid.*, 76(**1**), 24–37.
23. Siewert, T.A., McCowan, C.N., Olson, D.L. (1988) Ferrite number prediction to 100 FN in stainless steel weld metal. *Ibid.*, 67(**12**), 289–296.
24. Ames, N., Ramberg, M., Johnson, M. et al. (2001) *Comparison of austenitic, super austenitic and super duplex weld properties produced using GTAW flux*. KCI Publ.
25. Prasad Rao, K., Krishnan, K.N., Rama Rao, V. et al. (1986) Effect of welding parameters on the content of delta ferrite in austenitic stainless steel weld and clad metals. In: *Proc. of Nat. Welding Sem*. (India, 1986), 64–72.
26. Cui, Y., Lundin, C.D. (2004) Ferrite number as a function of the Larson–Miller parameter for austenitic stainless weld metals after creep testing. *Metallurg. and Mater. Transact. A*, 35, 3631–3634.
27. Vitek, J.M., Iskander, Y.S., Oblow, E.M. (2000) Improved ferrite number prediction in stainless steel arc welds using artificial neural networks. Part 1: Neural network development. *Welding J.*, 79(**2**), 34–40.
28. Vitek, J.M., Iskander, Y.S., Oblow, E.M. (2002) Improved ferrite number prediction in stainless steel arc welds using artificial neural networks. Part 2: Neural network development. *Ibid.*, 79(**2**), 41–50.
29. Balmforth, M.C., Lippold, J.C. (2000) A new ferritic-martensitic stainless steel constitution diagram. *Ibid.*, 79(**12**), 339–345.
30. Kotecki, D.J. (1999) A martensite boundary on the WRC-1992 diagram. *Ibid.*, 78(**5**), 180–192.
31. Barnhouse, E.J., Lippold, J.C. Microstructure/property relationships in dissimilar welds between duplex stainless steels and carbon steels. *www.aws.org/wj/supplement*
32. (2003) The metallographic examination of archaeological artifacts: Lab. Manual. MIT, Summer Inst. in Materials Sci. and Mater. Culture.
33. Vitek, J.M., David, S.A., Hinman, C.R. (2003) Improved ferrite number prediction model that accounts for cooling rate effects. Part 1: Model development. *Welding J.*, 82(**1**), 10–17.
34. Vitek, J.M., David, S.A., Hinman, C.R. (2003) Improved ferrite number prediction model that accounts for cooling rate effects. Part 2: Model results. *Ibid.*, 82(**2**), 43–50.
35. Palani, P.K., Murugan, N. *Modeling and simulation of wire feed rate for steady current and pulsed current gas metal arc welding* (commun. for possible publ. in the Int. J. of Computer Applications in Technology).
36. Kim, I.S., Son, J.S., Jeung, Y.J. (2001) Control and optimisation of bead width for multi-pass welding in robotic arc welding processes. *Australian Welding J.*, 46, 43–46.
37. Kim, I.S., Son, K.J., Yang, Y.S. et al. (2003) Sensitivity analysis for process parameters in GMA welding process using factorial design method. *Int. J. Machine Tools and Manufacture*, 43, 763–769.
38. Ramasamy, S. et al. (2002) Design of experiments study to examine the effect of polarity on stud welding. *Welding J.*, 81(**2**), 19–26.
39. Montgomery, D.C. et al. (1999) *Applied statistics and probability for engineers*. 2nd ed. New York: John Wiley & Sons.
40. Myers, W. (1998) *Probability and statistics for engineers and scientists*. 6th ed. New Jersey: Prentice Hall.
41. Cheremisinoff, N.P. (1987) *Practical statistics for engineers and scientists*. Techn. Publ. Co. Inc.
42. Cochran, W.G., Cox, G.M. (1957) *Experimental designs*. 2nd ed. Singapore: John Wiley & Sons.
43. Khuri, A.I., Cornell, J.A. (1996) *Response surfaces, designs and analyses*. New York: Marcell Dekker Inc.
44. Montgomery, D.C. (2001) *Design and analysis of experiments*. 5th ed. New York: John Wiley & Sons.

MODELLING OF THE SHOCK WAVE PROCESS IN LOCAL PULSED TREATMENT OF PLANE SAMPLES USING RING CHARGES*

B.I. PALAMARCHUK, N.A. PASHCHIN, A.T. MALAKHOV, A.V. CHERKASHIN, A.N. MANCHENKO and **A.A. CHAJKA**
E.O. Paton Electric Welding Institute, NASU, Kiev, Ukraine

Considered are the peculiarities of arresting the propagation of a fatigue crack through forming the field of compressive stresses and plastic strains in the vicinity of the crack using a pulsed explosive impact, involving focusing of energy in the crack location zone. The Neumann--Richtmyer method of end-to-end counting using artificial viscosity was employed to model shock waves in explosive loading of materials. Modelling of the shock wave (SW) process allows prediction of parameters of the pulsed impact on materials, which makes it easier to evaluate the effect on them by the density of explosive materials, explosion energy and damping interlayers. For complex schemes of pulsed loading of materials, the SW effect parameters can be directly measured using the developed electret pressure sensors.

Keywords: *shock wave treatment, structural steels, stressed state, numerical modelling, wave pressure, experimental procedure*

The pressing problem of current research is improvement of fatigue strength of structural materials based on light alloys. The main cause of deterioration of fatigue strength is initiation and propagation of fatigue cracks. In this connection, it was suggested that local pulsed treatment of sheet materials should be used to induce the field of residual compressive stresses to prevent free propagation of a fatigue crack in the material. This suggestion is based on the mechanism of complete elimination or re-distribution of the stress-strain state at the crack apex, which should lead to disorientation of the crack, and formation of barrier zones of residual compressive stresses in a direction of propagation of the crack to prevent its further development or arrest it for some time, depending upon the level and character of induced stresses.

Several schemes are available now for pulsed shock wave treatment (SWT) using the explosion energy. All of them differ in geometry, capacity, type of the used charges and loading schemes, which, in turn, provides a wide range of levels and sizes of the zones of residual stresses. However, most treatment schemes involve chemical condensed explosive materials (EM), the free use of which is limited now for a number of reasons. Therefore, the need to minimise the quantity of duplicate experiments made it necessary to apply numerical modelling of the stressed state of materials after pulsed SWT.

Non-stationary motion of an environment generated by explosion can be described by a system of differential equations in partial derivatives, which are usually integrated using specially developed difference methods. As a rule, the real flows are not one-dimensional. Nevertheless, solving one-dimensional problems with a spherical, cylindrical or plane symmetry of the flow yields plenty of the practically useful information.

The method of end-to-end counting with artificial viscosity was used to solve the problems in a one-dimensional statement. The main advantages of the method are versatility and possibility of end-to-end counting using homogeneous difference schemes realised with the same formulae in all points of the mesh, independently of the fact whether a given point coincides or does not coincide with the solution irregularity point. Homogeneity of an algorithm of difference counting is achieved through adding an artificial viscosity, or pseudo-viscosity, which smears discontinuities in the shock waves, this allowing them to be regarded as non-singularities.

The system of equations of one-dimensional motion of an environment and detonation products (DP) of EM can be written down on the Lagrangian co-ordinates in the following dimensionless form:

$$\frac{\partial u}{\partial \theta} = -v_0 \left(\frac{r}{x}\right)^{\nu - 1} \frac{\partial p}{\partial x}, \quad \frac{\partial r}{\partial \theta} = u,$$

$$v = v_0 \left(\frac{r}{x}\right)^{\nu - 1} \frac{\partial r}{\partial x}, \quad \frac{\partial e}{\partial \theta} = -p \frac{\partial v}{\partial \theta}, \tag{1}$$

where $u = U / a$ is the velocity; $\theta = t / \tau$ is the time; $r = R / \alpha$ is the Euler co-ordinate; $x = X / \alpha$ is the Lagrangian geometric co-ordinate; $v = \rho_0 / \rho$ is the specific volume; $e = E\rho_0 / P_0$ is the specific internal energy; $p = P / P_0$ is the pressure; and ρ_0 is the initial density of the environment. Making the motion di-

*The article is based on the presentation made at the 2nd International Conference «Mathematical Modelling and Information Technologies in Welding and Related Processes» (Katsiveli, Crimea, Ukraine, 13--17 September, 2004).

mensionless was performed using auxiliary values: $a = (P_0 / \rho_0)^{1/2}$; $\alpha = (W / P_0)^{1/\nu}$; $\tau = \alpha / a$; and $\nu = 1$, 2 and 3 for the flow with plane, cylindrical and spherical symmetry, respectively. Parameter W at $\nu = 3$ is the explosion energy, at $\nu = 2$, W is the explosion energy per unit length, and at $\nu = 1$, W is the same but per unit surface area. The system of equations (1) is closed by setting the equation of state in the form of $e(p, v)$. Naturally, different equations of state are set for the environment and DP. Calculations were made using the Neumann–Richtmyer method with artificial viscosity [1]. With this method, pseudo-viscous pressure q, which is more than zero in compression waves and equal to zero in rarefaction waves, is added to pressure p in equations (1). The use was also made of quadratic viscosity, which is advantageous over the other types of viscosity in that the width of smearing of the front of a shock wave does not depend upon its intensity.

The system of difference equations for numerical computations has the following form:

$$\frac{u_1^n - u_i^{n+1}}{\Delta\theta} = \frac{1}{2}\,(v_{0i-1/2} + v_{0i+1/2}) \times$$

$$\times \left(\frac{r}{x}\right)^{\nu-1} \frac{\delta p_i^n + \delta q_i^n}{x_i - x_{i-1}},$$

$$\frac{r_i^{n+1} - r_i^n}{\Delta\theta} = u_i^{n+1}, \tag{2}$$

$$v_{i+1/2}^{n+1} = v_{0i+1/2}\,\frac{(r_{i+1}^{n+1})^\nu - (r_i^{n+1})^\nu}{x_{i+1}^\nu - x_i^\nu},$$

$$e_{i+1/2}^{n+1} = e_{i+1/2}^n - \left(\frac{p_{i+1/2}^{n+1} + p_{i+1/2}^n}{2} + q_{i+1/2}^{n+1}\right)\times$$

$$\times\,(v_{i+1/2}^{n+1} + v_{i+1/2}^n), \tag{3}$$

$$q_{i+1/2}^{n+1} = \begin{cases} \dfrac{2(b\delta u_{i+1/2}^{n+1})^2}{v_{i+1/2}^n + v_{i+1/2}^n} & \text{if } \delta u_{i+1/2}^{n+1} < 0, \\ 0 \quad \text{if } \delta u_{i+1/2}^{n+1} \ge 0, \end{cases} \tag{4}$$

where $\delta p_i^n = p_{i+1/2}^n - p_{i-1/2}^n$; $\delta q_i^n = q_{i+1/2}^n - q_{i-1/2}^n$; $\delta u_{i+1/2}^{n+1} = u_{i+1}^{n+1} - u_i^{n+1}$; b is the dimensionless coefficient that determines pseudo-viscosity; and $\Delta\theta$ is the time step. The system of difference equations is solved by setting a specific type of the equation of state, $e = e(p, v)$, for the environment and DP.

The method of calculations by the «cross» differences scheme (2) (the second order of accuracy in approximation of differential equations by difference equations) has been applied roughly since 1950. It was verified on many intricate problems with known exact solutions.

The difference mesh for the environment and DP is assumed to be uniform in mass confined in cells between x_{i-1} and x_i. However, the environment and DP are differing in mass interval. The quantity of cells in the DP region remained unchanged in the calculations. For the environment, when the front of the head shock wave reaches a mesh point with some fixed number $m = i_{max}$, the cells are simultaneously doubled. After that the calculation is continued on the mesh with a doubled mass of the environment between the neighbouring points. The mass velocity and thermodynamic parameters of the flow in new cells are re-calculated on the basis of values for the old cells to conserve the mass, internal and kinetic energies. Based on the method described in [2], viscosity factor b' for the environment was changed in the calculation of b according to the following relationship:

$$b = b'\left(1 + \frac{i - k}{m - k}\right), \tag{5}$$

where b' = cost is the unchanged, initially set value of the viscosity factor; $k = (m + m_*) / 2$; and m_* is the quantity of points of the difference scheme for DP. In this case, if $b < b'$, it can be assumed that $b = b'$. This method of setting pseudo-viscosity maintains the width of smearing of the head shock wave front unchanged at a sudden doubling of the co-ordinate step, which eliminates fluctuations of the flow parameters in doubling the cells. 25 mesh points for DP and 350 mesh points for the environment were considered in the calculation of plane explosion. To control the accuracy of counting, the calculations were made with a halved co-ordinate step, and the conservation of the overall energy of the system at all stages of propagation of the shock wave was checked.

The calculations were made using the so called instantaneous detonation scheme that models the process of explosion loading of metal by a sliding detonation wave. With this scheme, pressure, density and other parameters of DP are assumed to be constant over the entire volume they occupy at the initial time moment. Further expansion of DP occurs on the basis of complex wave movements formed during interaction of DP with the environment.

The equation of state of DP was set in the form suggested in study [3]:

$$P = A\rho^n + (k - 1)\rho E \tag{6}$$

with isentropy

$$P = A\rho^n(n - 1) / (n - k) + B\rho^k. \tag{7}$$

According to [4], assume for trotyl that $k = 1.25$. Coefficients A, B and n are determined using the following relationships [3]:

$$P_{*0} = A\rho_0^n + (k - 1)\rho_0 Q = A\rho_0^n(n - 1) / (n - k) + B\rho_0^k,$$

$$P_* = A\rho_*^n(n - 1) / (n - k) + B\rho_*^k,$$

$$k_* = n - B\rho_*^k(n - k) / P_*,$$

where Q, P_*, ρ_* and k_* are the explosion heat, pressure, density and logarithmic slope of isentropy at the Chapman–Jouguet point. For trotyl with density $\rho_0 = 1600$ kg / m^3; the detonation velocity is $D = 6950$ m / s; $k_* = 3$ [5]; $Q = 1030$ kcal / kg [6]; $P_* = \rho_0 D^2 / (k_* + 1) = 1.932\cdot 10^{10}$ Pa; $\rho_* = \rho_0(k_* + 1)k_* =$

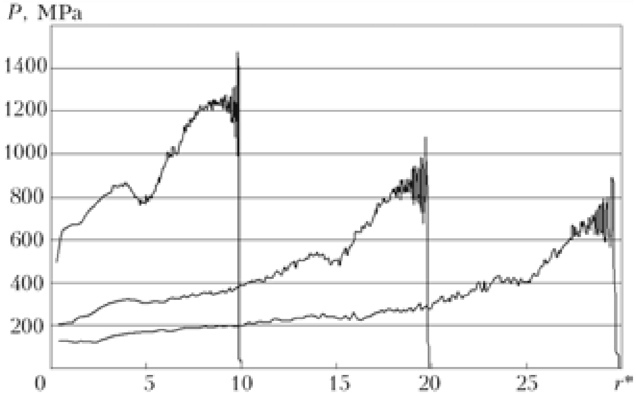

Figure 1. Profiles of pressure in aluminium and DP in the shock wave at different distances from the explosion point

= 2133.3 kg / m^3; A = 0.6622; B = 84560, and n = = 3.1186.

The equations of state for DP in the form of (6) and aluminium in the form of (4) allow the calculation of pressure p and internal energy e from the difference equation of energy (3) without iterations.

To avoid undesirable fluctuations of the parameters behind the wave front caused by quadratic viscosity, it is necessary to smear the front to a width of several steps of the difference mesh on the Lagrangian co-ordinates. Smearing by 3–4 steps is considered optimal. The calculations for aluminium were made at a constant viscosity factor b' determined by the relationship similar to the «classic» relationship for gas:

$$b' = \varphi[(\gamma + 1) / 2]^{0.5}, \quad \varphi = \text{const}, \quad 0.5 \le \varphi \le 2. \qquad (8)$$

To select the value of pseudo-viscosity in DP, the latter were assumed to be a perfect gas with an adiabatic exponent varying in expansion from $n \cong 3.12$ to $k = 1.25$ cm (7). The use of the relationship for gas (8) yields that coefficient b' at $\varphi = 1$ varies within a relatively narrow range of 1.06 to 1.43. As the quantity of cells in DP during the calculations remains unchanged, viscosity factor b is assumed to be constant and equal to a mean value of $b = b' = (1.06 + 1.43) / 2 = = 1.25$. In addition to the selection of viscosity, to perform calculations using explicit difference methods, it is necessary to meet the stability conditions that impose a limitation on a permissible value of the time step. Stability of the explicit difference «cross» scheme used by the authors was investigated for gas in studies [1, 7], and that for the environment with an arbitrary equation of state — in study [8]. The time step for the calculations was selected from the following condition:

$$t = M \min_i \frac{r_{i+1} - r_i}{c_{i+1/2}}, \qquad (9)$$

where r is the Euler co-ordinate; c is the sound velocity; and $M \le 1$ is the Courant number. It was assumed in the calculations that M = 0.2, which provided the calculation stability for aluminium and DP in all cases.

The calculations were made for aluminium (P_0 = = 101325 Pa ≈ 10^5 Pa = 1 bar; c_0 = 5250 m / s; ρ_0 = = 2710 kg / m^3; γ = 4.36) loaded at explosion of trotyl (ρ_0 = 1600 kg / m^3) by the instantaneous detonation scheme for the plane (ν = 1) and cylindrical (ν = 2) flow symmetry.

Figure 1 shows profiles of pressure for aluminium and DP depending upon the dimensionless distance to the cylindrical charge axis equal to $r^* = R / R_0$ (R_0 — radius) at the time moments when the shock wave front reaches distances of 10, 20 and 30 charge thicknesses. Parameter r^* is a similarity parameter for calculations of one-dimensional flows generated by detonation of EM. It can be seen that at a distance equal to about r^* = 30, the amplitude of pressure decreases to 800 MPa, i.e. the dynamic yield stress under explosion loading of aluminium alloys [5]. It is this distance that limits the region where it is possible to induce residual stresses in explosion treatment of aluminium and its alloys using cylindrical charges.

Figure 2 shows profiles of excessive temperature ($t - t_0$) of heating of aluminium in the cylindrical shock wave, depending upon the r^* distance at the time moments when the shock wave front reaches the distances of 10, 20 and 30 charge radii. It can be seen that the maximal heating temperature, which at these distances is not higher than 6 °C, is reached immediately behind the wave front, the initial temperature being t_0 = 15 °C. Further on, while the material in the unloading wave is expanded, adiabatic cooling to excessive temperatures of about 0.5–2.0 °C occurs. This proves the experimentally observed fact of insignificant residual heating of aluminium and its alloys after explosion welding or treatment.

Figure 3 shows profiles of mass velocity for the cylindrical shock wave (for aluminium and DP) at the time moments when its front reaches distances of 10, 20 and 30 charge radii. It can be seen that the mass velocity reaches 50–100 m / s at the shock wave front and increases to 170–270 m / s with a distance to the interface between metal and DP. This phenomenon of increase in the mass velocity is characteristic of spherical and cylindrical shock waves in metals and other hard-to-compress media, and is absent in plane shock waves.

All profiles of pressure, heating temperature, mass velocity and density can be taken from the calculations

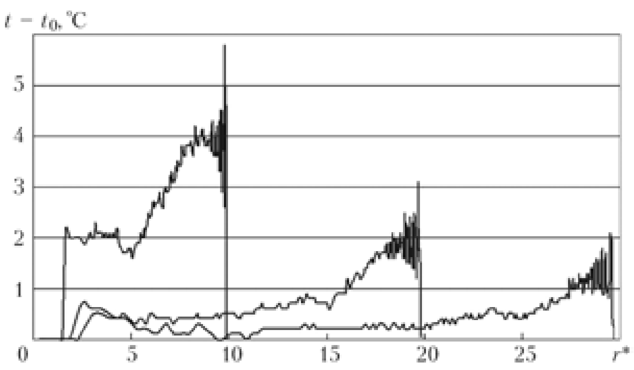

Figure 2. Profiles of excessive temperature ($t - t_0$) in heating of aluminium in the shock wave at different distances from the explosion point

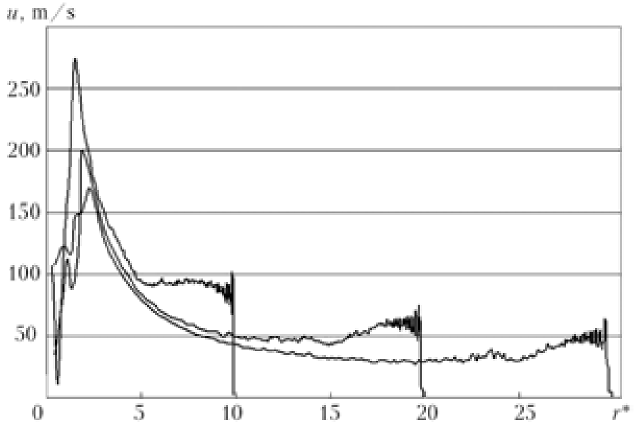

Figure 3. Profiles of mass velocity in the shock wave at different distances from the explosion point

without changes, according to the theory of similarity by parameter r^*. By correctly using the similarity theory for a one-dimensional flow, it is possible to make only one numerical calculation of the effect on environment by explosion of the charge of a certain thickness. At other thickness and other explosion conditions, characteristics of the explosion effect can be determined by corresponding scaling of the results of a single numerical calculation.

Numerical modelling shows that regulation of the shock wave amplitude and pulsed effect on a material can be achieved by varying the initial density of EM, as well as by using different types of interlayers (water, rubber, etc.). The latter makes it possible to produce the required effect on the material using standard EM. Thus, in the case of using EM with a density of 640 kg / m^3, the initial difference of pressure in the shock wave decreases 3 times, and the time of the effect increases. Utilisation of water interlayer between EM and a treated material with thickness of one radius of a cord charge causes a 1.5 times decrease in the intensity of an incident wave. This allows treatment of materials under soft conditions with no damage to the surface. Numerical calculations show that the plastic deformation zone on aluminium alloys in the case of treatment using cord charges is equal to approximately 10–30 charge radii, depending upon the employed pulsed loading scheme.

Increase in the intensity of the shock wave due to the cord charges can be achieved by arranging them in rings. In this case, the growth of parameters converging to the shock wave centre allows a more effective treatment of the central zone. To form the barrier zones to arrest initiation and propagation of cracks, the use can be made of spiral configurations of the charges. In a spiral arrangement of the charges, collisions of the shock wave between turns of a charge induce alternating stress fields in the treatment region, which also hinder propagation of cracks through the treatment region.

Plates of aluminium alloy D16 2 mm thick were used in the experiments. The plates were treated with cord charges arranged in rings, as shown in Figure 4.

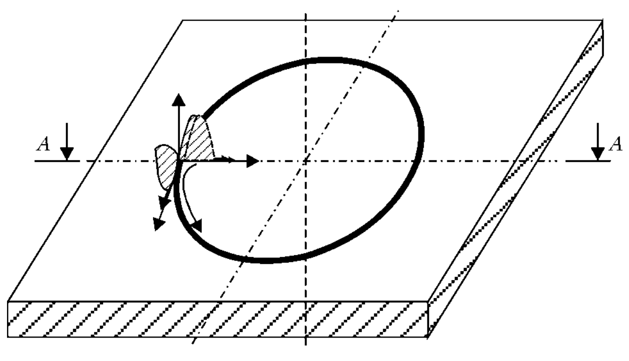

Figure 4. SWT scheme: *1* — plate treated; *2* — direction of mass velocity; *3* — propagation of the shock wave in a material at the beginning of the charge detonation process; *4* — direction of detonation of the cord charge; *5* — ring charge arrangement

Figure 5 shows schematic of propagation of the mass transfer front in a material at the end of the process of detonation of a cord charge in SWT by the ring scheme (see Figure 4). Here ε is the so called eccentricity, i.e. distance from the axis of symmetry of the charge to the point of convergence of two opposite flows of a material, where ε is determined by the following relationship:

$$\varepsilon = \pi d \left(\frac{(90 + \alpha)}{180}\right)\frac{u}{D},$$

where d is the diameter of the ring charge; α is the angle of rotation of the axis, on which convergence of the opposite flows is considered, relative to the point of initiation of the charge; D is the velocity of detonation of the cord charge; and u is the mass transfer velocity.

Figure 6 shows the general view of a sample after treatment with a ring cord charge. The Figure also

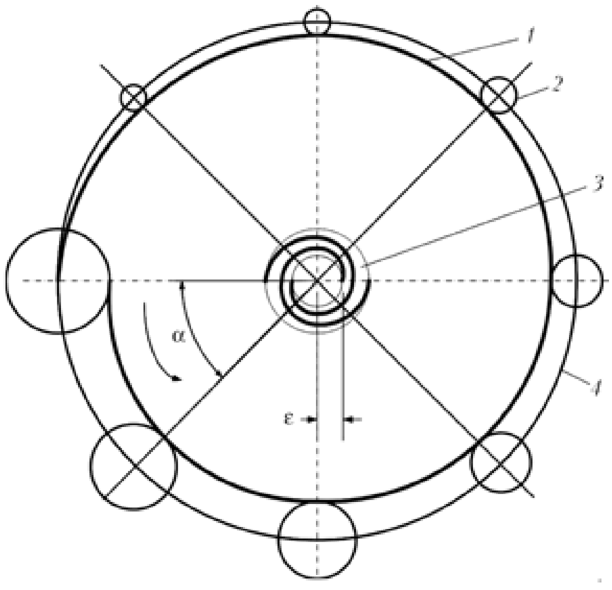

Figure 5. Basic diagram of location of the mass transfer front in a material during SWT: *1* — leading front of mass transfer converging into the zone limited by the charge; *2* — front of mass transfer at specific points of the load applied due to the cord charge; *3* — formation of the compression zone at the points of convergence of the shock waves in a material; *4* — initial position of the ring charge

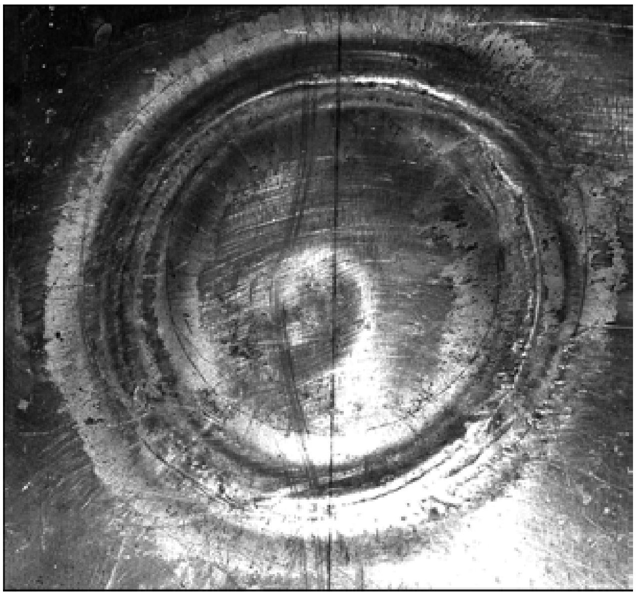

Figure 6. General view of sample after treatment by the ring scheme

shows the deformed central zone shifted with respect to the centre by the value of an order of ε.

As shown by the results of measurement of residual compressive stresses σ_{res} inside the treatment zone, in the case of a ring configuration of the cord charge with a ring diameter varied from 80 to 120 mm, σ_{res} = = 60 MPa at a maximal specific capacity of the charge equal to 33 g / m. In this case, according to the data of study [9], $\sigma_{res} = 0.5\sigma_{0.2}$ required for retardation of a fatigue crack for the material treated.

Application of spiral schemes for arrangement of the cord charges allowed the level of σ_{res} to be increased to 80--95 MPa, the maximal level of σ_{res} being 170--180 MPa at a satisfactory quality of the metal surface.

Procedure for measuring pressure in a shock wave was developed to check adequacy of the numerical method of evaluation of the SW parameters. Measurements are made using special pressure sensors, where the sensing element is a piezo-electret film 28 μm thick and a piezo-module of $8.9\cdot10^{-12}$ C / N, the total thickness of the sensor together with electrodes being not more than 40 μm, which allows the effects of reflection of the wave to be ignored in the measurements. This procedure makes it possible to experimentally evaluate parameters of the SW effect on a material with complex spiral schemes of materials treatment, numerical modelling of which involves much difficulties because of an intricate geometry of the charge. Utilisation of numerical modelling of the SW processes with the developed experimental procedures allows the number of experiments to be substantially reduced, and the technological schemes of SWT of materials to be optimised.

1. Richtmyer, R., Morton, K. (1972) *Difference methods for solving boundary problems*. Moscow: Mir.
2. Higbie, L.C., Plooster, M.N. (1968) Variable pseudo-viscosity in one-dimensional hyperbolic difference schemes. *J. Comput. Phys.*, **3**, 154–156.
3. Kashirsky, A.V., Orlenko, L.P., Okhitin, V.N. (1973) Influence of the equation of state on scatter of detonation products. *Zhurnal Priklad. Mekhaniki i Fiziki*, **2**, 165–170.
4. Baum, F.F., Orlenko, L.P., Stanyukovich, K.P. et al. (1975) *Physics of explosion*. Moscow: Nauka.
5. Baranov, E.G., Kovalenko, V.A., Lyakhov, G.M. (1980) Calculation of parameters of explosive waves in dense media using different detonation schemes. *Zhurnal Priklad. Mekhaniki i Fiziki*, **1**, 133–140.
6. Pepekin, V.I., Makhov, M.N., Lebedev, Yu.A. (1977) Heat of explosive decomposition of individual explosive materials. *Doklady AN SSSR*, 232(**4**), 852–855.
7. Samarsky, A.A., Popov, Yu.P. (1975) *Difference schemes of gas dynamics*. Moscow: Nauka.
8. Kalitkin, N.N. (1978) *Numerical methods*. Moscow: Nauka.
9. Knysh, V.V. (2000) Determination of cyclic life of structure elements in arresting fatigue cracks. *The Paton Welding J.*, **9 / 10**, 69–71.

THE E.O. PATON ELECTRIC WELDING INSTITUTE TECHNOLOGICAL PARK IS 5 YEARS

A.A. MAZUR
E.O. Paton Electric Welding Institute, NASU, Kiev, Ukraine

World experience of innovative activity of technoparks is considered. State support measures, as well as priority areas, goals, objectives, and results of activity of the «E. O. Paton Electric Welding Institute» Technological Park in the period of 2000–2004 are described.

Keywords: innovation activities, world experience, effectiveness, state support, technological parks, PWI, priority directions, targets and tasks, results

Technological parks and technological business-incubators are the main elements of innovation infrastructure with its main task to commercialize the results of scientific research of universities, academic and other research center, whose products are converted into industrial production. Merge of mutual interests of developers and consumers specified a boom of the number of scientific and technological parks. Now we have more than 700 technological parks in the word, most of which are located in USA, Europe, Japan and China, i.e. in most economically significant and dynamically developing regions. State power in these countries understanding the importance of technological parks is introducing a special regime with credit privileges, target financing of special innovation technologies and state procurement of innovation products. With such support from the state technological parks provide not only development of cost-effective businesses but also high-technological products for technological parks and creation of new jobs with stable supply of competitive products of these countries at the world market of products and services.

The Noble prizewinner Prof. Zh. Alfyorov is giving the following example of the state involvement into the financing of innovation activities in Singapore: «Two small applied institutes stuffed with 200 people have the budget of 25 million USD with 90 % of the state budget and only 10 % of contracts with the industry enterprises. I asked them: «You are developing applied projects why is the state financing you? The answer was simple. The industry is paying for what it needs today and the state is paying for what will be needed tomorrow if the state cares for tomorrow needs».

In Ukraine since 1999 eight technological parks were created. Legal framework providing economical interest in the innovation activities was developed. Starting from scratch the Ukrainian technological parks for the period 2000–2004 increased production of innovation products by 1.3 billion UAH a year. In this case not only Ukrainian domestic market is saturated, i.e. it becomes independent on import but also export volumes of high-technological competitive products grow.

Technological Park «E.O. Paton Electric Welding Institute» was created in Ukraine in 1999 as one of the first. The E.O. Paton Electric Welding Institute of the National Academy of Sciences of Ukraine as the world leading center became the scientific ground to accommodate the Technological Park. The research and developments of the Institute in the sphere of welding of materials, surfacing and spraying of protective coatings, special metallurgy, strength and serviceability of welded structures, modern structural and functional materials are well-known in the world. Among achievements of the Institute it is worth mentioning welding of the body of tank T-34, which was the best tank of the Second World War, welding technologies of practically any materials of any thicknesses (from micrometer to meter) under any conditions (from underwater to space). The latest achievement of the Institute is welding of living tissues of human organism.

From the moment of its foundation Prof. Evgeny O. Paton, the founder of the Institute, required from research staff that the developments should meet the urgent needs of domestic economy, be based on modern scientific tools and be widely introduced into the industry. Eventually multisectoral research and technical complex was set up on the basis of the Institute. The complex along with academic institute incorporated design and technological bureau, experimental production, three pilot plants and foreign trade firm. In the 1980s the administration of the Institute reorganized the complex and converted self-sustaining engineering centers into financial self-sufficiency units (a prototype of small and medium businesses).

Therefore, by the moment of creation of the Technological Park the Institute accumulated certain organizational experience, profound scientific potential and powerful production facilities. All this allowed creating not just a «hotel for small business» but a full-scale and effective innovation complex.

Main goal of the PWI Technological Park is to create favorable conditions for organization of research, developments, industrial production and sale of competitive innovation products and services in the sphere of welding and related technologies at the domestic and world markets. Priority activities of the Technological Park are centered on fostering maximal application of advanced achievements in the welding science and technology in the following areas:

• modern energy-effective and resource-saving technologies, equipment and structures;

• special electric metallurgy, metal scrap processing technologies, preparation of metallurgical raw materials, increase of the final metallurgical product quality;

• modern machines, mechanisms and new engineering facilities in rocket-space and aviation sectors, shipbuilding, railway and sea transport;

• soil processing machinery and crop harvesters with increased service life by using welding technologies and hardening of the operating elements;

• welding and related technologies for construction, operation and reconstruction of roads, bridges and transport systems including pipelines;

• rehabilitation of the environment and health improvement of humans by decreasing a technogenous effect of welding production on air, hydro and geoecology, application of welding and related technologies in medicines;

• upgrading of developers and consumers of welding products, development of their innovation culture.

The Technological Park registered 18 innovation projects, 4 of them are completed and 14 are under implementation. Research work and pilot-industrial production of innovation products are incorporated in ten projects. 2.8 ths specialists are involved into implementation of the projects, 1018 new jobs were created. Participants of the Technological Park (project implementers) are permanently increasing production volumes and payments to the budget from innovation and other activities.

Main welding equipment producers that during the last five years produced innovation products for 245.3 million UAH are involved into the Technological Park activities. A number of projects of the Technological Park are aimed at solving important problems in the national economy in line with the identified priorities.

Total sales volume of innovation products by the Technological Park for 2000–2004 amounted to 2.198 billion UAH including imported products for 335 million UAH. Budgets and state target funds received 179.2 million UAH. Financial resources from the special account of the Technological Park were allocated for financing research and technical sphere in the amount of 142.8 million UAH.

The Technological Park «E.O. Paton Electric Welding Institute» is the only technopark in Ukraine whose deductions to the budget and extra-budgetary funds exceed the benefits of a special regime. 93.9 % of finances from special accounts were spent for creation, modernization and reconstruction of scientific-technical and pilot-experimental sites, purchase of scientific and production equipment, i.e. creation of the material base for innovation activities; 5.9 % were used for carrying out research works and R&D activities, preparation of design and technological documents, specifications, patents, purchase of rights for intellectual property objects; 0.2 % were used for organization of conferences, seminars and exhibitions, publication of research and innovation activities results.

State support of innovation projects by reinvesting funds of the special account formed as a result of applying a special regime is about 10 % of all expenditures for implementation of the projects, the rest of funding is provided from own means of the project implementers or investors. However, even such small financing allows solving the problems left untouched for years.

So, implementation of a joint project of the Technological Park and Simferopol Electric Machine-Building Plant SELMA permitted a considerable renewal and broadening of the range of equipment for arc welding widely applied in the industry and construction. In this situation it has become possible not only meeting demand of Ukrainian market in welding equipment but also providing increased export of this equipment abroad. A share of export in the total production volume of the enterprise is 65 %.

The E.O. Paton Electric Welding Institute together with the Engineering Center for Pressure Welding developed technologies and designed new generation machines for electric resistance welding of high-strength railroad rails. Such machines are produced at the Kakhovka Plant for Electric Welding Equipment and are currently applied for construction of high-speed railways and «velvet» ways of metros. By the end of 2005 the project will increase a share of export from 20 to 75 % of the total production volume. The contracts for supply of the newest units for butt welding are concluded with China, Korea, Austria and Russia. Currently the funds of the special account are used for designing of a new generation pipe-welding machine for lying main oil and gas pipelines.

The innovation project of the Zaporozhie Plant for Welding Fluxes and Glasswork is aimed at commercializing and industrial implementation of the duplex-technology for melting welding fluxes developed at the Institute. This will allow producing both conventional well recognized flux grades and new high-quality welding fluxes. They are applied in bridge construction and ship-building and in pipe industry also in the northern areas. Consumption of deficit and expensive import charge components decreased twice. They are replaced by slag wastes of metallurgical plant and pipe welding plants of Ukraine.

Innovation project on preliminary processing of iron ore by the method of dry magnetic separation and magnet-flotation conditioning of the concentrate was launched at the Ingulets Mining and Processing Integrated Works (InGOK). The aim of the project is to implement a set of activities for producing iron ore concentrate with the iron content 69–70 % instead of current 63.7 %. This will solve one of the most important problems of the domestic metallurgy, namely a low quality of the initial raw material and will allow bringing InGOK to the level of ten world leading mining and processing integrated works who work with quality raw materials. Swedish works LCAB (70.8 %) is the world leader, the Lebedinsky GOK in Russia (66 %) occupies the tenth place. Implementation of the project will considerably decrease a technogenous load on the environment, create technical and economical conditions providing stable work of the InGOK in the future also as a city-forming integrated works.

The PWI Technological Park together with Joint Stock Company VESTA-Dnepr works on the developments and creates production of modern energy sources including at the first stage non-maintainable industrial and starter batteries of a new generation for normal and hard working conditions, at the second — autonomous energy systems including power accumulators, solar power systems and wind power mills with power capacity of 10–30 kW. Implementation of the project will meet the demands of remote small capacity power consumers (farms, field camps, mountainous villages, frontier outposts, irrigation systems and others) without switching them to operational power systems and will provide essential energy saving by using renewable energy sources, such as sun and wind.

The E.O. Paton Electric Welding Institute of the NASU as the basic scientific organization of the Technological Park together with the Research and Technical Complex of the Institute received in 2000–2005 financing from the funds of Technological Park the amount of 8.1 million UAH for renovation of its laboratory facilities and development of new projects. Currently a number of innovation projects for which the state cannot allocate money neither now no in the nearest future ar at their preparation stage.

One of the projects is the development of the technology for high-frequency welding of living human tissues by the Institute research workers together with Ukrainian surgeons. Experimental equipment produced at the E.O. Paton Electric Institute received approval from the Ministry of Health Care of Ukraine and is currently being used in some hospitals of Kiev and Donetsk. More than 6 ths patients were operated without any lethal cases or dangerous complications.

In May 2004 the Ukrainian scientists demonstrated in USA possibilities of the welding equipment in surgery to American surgeons and medical industry producers. Demonstration operations received the highest appreciation of the American specialists. J. Kuts, the leading American surgeon, stated that the development of the Ukrainian scientists is the breakthrough into the medicine of the 21st century, which may in 2–3 years produce a revolution in surgery.

The project is based on the works protected by four patents of Ukraine, two patents of the USA and one patent of Australia. The team of authors received in 2004 the National Award of Ukraine. Despite of the achieved results the project is still at its beginning stage. Further improvement of the operations methodology is needed as well as broadening of a range of human organs eligible for welding operations. It is also necessary to improve equipment and tools, create their commercial versions and launch production in the volumes enough to provide export supplies (CIS, China, Korea, Japan, Middle and Far East). Eventually the medical projects of the PWI Technological Park will continue. Now the project on development of the technology and equipment for utilization of medical and other high-toxic wastes by using plasma technology is at its preparation stage.

The E.O. Paton Electric Welding Institute jointly with the department of economical studies carries out a focused search, analysis and processing of the information on activities of techoparks in the world, develops proposals on the use of the world experience in the practice and functioning of the technoparks in Ukraine. Materials on scientific and methodological support of the technoparks activities developed at the Technological Park of the Institute, information of its own and world experience are widely used by other technoparks in their activities and by the state power bodies in improvement of the relevant legal framework. There is a business club that functions under the Technological Park umbrella and allows its members to get together and discuss critical problems. The PWI Technological Park concluded cooperation agreements with National Technical University of Ukraine «KPI» and Kherson University. In compliance with these agreements the Technological Park is providing assistance in creation and organization of activities of technoparks «Kievskaya Politekhnika» and «Tekstil».

The PWI Technological Park whose innovation products amount to 57 % of its total production volume, is the only one of all providing in 2000–2004 an excess of deductions to the budget and target funds over benefits in the amount of 36 million UAH. Not a single kopeck from the budget was spent, high technology products were produced and new jobs were created. Regular audit of financial activity of the Technological Park and the target disbursement of the funds from the special account exposed full compliance to the current legislation. This shows that the current legal framework regulating activities of technological parks on condition of its full observance allows providing such results that any reference to the activities of technological parks as «budget holes» and a sphere of total embezzlements is nothing but an attempt to purposefully discredit the sphere so vitally important for the country.

P.S. The Parliament of Ukraine adopted on January 12, 2006 a new Law of Ukraine on Introducing Changes to the Law of Ukraine «On Special Regime of Investment and Innovation Activities of Technological Parks» that will allow further development of technological parks and increase of their project efficiency.

FLAME SOLDERING FOR JOINING MICROELEMENTS TO PRINTED CIRCUIT BOARDS

S.P. PAVLYUK[1], **G.N. KUTLIN**[1], **V.M. KISLITSYN**[2] and **A.G. MUSIN**[2]
[1]T. Shevchenko Kiev National University, Kiev, Ukraine
[2]E.O. Paton Electric Welding Institute, NASU, Kiev, Ukraine

Described is a new process for joining microcircuit leads to tracks on printed circuit boards. The soldering method is suggested, allowing increase in element packaging density and elimination of operator's mistakes. Results of comparative tensile tests of the joints heated by a hydrogen-oxygen mixture flame and hot gas are given.

Keywords: soldering, printed circuit board, flame heating, hydrogen-oxygen mixture, forced cooling, strength of joints

There is a trend now to an increasing gap between the achieved high density of microcircuit elements in the bulk of silicon chips, measured in nanometres, and relatively low density of packaging of added components (microcircuits, capacitors, connectors and other discrete elements) on printed circuit boards.

Topicality of development of new designs of printed circuit boards and methods for assembly of added components using soldering is determined, on the one hand, by a tendency to miniaturisation of electronic components and, on the other hand, by requirements for making the assembly process less expensive and improving operational reliability of the electronic components.

Resistance heating is one of the promising heating methods for assembly of unpackaged microcircuits directly on printed circuit boards [1]. However, it can be applied for the assembly only by the flip-chip method, i.e. for microcircuits the contact pads of which face the metal wiring of a printed circuit board.

At present, wide acceptance has been received by unpackaged microcircuits with wire leads. For soldering this type of microcircuits, of a certain interest are the results of studies of new heat sources based on silicon single crystals doped by a special method, which, in addition, provide the compression force on the components soldered [2], as well as the laser energy, which in this case is supplied to a lead joined via a flexible light guide [3].

The level of miniaturisation of electronic components can be increased through upgrading existing designs of printed circuit boards, as well as methods for joining added components to a board. Also, this should be accompanied by both reduction of costs of the assembly process and improvement of reliability of finished products.

As these problems can be solved not by any heating method, this study considers the variant of flame soldering of leads of added electronic components to the special design of a printed circuit board.

For this, the authors selected that design of a soldered component (Figure 1) which, in their opinion, could meet requirements of further miniaturisation to the highest possible degree. According to this design, leads *4* of unpackaged integrated circuit *5* are joined by mass soldering to printed circuit board tracks *6*. In gluing the base of an integrated microcircuit to the printed circuit board, its leads in the form of gold wire 0.06 mm in diameter are placed in special slits. During soldering, the leads are pressed to the board tracks by a corrugated shoulder of heater *1* with a force sufficient for insignificant, but assigned deformation, and pressing out of a thin layer of solder from

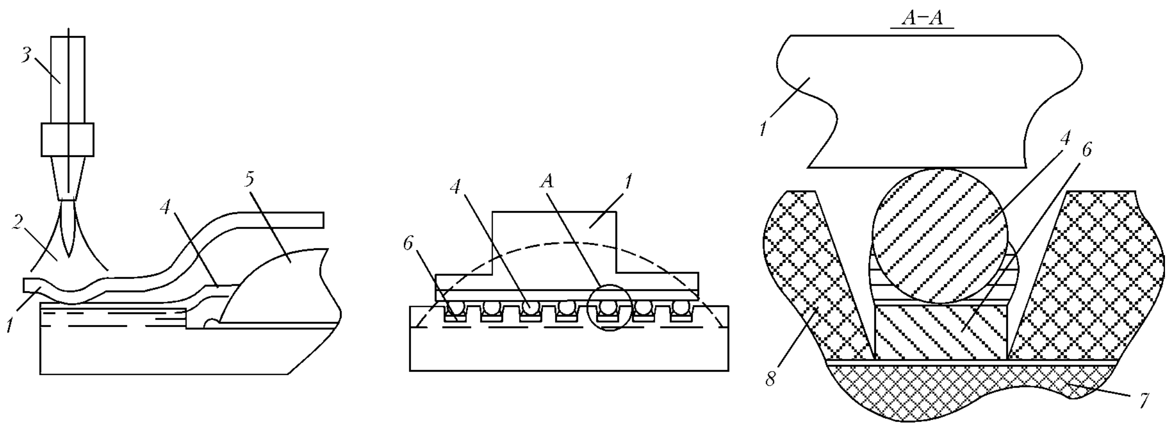

Figure 1. Schematic of soldered component: *1* — heater; *2* — jet of hot gas or hydrogen-oxygen mixture; *3* — nozzle; *4* — microcircuit leads; *5* — unpackaged integrated microcircuit; *6* — track of printed circuit board; *7* — printed circuit board; *8* — mask

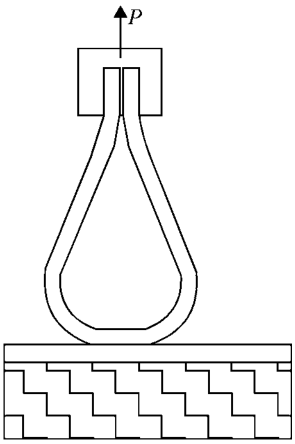

Figure 2. Tensile test diagram: P — applied force

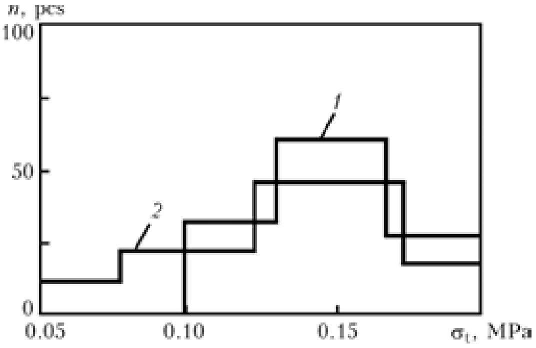

Figure 3. Density of distribution of tensile strength values for soldered joints heated by flame of hydrogen-oxygen mixture (*1*) and hot gas (*2*)

the zone of contact of the lead with the tinned board tracks.

According to this design, printed circuit board *7* consists of a base, on which copper tracks *6* with the contact pads tinned by a solder are deposited according to the electronic circuit layout, and mask *8* glued to it. The mask is made from an electric insulating material with through holes of a rectangular shape located against each of the contact pads of the board. Therefore, each contact pad is immersed into a special slit on the board. This eliminates the probability of mistakes in placing the leads into the slits, which is the case where width of the contact pads is almost equal to diameter of the joined leads (60 μm), and prevents the electric contact between the neighbouring leads of an integrated microcircuit, which is the case where the distance between the tracks is about 60 μm.

The presence of the mask allows realisation of a version of mass soldering of several leads of the unpackaged microcircuit to contact pads of the printed circuit board, avoidance of a mistake in arranging the leads, and reduction of the time of preparation for the soldering process.

Soldering of the above design of the board was performed using two heating methods: with the jet of a hot gas and flame of the hydrogen-oxygen mixture directed to the corrugated shoulder of heater *1*, which acts as a sort of a flame collector and spreader. In both cases, the heater comprises nozzle *3*, from which the hot gas jet or hydrogen-oxygen mixture flame *2* flows out.

Controlled parameters of the soldering process are the force of compression of the leads soldered and temperature of the beginning of melting of the solder preliminarily deposited on the contact pads of the printed circuit board. The beginning of melting of the solder was determined from upsetting of the heater plate, which is an indirect proof of the presence of deformation of the leads joined and pressing out of the solder interlayer from the zone of contact of the leads with the board tracks. Feed of the hot gas or hydrogen-oxygen mixture is automatically switched off by a signal of the upsetting sensor, i.e. heating of the leads joined is stopped, and forced cooling of the soldered joints is started by feeding a jet of a cooling air via the same nozzle.

Each heating method was studied on a batch (120 pcs) of specimens of soldered joints. The quality of soldering was assessed by values of tensile strength of a soldered joint. Considering the special design of a soldered joint that does not correspond to requirements of the test standards in force, the authors used a tensile test diagram shown in Figure 2. According to this diagram, two ends of a soldered lead are simultaneously fixed in clamping jaws of the tensile test machine, this bringing the tests closer to actual service conditions.

Length of the joining zone in the majority of specimens soldered by heating with a hot gas or hydrogen-oxygen mixture flame was not in excess, as a rule, of width of the corrugated shoulder of the heater, and its width was equal to that of the preliminarily tinned contact pad.

Examinations of fracture regions of the soldered specimens revealed a relationship between strength of the joints and thickness of the solder interlayer located between a lead and board track, the specimens that fractured at a higher load having a thinner solder interlayer within the joining zone.

Intensive heating and forced cooling, which is the case of heating with the hydrogen-oxygen mixture flame, provide a more complete pressing out of solder from the lead to board track contact zone.

Dependence of tensile strength of the soldered joints made using both heating methods upon their quantity n is shown in Figure 3.

Location of the lead to track contact zone in a slit of the mask glued to the printed circuit board eliminates the probability of contact of the pressed out solder with the neighbouring tracks and, therefore, prevents the undesirable electric contact between them. Tensile strength of some specimens of the soldered joints is 0.2 MPa, which is 10–15 % higher than that of the tin-lead solder, this proving formation of the soldered bonds.

CONCLUSIONS

1. The method of soldering with pressing out of a major part of the solder from the zone of contact between the joined components at a temperature close

to that of melting of the solder, followed by forced cooling, provides a 10–20 % increase in strength of the soldered joints, compared with the joints made without forced cooling.

2. More intensive heating of the components being soldered, provided by the hydrogen-oxygen mixture flame, compared with heating with a hot gas, and rapid cooling of the joining zone to a temperature of solidification of the solder allow improvement in the quality of soldering and a 30–50 % increase in the process productivity.

3. New design of a printed circuit board, which is made slightly more complicated due to gluing the mask with slits against the contact pads, provides a substantial increase in packaging density and eliminates the probability of reject, which may be formed in short circuiting of the leads to each other or to contact pads because of displacement of the leads caused by operator's mistakes.

1. Kislitsyn, V.M. (1987) *Technology of resistance soldering of silicon diodes*. Syn. of Thesis for Cand. of Techn. Sci. Degree. Kiev.
2. Pavlyuk, S.P., Rossoshinsky, A.A., Kislitsyn, V.M. et al. (1999) Application of silicon as heating element of microsoldering tools. *Avtomatich. Svarka*, **2**, 41–44.
3. Azdasht, G., Zakel, E., Reichl, H. (1996) Implementation of low power diode laser for soldering by FPS method. *Soldering and Surface Mount Technology*, **22**, 51–54.

FEATURES OF WELDING PRODUCTS WITH PROTECTIVE ENAMEL COATINGS

A.M. SAVITSKY, V.N. VASHCHENKO and **I.V. BOBROV**
E.O. Paton Electric Welding Institute, NASU, Kiev, Ukraine

Considered are the main problems arising in arc welding of parts with a protective enamel coating on their inside surface. It is shown that enamel can resist the short-time (up to 3–5 s) high-temperature effect right up to the melting temperatures of steel. This short-time soaking of metal of a welded joint at the above temperatures can be provided by pulsed-arc welding.

K e y w o r d s : pulsed-arc welding, enameled products, coating, welded joint, pulsed thermal cycle of welding, heating and cooling conditions, enamel vitrification

The problem of corrosion protection of products operating in media of various degrees of aggressivity is currently being solved by development and introduction into production of various protective coatings (polymer, lacquer-paint, epoxy, etc.).

Vitreous enamels are quite promising protective coatings. Application of the latter for protection of the inner surfaces of pipes in heat-and-power engineering and petroleum processing industry, as well as chemical engineering products, extends their service life by 4 to 5 times.

In case of enameling of products after welding, its implementation does not run into any problems. However, if it is impossible to perform product enameling after welding, as in welding of butt joints of pipelines, for instance, of a small diameter, or closing welds of shell structures without free excess to the inner surface, welding has to be performed over a layer of pre-deposited enamel. This runs into a number of problems, which are due to a comparatively low heat stability of enamel, which is limited by temperatures of 800 to 900 °C. Temperature rising above 900 °C leads to enamel burning out, whereas below 800° C no vitrification of the enamel layer is achieved, as the enamel is only partially sintered. It forms cracks and gas bubbles, which later leads to its complete or partial fracture, and violation of the item anticorrosion protection. Such a narrow temperature interval of vitrification essentially limits the application of vitreous enamels for welded joint protection. As in full penetration welding the reverse side of the joint is heated up to temperatures close to that of metal melting, and temperatures either equal to or exceeding it are achieved in the weld, the enamel burns out in this area.

Several techniques are currently used to solve the problem of welding butt joints of enameled pipes, which are based on application of the lock welded joints with incomplete penetration of the edges, use of special forming devices; prior deposition of corrosion-resistant materials on the edges. Also transition inserts from corrosion-resistant materials are used, which are first welded to the pipe edges. All these methods are described in detail and analyzed in [1]. They are quite reliable, but not without drawbacks (rather high cost and labour consumption). In addition, some of them lower the welded joint performance. Therefore, more promising is the method based on a preliminary deposition of a cladding layer on the pipe inner side in the butt joint area [1].

Analysis of the modern approaches to solving the problem of welding enameled products is indicative of the fact that most of them require rather complex and labour-consuming preliminary preparation of pipe edges for welding. Therefore, the objective of this work was finding the possibility of welding enameled products over the enamel layer without any special preliminary preparation of the edges being welded or application of any special forming devices. As standard heat treatment of the enamel envisages its heating up to 800–900 °C and soaking at these temperatures for a certain time, it was necessary to determine its ability to stand higher-temperature impact, close to the steel melting temperature. With this purpose, samples with the applied and dried up enamel were heated up to temperatures of 800–1500 °C. Duration of soaking up to the start of the enamel vitrification or its combustion was recorded.

Temperature-time dependences given in Figure 1 are indicative of the fact that the enamel resistance decreases at temperature increase. For instance, at heating up to 900 °C, enamel vitrification takes 4 min, at heating up to 1200 °C enamel vitrification takes place 45 s after heating, and it burns after 50 s. The time interval of enamel vitrification is 5 s. At heating up to temperatures, close to that of steel melting, enamel can stand a thermal impact for 3 to 4 s without burning.

Therefore, in welding of enameled products, it is necessary to seek such a welding process, in which it is possible to accurately enough adjust the conditions of the welded joint heating and cooling, limiting the duration of metal staying in the temperature range above 1000 °C to seconds. Duration of contact of protective enamel with liquid metal of the weld pool should not exceed 2 to 3 s.

With the traditional processes of welding with a constant power arc, it is extremely difficult to implement such stringent conditions of heating and cooling. Welding should be performed at such low values of the heat input, that producing sound welded joints becomes problematic, because of lacks-of-penetration or lacks-of-fusion, but even that does not provide a solution of the problem. Enamel either burns, or is partially sintered with formation of cracks and gas bubbles, which is accompanied by its subsequent destruction.

Acceptable thermal conditions in the welded joint without impairing its quality can be provided by using pulsed thermal cycles of the type of those given in [2]. Such or similar conditions of heating and cooling can be provided by pulsed-arc welding [2, 3], welding with a constant power arc with electrode oscillations [4], and welding by multilayer welds [5].

Results of comparison of various welding processes showed that automatic step pulsed-arc welding offers the broadest capabilities for controlling the conditions of welded joint heating and cooling. A feature of this welding process is periodical variation of the arc thermal power. In view of that, and due to adjustment of the duration of pulses, pauses and welding speed, this process ensures the possibility of formation of a whole range of thermal cycles [2] in the welded joint. Depending on a combination of mode parameters in the welded joint, traditional thermal cycles similar to the one given in Figure 2, *a*, cycles with low rates of heating and cooling, as well as cycles with a long duration of welded joint metal soaking in the region

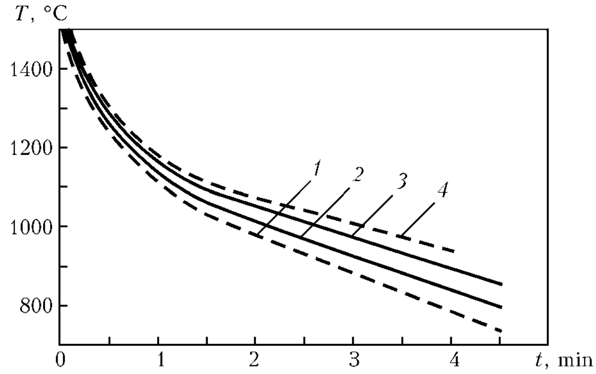

Figure 1. Thermal characteristics of vitrified enamel: *1* — sintering; *2, 3* — vitrification; *4* — burning

of high temperatures, can be formed. With such thermal cycles the enamel coating under the weld and in the adjacent regions burns out completely.

At a respective combination of the mode parameters, pulsed thermal cycles can form in the welded joint with a sufficiently large number of periods of heating and cooling and high requirements to temperature change [2]. Such cycles ensure a compara-

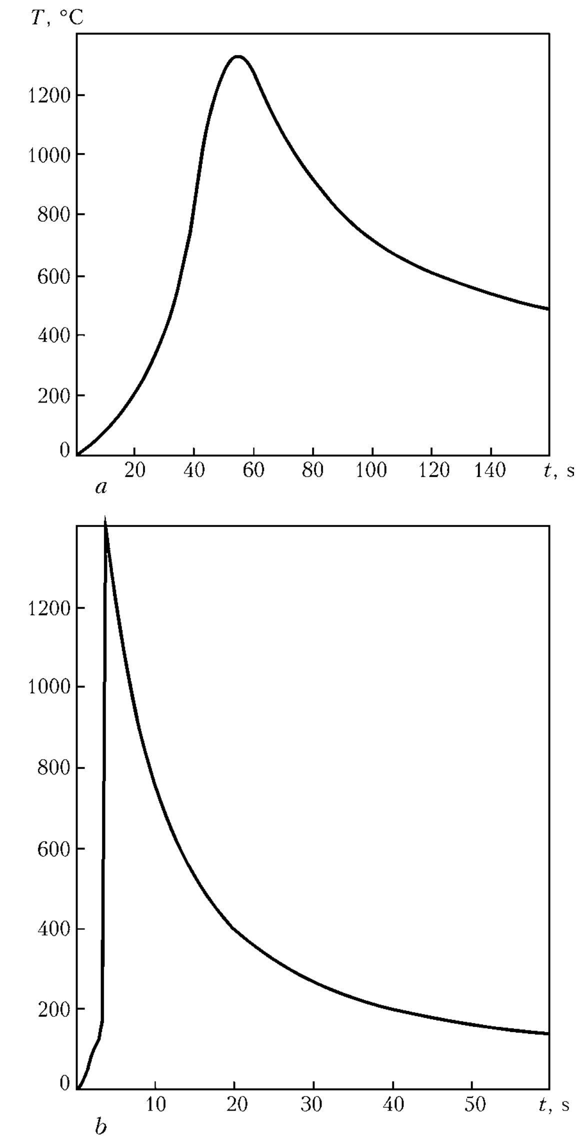

Figure 2. Thermal cycles in pulsed-arc welding [2]: *a* — traditional low-speed; *b* — high-speed

Figure 3. Butt joint of enameled pipes made by pulsed-arc welding over a layer of enamel

tively small total duration of the welded joint metal soaking at temperatures above 1000 °C. Depending on the number of heating and cooling periods, as well as a combination of welding mode parameters, it may be reduced to 2 to 5 s.

Results of experiments performed on flat samples 3 to 5 mm thick and pipe samples of 57 to 325 mm diameter with 4 to 10 mm wall thickness showed that the selected welding process ensures a guaranteed vitrification of the enamel under the weld and its fusion with the protective layer applied and vitirified earlier. As a result, a thin enamel layer without defects or cracks forms on the product inner surface (Figure 3).

Welding of flat samples was performed in the downhand position, that of pipe samples in different positions in space with sample rotation to simulate the conditions of welding the position butt joint. Thermal power of the arc was equal to 1.9 to 4.8 kW, depending on metal thickness or root face. In case of welding samples with more than 4 mm edge thickness, it is rational to apply edge preparation with the groove angle of 60°. Enamel with layer thickness of up to 0.5–1.0 mm was applied onto the butt edges before welding, and dried at the temperature of not more than 80 °C to avoid porosity. Welding was performed on samples from St.3, 10, 20, and 09G2S steels. Welds were made without applying any forming backing.

Pulsed-arc welding allows forming thermal cycles in the welded joint similar to those given in Figure 2, *b*. They have a traditional shape, but differ by high heating and cooling rates. Duration of metal soaking in the region of temperatures above 1000 °C can be limited to several seconds. At such welding thermal cycles, however, no guaranteed vitrification of the enamel along the butt length is provided. The enamel layer, which is partially sintered, but not vitrified, forms cracks and bubbles. This layer does not completely fuse with the earlier deposited and vitrified enamel. Such a low-quality treatment of the enamel under the weld, leads to its premature fracture.

Thus, investigation results show that for a guaranteed vitrification of the enamel and its reliable fusion with the earlier deposited and vitrified layer, it is necessary to ensure the heating and cooling conditions, corresponding to pulsed thermal cycles of the type of those given in [2]. In this case the duration of the high-temperature impact on the enamel under the weld is sufficient for its vitrification and fusion with the earlier deposited one, but is insufficient for enamel burning.

As shown by the results of the conducted studies, application of pulsed-arc welding is the most rational approach to create such conditions of heating and cooling in the welded joint. Among all arc welding processes, this method opens up the widest possibilities in terms of adjustment of the thermal condition of the welded joint, irrespective of the thickness of the metal being welded.

CONCLUSIONS

1. Quality of the layer of protective enamel under the welded joints is determined by the conditions of its heating and cooling.

2. Thermal condition of the welded joint in welding with a constant power arc does not provide a guaranteed vitrification of the enamel under the weld, or its reliable fusion with the protective layer earlier deposited on the item and vitirified. The enamel either burns, or is partially sintered with formation of cracks and gas bubbles, which is accompanied by subsequent fracture of the sintered layer.

3. Pulsed-arc welding provides the conditions of heating and cooling in the welded joints, under which the enamel under the weld is vitrified and fused with that earlier deposited on the product and vitrified, but it does not burn.

1. But, V.S. (2003) Arc welding of pipes with inner protective coating. *Svarshchik*, **2**, 8–11.
2. Dudko, D.A., Savitsky, A.M., Savitsky, M.M. et al. (1998) Specifics of thermal processes in welding with thermocycling. *Avtomatich. Svarka*, **4**, 8–12.
3. Vagner, F.A. (1980) Thermocycling in tungsten electrode welding. *Svarochn. Proizvodstvo*, **2**, 4–6.
4. Makara, A.M., Mosendz, M.A. (1976) *Welding of high-strength steels*. Kiev: Tekhnika.
5. Prokhorov, N.N. (1976) *Physical processes in metals during welding*. Moscow: Metallurgiya

EXTENSION OF SERVICE LIFE OF A PIPELINE WITH DEFECTS ON THE INNER SURFACE

P.S. YUKHIMETS[1], **S.V. KOBELSKY**[2], **V.I. KRAVCHENKO**[2], **I.A. KLIMENKO**[2] and **V.P. LESOVETS**[3]
[1]E.O. Paton Electric Welding Institute, NASU, Kiev, Ukraine
[2]G.S. Pisarenko Institute for Problems of Strength, NASU, Kiev, Ukraine
[3]Company «Naftogas Ukraini», Kiev, Ukraine

The stressed state of a pipeline with volume defects on the inner surface of a pipe was analyzed in terms of different variants of repair operations aimed at extension of remaining life of the pipeline. It is shown that the use of two bands located symmetrically relative to a defect at a distance of the double defect length allows a substantial decrease in stress concentration factor and increase in the remaining life of the pipeline, with the possibility of post-repair monitoring of the defective region.

Keywords: pipeline, corrosion damage, repair, extension of service life, band

Pitting (bulk surface) defects resulting from corrosion or erosion-corrosion processes (Figure 1) are widely spread kinds of damage in pipelines with a long operating life. Influence of a defect on the static and cyclic strength is assessed on the basis of evaluation of the defect geometrical parameters by direct measurement (external) and by NDT means (inner surface) [1, 2].

Performed calculations may show that the pipeline residual life is insufficient. In such a situation a decision is taken on performing repair by welding-in the so-called «shell», i.e. a pipe section instead of the removed defective one, or lowering the working pressure down to the respective value (based on the conditions of provision of the residual life).

The above methods of extension of the pipeline service life may turn out to be inacceptable because of the requirement of continuity of the technological cycle or stability of the mode of product pumping. Recently a number of fundamental developments were performed on an alternative repair method, namely welding up individual corrosion defects on the outer surface of the pipe wall section without shutting the pipeline down [3, 4].

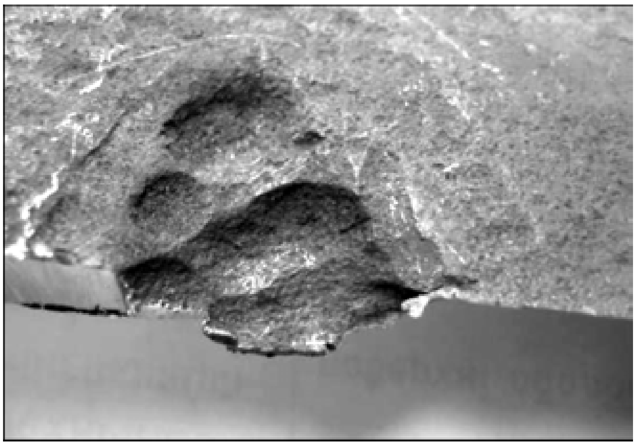

Figure 1. Outer surface of the pipe with crevice damage (sample is cut out of Dn 273 × 8 pipe)

This paper presents analysis of the stressed state of a pipeline with a bulk defect on the inner surface, in order to develop measures for performance of repair work, aimed at extension of the pipeline residual life without shutting it down.

Cyclic deformation range (stress concentration factor (SCF)) calculated in the defect zone by finite element method (FEM) was selected as the determinant factor influencing the cyclic strength.

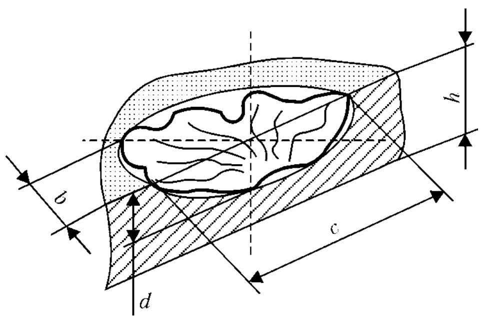

Figure 2. Schematic of a surface defect simulated by half of ellipsoid: c — length; b — width; d — depth of defect; h — pipe wall thickness

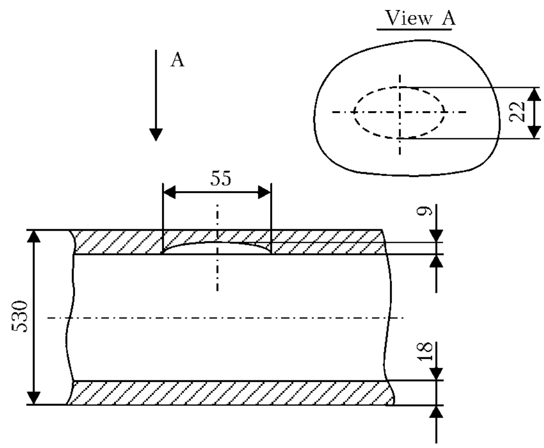

Figure 3. Schematic of a pipe with a defect on the inner surface

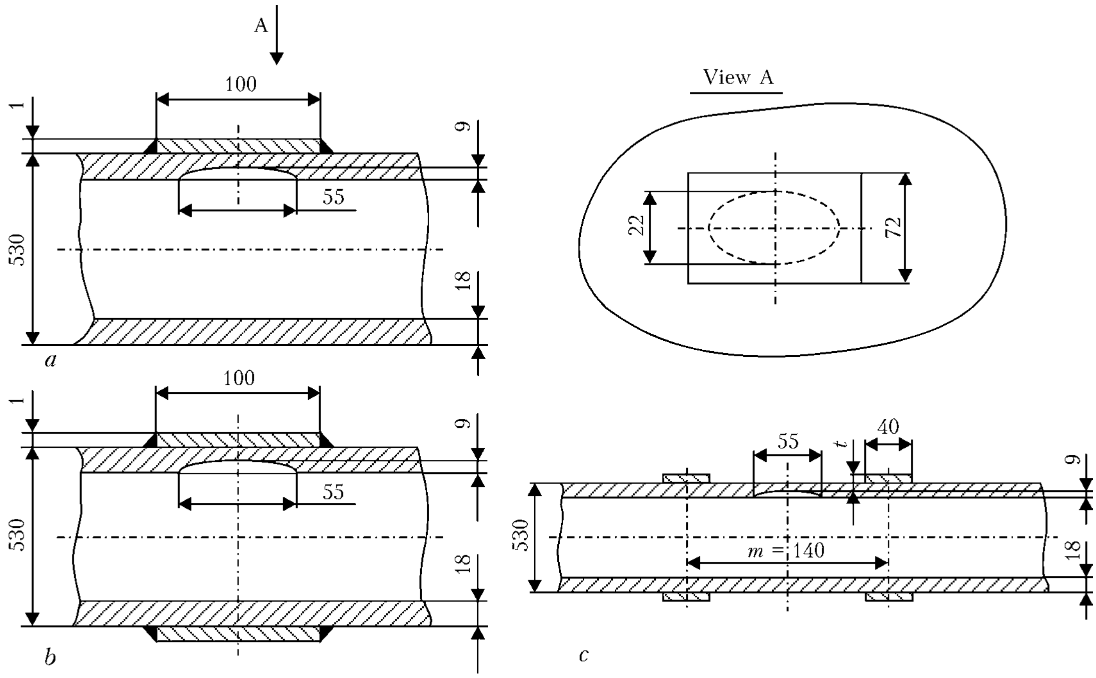

Figure 4. Schematics of variants of pipelines with crevice defects: *a* — pipe with welded-on coverplate; *b* — with a band; *c* — with a double band

Calculations were performed using SPACE software designed for FEM simulation of a three-dimensional thermal and stress-strain state of structural elements, developed and successfully applied at G.S. Pisarenko Institute for Problems of Strength of NASU. Software for finite element analysis is based on a mixed FEM schematic, providing a stable numerical solution and high accuracy of obtaining results both for displacements and for stresses and strains [5, 6]. This circumstance is extremely important for solving the problems of residual life design, as these are exactly strains and stresses that should be determined with maximum accuracy.

Software includes an open-ended library of parametrized models of typical pipeline elements, including different types of tee joints (of equivalent and non-equivalent opening, cylindrical and conical), tapers, branch-pipes, flange joints, pipe fragments with a corrosion defect on the inner or outer surface [7].

Half of an ellipsoid, where the axes of symmetry are the largest defect dimensions in the axial, circumferential and radial directions (Figure 2), was used as the geometrical model of the considered surface defects of the pipelines. Testing of the effectiveness of different variants of pipeline repair was based on calculations of the stressed state of Dn 530×18 pipe with a

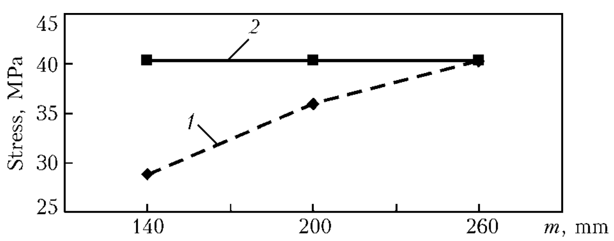

Figure 5. Influence of band spacings on maximum stresses in the defect zone (t = 18 mm; ΔP = 1 MPa): *1, 2* — pipe with a band and without it, respectively

semi-elliptical defect on the inner surface (Figure 3). The following repair variants were considered (Figure 4):

- welding of a coverplate to the pipe outer surface, which is located above the defect (Figure 4, *a*);
- mounting / welding a metal band, covering the defect (Figure 4, *b*);
- mounting / welding two bands located symmetrically relative to the defect (Figure 4, *c*).

As follows from the above data (Table), the most effective method to lower the stress concentration (increase the residual life) at the same thickness of the fastening element is overlapping the defect zone by a circular band (variant 2). When mounting a band of the thickness equal to 1.5 of the pipe wall, the level of stress concentration in the defect zone drops 2 times.

Methods to improve the residual life of pipelines

No.	Repair variant	Thickness of strengthening elements t, mm	SCF in defect zone	Admissible cycle number $[N]^*$ at ΔP = 20 MPa
1	Cover plate	9	3.11	14610
		18	2.90	20880
		27	2.65	34310
2	Band	9	2.29	87210
		18	1.85	666000
		27	1.63	$> 1 \cdot 10^6$
3	Double band (m = 140 mm)	9	2.59	39230
		18	2.34	74940
		27	2.10	171900
4	Without fixing element	–	3.26	11610

*Calculation was performed for a low-carbon steel pipe.

Strengthening the defect area by welding-on a cover-plate is the least effective. Mounting of two bands located symmetrically relative to the defect (variant 3) at a distance of approximately 2c between the inner edges (two defect lengths) also allows achieving a considerable lowering of SCF. In this case, its dropping to the same level as in the case of one band (variant 2) is achieved with a doubled thickness of the bands. Band spacing m has a marked influence on stress concentration (Figure 5). At m = 300 mm the positive influence of the design measures is lost completely.

Mounting double bands having the thickness equal to that of the pipe wall, under the conditions of a cyclic impact of pulsed inner pressure ΔP = 20 MPa increases the admissible number of cycles by approximately 6 times.

Thus, comparison of the considered repair variants is indicative of the fact that one of the measures to extend the life of a pipeline with crevice type defects on the inner surface can be defect strengthening using two bands located symmetrically relative to the defect at the distance of a double length of the defect. Despite the fact that this method is somewhat inferior to that of welding-on a band covering the defect, in terms of effectiveness of SCF lowering in the defect zone, and has the highest material content, it still allows tracing the dynamics of the change of geometrical parameters of the defect in post-repair period.

1. Garf, E.F., Netrebsky, M.A. et al. (1999) Strength of pipelines with erosion-corrosion damages. *Tekhn. Diagnostika i Nerazrush. Kontrol*, **1**, 44–49.
2. Yukhimets, P.S., Garf, E.F., Nekhotyashchy, V.A. (2005) Experimental substantiation of method for calculation of residual life of pipelines with corrosion damages. *The Paton Welding J.*, **11**, 11–15.
3. (1999) *API Standard 1104:* Welding of pipelines and related facilities. Appendix 13. Service welding. API.
4. Makhnenko, V.I., But, V.S., Velikoivanenko, E.A. et al. (2001) Mathematical modelling of pitting defects in active oil and gas pipelines and development of a numerical method for estimation of permissible parameters of arc welding repair of defects. *The Paton Welding J.*, **11**, 2–9.
5. Bojko, V.B., Voroshko, P.P., Kobelsky, S.V. (1991) Modelling of three-dimensional thermal and stress-strain state of elastic bodies using the mixed variant formulations of FEM. Inf. 1. *Problemy Prochnosti*, **2**, 72–77.
6. Chirkov, A.Yu. (2003) *Mixed schematic of finite element method for solution of boundary problems of elasticity theory and low elastic-plastic strains*. Kiev: G.S. Pisarenko IPP.
7. Kobelsky, S.V., Kravchenko, V.I., Lisovers, V.P. (2004) Special software for calculation of strength of pipeline parts in oil-and-gas industry. *Naft. i Gazova Promyslovist*, **1**, 52–54.

ALGORITHM OF AUTOMATIC ORIENTATION OF MANIPULATION ROBOT RELATIVE TO TESTED SURFACES

G.A. TSYBULKIN
E.O. Paton Electric Welding Institute, NASU, Kiev, Ukraine

Suggested is the algorithm for ensuring orientation of the manipulation robot normal to the test surface under the conditions of ambiguity of its position in the robot work space. The algorithm was synthesized as a result of solution of the problem of minimizing the functionals that characterize the current distance from some virtual plane to the test surface at movement of the robot along the set paths.

Keywords: robotization of welding processes, measurements, algorithm, automatic orientation

Robotization of the processes of building-up the worn parts or thermal straightening of deformed sheet structures runs into a number of problems, associated with the need to preliminarily (and during running of the processes) determine the geometrical parameters of the processed part surfaces. Sometimes, measurement of deformations just in the characteristic points of these surfaces is sufficient. One of the algorithms of localization of such points and determination of deformations in them using manipulation robots is proposed in [1], and is implemented in practice in development of an automated complex for thermal straightening described in [2].

In [1] it was assumed that the measuring device (MD) with which the robot is fitted, is oriented beforehand normal to the so-called level planes [3], characterizing the relief of the tested surface. Questions related to the actual procedure of MD orientation were not considered in [1]. On the other hand, if the above surface is randomly located in the robot working space, namely so that the above level planes were not necessarily parallel to one of the coordinate planes of the robot co-ordinate system, the process of MD orientation becomes much more complicated in this case. This is attributable to the fact that orientation is usually performed by teaching the robot. A sequence of MD purpose-oriented motions is performed in the manual mode with simultaneous measurement of its position relative to the normal to the tested surface by some method. Recording of angular coordinates in the memory of the robot control system is performed only after MD longitudinal axis is combined with the above normal.

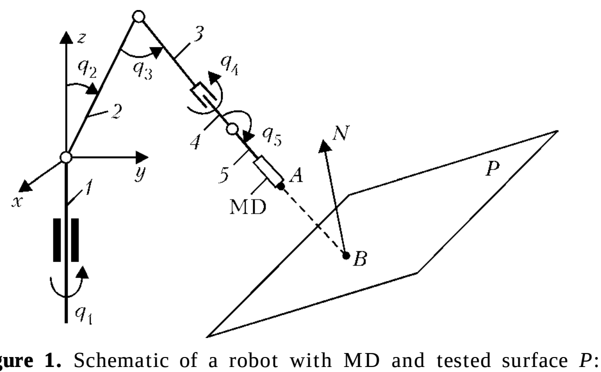

Figure 1. Schematic of a robot with MD and tested surface P: *1–5* — here and furtheron are link numbers; for other designations see the text

It is obvious that such a method of orientation has several drawbacks. In particular, robot teaching time is quite extensive (being commensurate sometimes with that of performance of the main technological operations), while orientation accuracy is low and depends on the operator experience and qualifications. As a result the accuracy of subsequent measurement of the relief of the tested surfaces can turn out to be inadmissibly low.

In this connection, it appears to be quite urgent to solve the problem of automation of the actual process of MD orientation relative to the surfaces being tested. However, as far as we know from publications [4–8], progress in this area is quite negligible so far.

This work presents one of the automatic orientation algorithms, ensuring the specified accuracy of orientation under the conditions of indeterminate position of the tested surface and essentially simplifying the procedure of manipulation robot training. The algorithm is synthesized as a result of solving the problem of minimizing the functionals, characterizing the current distance from a certain assigned virtual plane to the tested surface at motion of the measuring device along pre-set trajectories.

Problem definition. Let us consider the classical (anthropomorphous) kinematic diagram of a manipulation robot (Figure 1). According to this diagram, the robot is a five-link mechanism, connected by rotational joints. Cartesian coordinate system $0xyz$ is used as the basic system of robot coordinates. Relative position of the links is determined by angular coordinates q_i ($i = 1, ..., 5$). The last (fifth) link is connected to MD designed for determination of distance D from point A to surface P along MD axial line. MD longitudinal axis coincides with this axial line.

Flat surface P is located in the robot working space. Its position relative to the basic coordinate system of the robot is unknown, and, therefore, orientation of MD longitudinal axis (section AB in Figure 1) relative to the above surface is not determined. It is only possible to measure distance D using MD. According to Figure 1, point A is located on MD end face, point B is on surface P, N is the normal to plane P.

Let us define the problem of automation of the process of MD orientation as follows: it is required to synthesize such an algorithm of variation of angular coordinates q_i, which based on current information on distance D would provide automatic orientation of longitudinal axis MD along a normal to surface P.

Synthesis of orientation algorithm. At first glance it may seem that this robotic problem is unsolvable, because of deficit of information on the position of the surface in the robot system of co-ordinates. However, at closer consideration it turned out that if a certain technique is used, which provides the lacking information, the problem becomes quite solvable.

The essence of one of such techniques consists in the following. Let a certain position (configuration) of the manipulation robot with a rough orientation of measuring device MD be fixed relative to a plane, for instance, the one shown in Figure 1. In addition, let condition $q_5 = \pi - \Delta q_5$ be satisfied, where Δq_5 is a quite small increment of angular coordinate q_5. Now, if MD is brought into motion by changing just one angular coordinate q_4, then point A will move around a circumference, located in a certain virtual plane W, orthogonal relative to longitudinal axis of link *4*, and image point B in this case will circumscribe an ellipse in plane P (Figure 2). Axis UV of this ellipse is normal to the line of crossing of planes W and P. It is obvious that only when the image point is in one of the ellipse vertices U or V, UV line and axial lines of links *4* and *5* are in the same plane normal to plane P (Figure 3). Therefore, if now we were to move image point B along line UV, for instance, from point U towards point V by varying angular coordinate q_5 with the rest of the co-ordinates «frozen», then in point B_* axial line AB will be combined with normal N to plane P.

Thus, to get a final solution of the problem, points U and B_* have to be localized. For this purpose let us use MD. As in the general case planes W and P are non-parallel, distance D (equal to section AB) will change at motion of point B around an ellipse (see Figure 2), and become minimum in point U. According to [9], coordinates of this point can be determined from the following relationship:

$$q_4^U = \underset{0 \le q_4 \le 2\pi}{\arg\min} \; D[q_i(t)], \tag{1}$$

where q_4^U is the as yet unknown angular coordinate of point U; $D[q_i(t)]$ is the functional characterizing distance D, depending on coordinates q_i. Coordinate of point B_* (see Figure 3) can be found from a similar relationship:

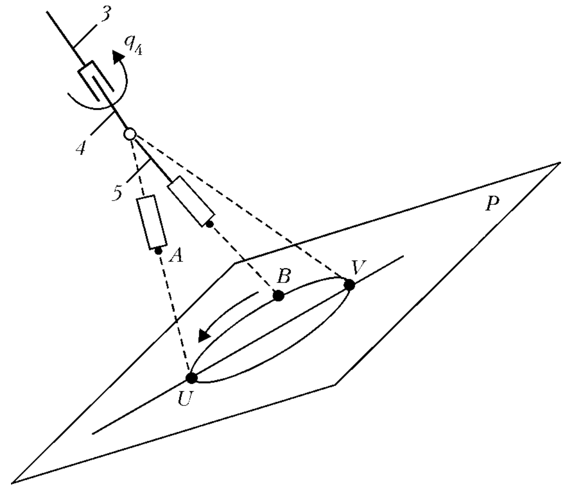

Figure 2. Schematic of motion of image point B along an ellipse at change of angular coordinate q_4

$$q_5^{B_*} = \underset{q_{l5} \le q_5 \le q_{u5}}{\arg\min} \; D[q_i(t)], \tag{2}$$

where q_{l5} and q_{u5} are the lower and upper limits of the magnitudes of angle q_5 assigned earlier when solving a specific problem.

So, algorithm of MD orientation relative to the tested surface P functions as follows. First in the teaching mode MD is mounted near tested surface P at the required distance and it is rather roughly oriented along a normal to this surface. Then a program is run, ensuring step-by-step (point-by-point) motion of MD around a circumference above surface P by changing coordinate q_4 with other coordinates «frozen». Distance D is measured in each local point, and the following condition is verified:

$$D_k - D_{k-1} < 0, \tag{3}$$

where $k = 1, 2, \ldots$ is the number of the local point. The program is performed until condition (3) is disturbed, i.e. until image point B coincides with point U (see Figure 2).

After that a similar program is started, which also performs point-by-point MD motion, but now along

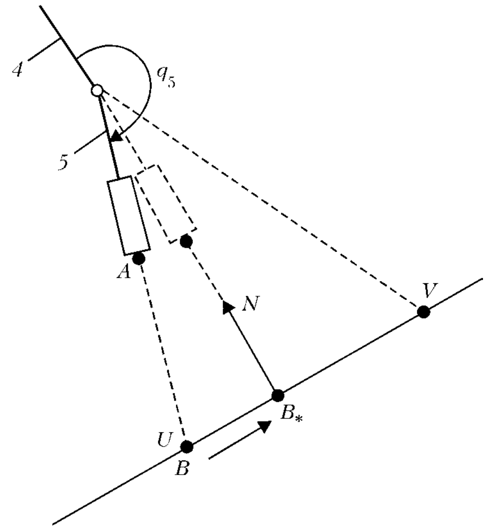

Figure 3. Schematic of motion of image point B along line UV at change of angular coordinate q_5

UV line by varying angular coordinate q_5 with other coordinates being unchanged. As before, distance D is measured in each point k, and condition (3) is verified. As soon as this condition is disturbed, point B coincides with the target point B_*, in which MD longitudinal axis is combined with normal N to plane P. At the end of the algorithm operation angular coordinates are entered into the memory of the robot control system. The process of MD automatic orientation relative to plane P is over.

Experimental verification of the algorithm. Several experiments were performed to verify the operation of the synthesized algorithm, using a six-link manipulation robot RM01 (PUMA-560). Kinematic diagram of RM01 differs from the schematic shown in Figure 1 just by an additional (sixth) link, which provides MD rotation around a longitudinal axis of this link.

Potentiometer type range-finding sensor is used as MD. As the sensor is designed so that its longitudinal axis coincides with the longitudinal axis of RM01 sixth link, variation of angular coordinate q_6 does not have any influence on MD position or orientation. Tested flat surface of 500 × 500 mm size was placed in RM01 working space at an angle of 36° to plane xy of the robot coordinate system. In the teaching mode MD was installed approximately in the center of the tested surface and it was oriented approximately relative to the normal to this surface.

Such simple preparatory operations were followed by starting a program, implementing the algorithm of MD automatic orientation. Program retrofitting took about 35 s. As a result MD was automatically positioned normal to the tested surface.

To make a final conclusion on the effectiveness of the proposed algorithm, experimental verification of the accuracy of MD orientation was conducted, which consisted of the following. Three points spaced at $\Delta l =$ $= 200$ mm were selected in virtual plane W, which now is parallel to coordinate plane τb of the so-called tool coordinate system $F\tau bn$. In these points (of a preset orientation) MD was used to measure distances D_1, D_2, and D_3. Since axis n is aimed along MD longitudinal axis, $D_1 = D_2 = D_3$ condition should be satisfied in the case of accurate orientation relative to the tested surface. It is exactly the degree of violation of this condition that will characterize the error in MD orientation relative to the tested surface.

The following averaged data were obtained as a result of measurements: $D_1 = 52.3$ mm, $D_2 = 52.9$ mm, $D_3 = 52.7$ mm. Substituting these values into formulas

$$\psi_\tau = \text{arc tg}\,\frac{D_2 - D_1}{\Delta l},\quad \psi_b = \text{arc tg}\,\frac{D_3 - D_1}{\Delta l},$$

we obtain $\psi_\tau = 10.3'$, $\psi_b = 6.8'$.

As was to be anticipated, deviations of MD axial line from the normal to the tested surface, characterized here by angles ψ_τ and ψ_b, are negligible. It should be noted that these angles usually are by an order of magnitude greater at MD orientation in the manual mode.

Thus, experimental verification showed a sufficiently high effectiveness of the proposed algorithm of MD automatic orientation relative to the tested surface, randomly arranged in the robot working space: first of all, orientation accuracy was significantly increased; secondly, the orientation procedure proper was markedly simplified; thirdly, the time consumed in orientation, was markedly decreased.

1. Tsybulkin, G.A. (1999) Search algorithm of maximum deformations of sheet structures using the manipulation robot. *Avtomatich. Svarka*, **6**, 55–57.
2. Paton, B.E., Lobanov, L.M., Tsybulkin, G.A. et al. (2003) Automated thermal straightening of welded thin-sheet structures. *The Paton Welding J.*, **7**, 2–6.
3. Torp, J. (1982) *Initial chapters of differential geometry*. Moscow: Mir.
4. Coife, F. (1985) *Interaction of robot with environment*. Moscow: Mir.
5. Chernousko, F.A., Bolotnik, N.N., Gradetsky, R.G. (1989) *Manipulation robots: dynamics, control, optimization*. Moscow: Nauka.
6. Wukobratovich, M., Stokich, D., Kirchansky, N. (1989) *Nonadaptive and adaptive control of manipulation robots*. Moscow: Mir.
7. Horn, B.K.P. (1989) *Vision of robots*. Moscow: Mir.
8. Kozlov, Yu.M. (1990) *Adaptation and training in robotics*. Moscow: Nauka.
9. Tsybulkin, G.A. (1995) Two-level coordinating control of manipulation robot with kinematic redundancy. *Problemy Upravl. i Informatiki*, **3**, 143–150.

NEW MACHINE FOR STUDDING OF HEATING SURFACES

G.V. ZHUK[1], **V.M. LUKIANETS**[2] and **S.V. MAZUR**[3]
[1]Closed Joint Stock Company «Ukrspetsterm», Kiev, Ukraine
[2]Company «Atol», Kiev, Ukraine
[3]Tripolskaya Heat Power Station, Ukrainka, Ukraine

New machine for realisation of the process of welding of studs to steam boiler water walls is described. Technical characteristics of the machine are given, and the efficiency of its application in manufacture and repair of boilers at heat power stations is shown.

Keywords: arc welding, carbon and low-alloy steels, machine, welding technology, productivity, quality of joints

Repair of heat power stations involves a substantial amount of work associated with manufacture of studded walls of steam boiler furnaces. The high quality of work is one of the requirements for their reliable and safe operation.

The most efficient technology for manufacture and repair of studded water walls is arc welding.

In operation of steam boilers, a heat flow is transferred to the water wall tubes through a liner and, primarily, through studs. The ratio of temperature levels in the liner and studs depends upon the temperature of plume, weight and viscosity of liquid slag, quality of deposition and material of the liner, material, size and quantity of the welded studs, their arrangement, and quality of the stud to tube welded joints.

As the studs welded to the water wall tubes serve also for fixation and cooling of the liner, they determine to a high degree its strength and operational reliability of a studded water wall as a whole. Decrease in distance between the studs and increase in their diameter should provide better retention of ramming masses and their more efficient cooling. Arrangement of the studs on water walls is specified by OST 108.130.01--79. The studs are made from steels of grades 10 and 20 according to GOST 1050--74, steel 12Kh1MF according to GOST 20072--74, and SiCrAl steels according to GOST 5632--61.

Long-time and reliable operation of a studded water wall is ensured, first of all, by implementation of the approved flow diagram of studding and quality of welded joints between the studs and tubes. Minimal length of a stud is determined by conditions of its clamping in the studding gun collet.

The method for arc welding of the water wall studs should provide welded joints with a quality that meets the following requirements: sufficient strength of welded joints to ensure their integrity in technological operations associated with manufacture of a studded water wall, and in long-time exposure to service temperatures and corrosive environment under the steam generator furnace chamber conditions, reliable thermal contact between the stud and tube wall to ensure a required (designed) heat flow through it, and absence of considerable changes in structure of the tube metal within the fusion and heat-affected zones, which can cause deterioration of its performance.

According to the «Instructions for Manufacture and Repair of Studded Water Wall Tubes of Boilers under Electric Station Conditions», strength of the welded joints in studs is considered sufficient unless the studs break off under slight tapping with a hammer 250 g in weight on the side of lack of penetration or, at its absence, on the side of the smallest bead. The studs should not break off in bending to 30° either. The quantitative assessment of mechanical strength of the welded joints should be made by testing the studded tube specimens to static shear with bending.

Equipment of foreign companies NELSON, BTH and KOCO is sold now in the market of welding equipment. According to its specifications, this equipment meets requirements for studding. However, its wide application is limited by high prices and increased requirements to service conditions.

Closed Joint Stock Company «Ukrspetsterm» in collaboration with the Design Bureau of the E.O. Paton Electric Welding Institute developed and manufactured the U-1152 machine for welding of studs with a diameter ranging from 4 to 14 mm. The machine consists of a power supply with control box (Figure) and a welding gun (1 or 2 guns). The machine provides welding of studs by the gas shielded or submerged-arc method, using protective ceramic rings, or without

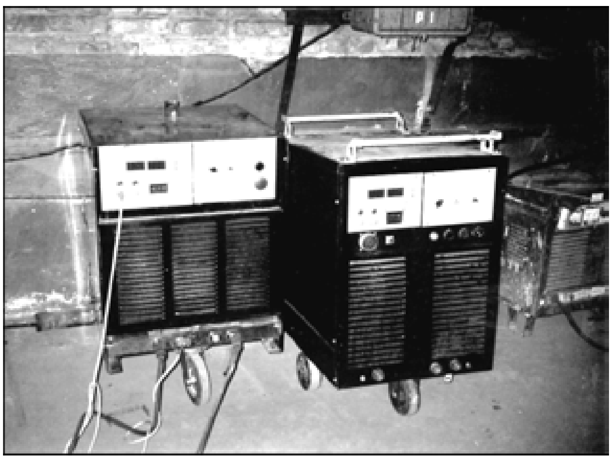

Specifications of the U-1152 machine

Parameter	Standard	
	Characteristic	
	Constant	Drooping
Rated welding current, A	1000	
Power consumption, kV·A	40	
Rated duty cycle, %	10	
Welding current regulation range, A	250–1300	
Rated working voltage at rectifier clips at rated current, V	26	26
Arc time regulation range, ms	5–999	
Efficiency, %, not less than	84.5	83.5
Open circuit voltage, V, not more than	85	
Dimensions, mm, not more than:		
length	1000	
width	800	
height	1000	
Weight, kg, not more than	300	

shielding, and can be applied for repair or manufacture of studded water walls under shop or field conditions.

For example, three panels of the lower radiation part (LRP) with 150,000 studs welded to them were installed in overhaul of power unit 4 at the Tripolskaya Heat Power Station.

Application of the suggested technology allowed avoidance of the problems associated with burns-through of the tubes, reduction in buckling of the tubes after studding, and decrease in consumption of shielding gases and auxiliary components (collets, nozzles).

The experience of operation with the U-1152 machine at the Tripolskaya Heat Power Station showed that welding of studs could be performed by low-skilled operators, e.g. graduates of vocational schools, with no complaints for the quality of welding of the studs. Later on, in overhaul of boiler TPP-210-A by replacing LRP of both casings, it was necessary to weld 1500,000 studs. According to time regulations, it is required to weld 1500 studs per shift, i.e. it takes 1000 shifts to stud a boiler.

The average speed of studding with the U-1152 machine is 6 studs per minute using one gun. In this case, 2200–2500 studs can be welded per shift, and studding of the boiler will take 600 shifts. Given the absence of burns-through, the probability of repeated pressurisation of the boiler after repair is eliminated. Arc blow can be avoided in each particular case without any problems. Certain difficulties arise in loading the collet with studs, as both collet and nozzle of the gun are heated after welding of 200–250 studs. The welding gun allows achievement of different speeds of upsetting of a stud to the weld pool to provide the required welding quality. The tip angle of a stud is 90° for tubes more than 5 mm thick, 120° — for tubes 4.5–5.0 mm thick, and 160° — for tubes less than 4.5 mm thick. The shape and size of the tip angle of a stud are affected also by the stud material or, to be more exact, by its thermal-physical properties. The welding current and arcing time should be selected depending upon the kind of the current, method used for shielding the welding zone, stud diameter, steel grade, and spatial position of the tube (Table).

INFLUENCE OF RAMSAUER EFFECT ON THE PARAMETERS OF CATHODE REGION OF ARGON ARC WITH NONCONSUMABLE ELECTRODE

O.M. CHERNY
OJSC «Rostvertol», Rostov-on-Don, RF

It is shown that the length of electron free path and number of collisions of electrons with atoms in the cathode region of the arc are determined by the Ramsauer effect.

Keywords: arc welding, welding arc, cathode region, Ramsauer effect, electron free path

Processes running in the cathode region depending on polarity have an essential role at heating of the electrode or the product. Numerous studies are devoted to investigation of these processes. However, many questions are still unstudied, for instance, length λ of the electron free path in the cathode region and number N of electron collisions with the atoms at their passage of the cathode region. In this work at attempt has been made to study these problems.

Let us consider an arc running between two tungsten electrodes in argon, in which according to [1] the total drop of cathode U_c and anode U_a voltages is equal to approximately 9 V. According to [1], $U_a \cong$ $\cong$ 4 V and does not depend on electrode material. Therefore, it may be assumed that in the considered case $U_c \cong 5$ V.

Change of section S of collision of electrons with argon atoms depending on energy W of the electrons (Ramsauer effect) is studied in [2, 3] and is expressed by the following formula:

$$S = 24.9W^2 - 14.9W + 2.4. \quad (1)$$

In the first approximation let us assume that the drop of electric potential in the cathode region is described by a linear function, depending on length l_c of the cathode region. Then the energy acquired by the electron when covering the path between the two collisions, will be equal to

$$W = \lambda U_c / l_c. \quad (2)$$

Value λ according to [4] is calculated by the following formula $\lambda = 1 / \pi\sqrt{2}\, d^2 n$, where d is the atom diameter, m; n is the atom concentration in a unit of volume, 1 / m^3. As $S = \pi d^2 / 4$, then

$$S = 1/4\sqrt{2}\lambda n. \quad (3)$$

Substituting expressions (2) and (3) into (1) and assuming that $l_c = \lambda N$, we obtain

$$\lambda = 1 / A[622 / N^2 - 74.7 / N + 2.4], \quad (4)$$

where A is the coefficient of proportionality.

Furtheron we will proceed from the principle of a minimum of the system energy, in keeping with which any system consisting of many bodies, is striving to a minimum of energy concentration in it, which in our case at the set U_c is achievable, if l_c has a maximum value. At limited number N of electron collisions with argon atoms in the cathode region, this is possible at the maximum value of λ, which proceeding from (4) is achieved at $N = 16.5$. According to dependence of S on W given in [2, 3], minimum section of electron collisions with argon atoms (Ramsauer section) is equal to $S_R = 1.6 \cdot 10^{-20}$ m^2. Then the maximum value of λ corresponding to S_R according to (3) is found from the expression

$$\lambda_R = 1/4\sqrt{2}\, S_R n. \quad (5)$$

Let us determine value n by the formula $n = P / kT$ [4], where P is the specific pressure of gas, N / m^2; $k = 1.38 \cdot 10^{-23}$ J / deg is the Boltzmann constant; T is the temperature. Assuming $P = 1 \cdot 10^5$ N / m^2 and $T = 1 \cdot 10^4$ K, we obtain $n = 7.2 \cdot 10^{23}$ 1 / m^3. Substituting S_R and n into (5), we obtain that $\lambda_R = 1.5 \cdot 10^{-5}$ m.

It should be noted that presence of a maximum in equation (4) obtained from (1), describing the Ramsauer effect, is indicative of stable values l_c and λ in the cathode region, as any deviation from $l_c = 16.5\lambda$ leads to a lowering of values λ and l_c, respectively, and, therefore, in keeping with the above-said, also to increased energy concentration in the cathode region, which is impossible. This leads to the conclusion that not only λ but also l_c values are determined by the Ramsauer effect.

Thus, the free path length of the electrons and number of electron collisions with atoms in the cathode region of the welding arc are determined by Ramsauer effect and are equal to $\lambda_R = 1.5 \cdot 10^{-5}$ m and $N =$ $= 16$–17, respectively.

1. Leskov, G.I. (1970) *Electric welding arc*. Moscow: Mashinostroenie.
2. Golden, D.E., Bandel, H.W. (1966) Low-energy e-Ar total sputtering cross section. *Phys. Rev.*, 149(**58**), 10–12.
3. Drukarev, G.F. (1978) *Collisions of electrons with atoms and molecules*. Moscow: Nauka.
4. Telesnin, R.V. (1973) *Molecular physics*. Moscow: Vysshaya Shkola.

NEWS

Simferopol Electric Machine-Building Plant SELMA Mastered Production of Low Voltage Universal Welding Converters KSU-320

KSU-320 is used for manual arc welding with covered electrodes and semi-automatic electrode wire welding (when being completed with the feeding mechanism) with power supply from multi-station power sources of VDM type without using ballast rheostats (RB), including use outside closed premises, where use of welding sources powered from industrial networks, is complicated.

The converter ensures:

• smooth regulation of welding circuit induction resistance;

• possibility of preliminary setting welding current in MMA welding mode;

• low voltage with rigid external characteristics for semi-automatic welding and falling external characteristics for manual arc welding;

• exclusion of mutual influence of welding stations when working from one welding source;

• increasing number of stations for welding from one multi-station source due to high efficiency and reduction of power consumption;

• stabilization of established welding mode within power supply voltage range from 45 to 90 V;

• «hot start» in MMA welding mode;

• possibility of using available electric welding equipment stock irrespective of year of production, functional complexity, and a manufacturer;

• possibility of placing welding station at a distance up to 200 m from welding sources and performing welding works at significant height;

• increase of deposition coefficient by 5--8 % and reduction of costs connected with removal of metal spatters in the welded joint zone;

• possibility of ensuring multi-station semi-automatic welding or simultaneous operation of stations in MMA and MIG / MAG welding modes from one source;

• power supply (due to the built-in generator) of own control circuits and the welding wire feeding mechanism;

• automatic cut-off in case of breaks in welding for more than 4 min (output voltage is cut off and a repeated switching takes place when an electrode is closed on a welded item);

• high degree of protection against negative effect of environment (mechanical damages, humidity, etc.);

• small mass and overall dimensions;

• establishment of digital indication instruments of welding current and voltage is possible on additional order.

Application of KSU-320 ensures the following advantages in comparison with the inverter equipment:

• KSU-320 is powered by the welding source open-circuit voltage, due to which voltage that is supplied to KSU-320 is electrically safe, thus making it possible to protect a welder against high voltage when working at height and on a metal surface;

• by using multi-station source with minimum open-circuit voltage 60 V it is possible to connect at any necessary for welding place within power bussing at a distance up to 200 m from the source;

• several welders may work simultaneously from one source on the current up to 300 A, whereby mutual influence of the stations is excluded;

• in case of connection to a multi-station source it is possible to establish a multi-station system for manual arc welding with covered electrodes, and multi-station system for semi-automatic welding (in case of connecting feeding mechanism to KSU-320), whereby simultaneous use of manual and semi-automatic welding stations is allowed;

• mass of KSU-320 is only 8 kg, which makes its transportation easy under mounting conditions.

Technical characteristics of KSU-320 converter

Power supply voltage, U_{in}, V	45–90
Output voltage, V	0–90
Rated welding current, A (duty cycle, %)	250 (100)
	320 (60)
Limits of regulated welding current, A	MMA 30–320
	MIG / MAG 40–320
Consumed power, kW·A	11
Mass, kg	8
Overall dimensions, mm	190 × 570 × 260

Calculation of economic efficiency of using KSU-320 in composition of welding rectifiers of VDM type

Let us assume welding parameters of a welding station as follows: I_2 = 200 A, U_2 = 28 V.

Now we'll calculate consumption of electric power for two cases:

• using RB, and

• using KSU-320.

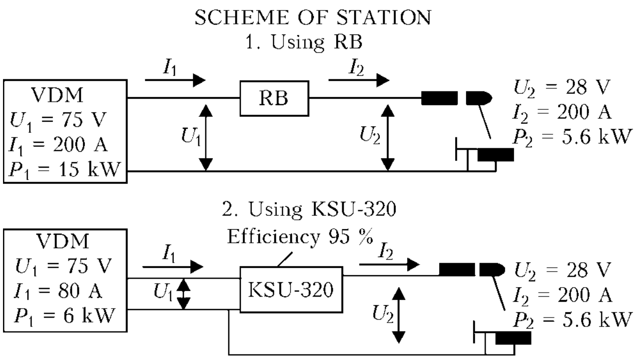

Difference in consumption of electric power between $P_{1\ RB}$ and $P_{1\ KSU}$ is 9 kW·h (for one station).

Initial data for calculation: working shifts — 2; cost of KSU-320 — 1358 USD (7200 UAH); cost of RB-302 — 126 USD (669 UAH); approximate price of electrodes is 5 UAH; total volume of deposited metal per year is 1500 kg; annual planned time of the equipment operation — 4000 h, 2500 of them under load; number of working days per year — 250; duration of a working shift — 8 h, within 5 h of which welding operations are performed; optimum welding current at the station is 180–200 A.

It was established in the course of comparative tests that in case of using KSU-320 deposition coefficient increases by 5–8 %. Spattering is insignificant or absent, formation of the weld is of fine-ripple character, whereby it was established that consumption of electrodes necessary for deposition of 1 kg of metal reduces by 3 %. If we transform it into the cost we'll get 0.05·5 UAH = 0.25 UAH. The annual volume of deposited metal being 3000 kg, the saving will make up 750 UAH or 150 kg of electrodes at one station.

High quality of the works performed with this equipment significantly reduces duration of auxiliary time necessary for fettling welds from slag and metal spatters in the welding zone.

At present there is a great number of welding sources of VDM type at the enterprises. Application of KSU-320 makes it possible to improve quality of welded joints while significantly reducing stock of used welding equipment, and, as a result, time for its servicing. Transition to the new scheme of operation will allow significant reducing electric power consumption.

It should be taken into account that RB require within a year for repair and replacement of spirals (80 % of used RB require after one year of operation for overhaul, and 30 % of them for replacement for new ones).

Main advantages of the scheme VDM-1202S + KSU-320 are as follows:

• reduction of power consumption by a station by 6800 UAH per year;

• increase of simultaneously operating stations from one source: in our case KSU-320 — 12 stations (200 A), RB-302 — 6 stations (200 A);

• increase of deposition coefficient by 5–8 % and reduction of consumption of welding electrodes up to 150 kg / year at one station;

• installation of a welding station, if necessary, at a distance of up to 200 m from the source;

• performance of welding operations by electrodes with both basic and cellulose cover;

CALCULATION DATA

Indices	1st option	2 option	Difference
	KSU-320 (7200 UAH)	RB-302 (669 UAH)	
1st year			
Cost of welding equipment necessary for organization of one station	$ 1358	$ 126 × 2 = $ 252, because in case of two-shift work within one year 1 RB will fail	–$ 1106
Electric power consumption per year by one station (two shifts)	4500 UAH ($ 840)	11,250 UAH ($ 2125)	6750 UAH (+$ 1285)
Total	$ 2198	$ 2377	+$ 179
Efficiency of introducing KSU-320 in the first year of operation:			
reduction of power consumption			6750 UAH
saving on welding consumables			750 UAH
Total			7500 UAH
2nd year			
Electric power consumption per year by one station	4500 UAH ($ 840)	11,250 UAH ($ 2100)	6420 UAH (+$ 1200)
Efficiency of introducing KSU-320 within the period of operation			7500 UAH

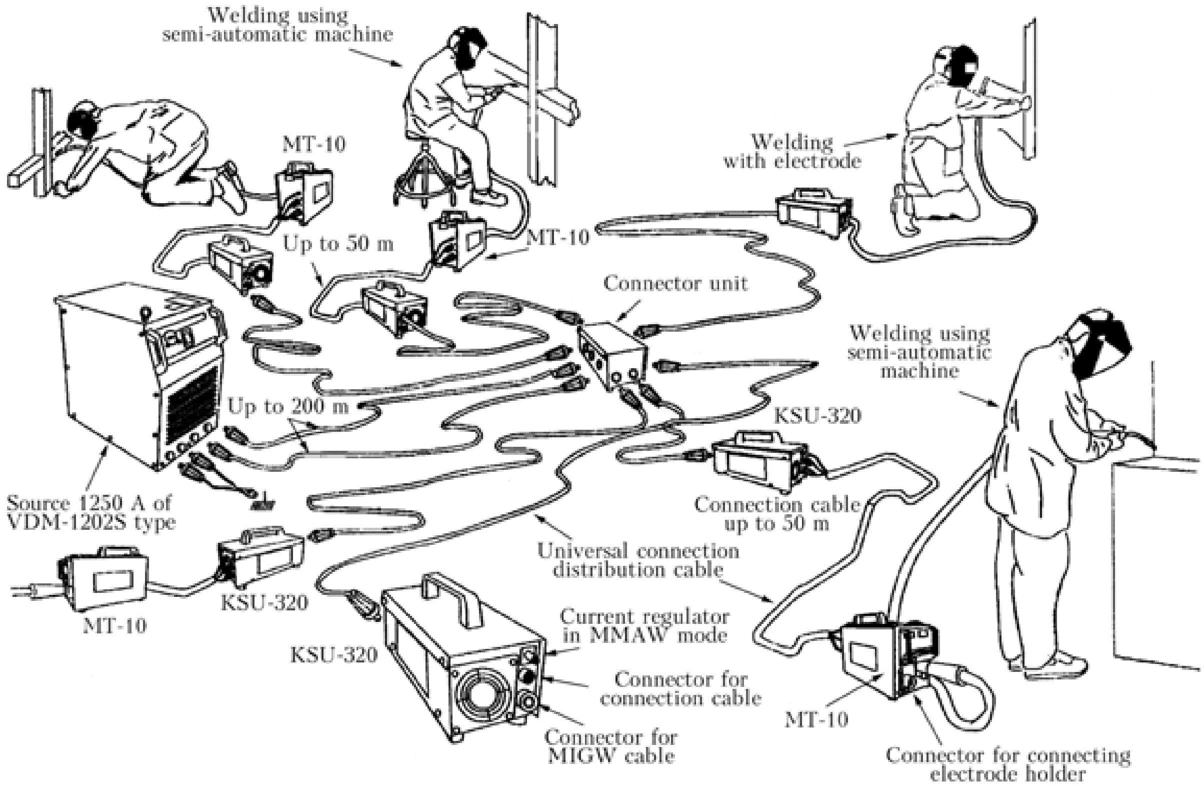

Scheme of KSU-320 and feeding mechanism MT-10 connection to the multi-station source for ensuring multi-station welding by covered electrodes and / or shielded gas semi-automatic welding

• assignment of a technologically necessary welding current value and its fixing on an item by means of multi-turn resistors Multi-Lock;

• smooth regulation of inductivity;

• mass of KSU-320 is 2.5 times less than mass of RB-302;

• section of welding cables between VDM--KSU is reduced two-fold, which allows saving up to 10 UAH per running meter of a welding cable;

• organization of multi-station semi-automatic welding system by series connection to the circuit of welding semi-automatic machine of MT-10 and PDG-422 type.

THESIS FOR SCIENTIFIC DEGREE

E.O. Paton Electric Welding Institute of the NAS of Ukraine

I.I. Ryabtsev (PWI) defended on 15th of February 2006 candidate's thesis on topic «Development of Phosphorus-Containing Materials for Electric Arc Surfacing of Layers with Advanced Tribotechnical Characteristics».

The work is devoted to study of regularities of forming in iron-base alloys structures, strengthened by phosphides, and creating on this basis new class of surfacing materials having advanced tribotechnical properties. New surfacing materials are designed for renovating and strengthening parts, which operate under conditions of metal on metal friction without lubrication.

Calculations of isobaric potentials of phosphide-forming reactions of the main alloying elements were carried out using entropic method. It is established that the most probable is formation, first of all, of molybdenum, chromium and manganese phosphides. Exactly these phosphides have the highest melting point. On the basis of thermodynamic calculations and experience of creating materials for surfacing of friction pair components deposited metal 20KhGSP was selected.

On the friction machine tribotechnical characteristics of deposited metal 20KhGSP with different contents of phosphorus were studied according to the test scheme «shaft–plane». It is established that when phosphorus content increases by up to 1 %, friction coefficient of deposited metal 20KhGSP reduces approximately 1.5 times. When phosphorus content is 1.0–1.6 %, wear of a deposited specimen reduces 4–4.5 times, and of a 45 steel counter-body — 1.5 times.

It is established that in open arc surfacing using flux-cored wire PP-Np-20KhGSP or using flux AN-348A practically the whole phosphorus is assimilated by a deposited metal. It allows performing with the same success surfacing with flux-cored wire PP-Np-20KhGSP using self-shielding option or flux.

Phosphorus, depending upon its content, partially dissolves in the matrix and partially forms phosphides and phosphide eutectics in deposited metal 20KhGSP. Alloying by chromium and manganese increases solubility of phosphorus in a deposited metal up to 1.45 % and more, while its solubility in pure iron is 1.2 %.

It was established in surfacing of a rigid technological sample that hot cracks in a deposited metal 20KhGSP don't form when phosphorus content makes up 0.3–3.5 %. At phosphorus content up to 1.2 % deposited metal has a narrow range of solidification, which positively affects its resistance against formation of hot cracks. At its higher content in a deposited metal big amount of low-melting phosphide eutectics form, which «cure» nuclei of hot cracks.

Cold cracks in deposited metal of studied type form at phosphorus content above 1.6 %. Loci of origination and distribution of cold cracks are brittle phosphide eutectics precipitated on grain boundaries. Taking into account difficulties of controlling processes of forming phosphide eutectics, phosphorus content in the deposited metal 20KhGSP is limited from the viewpoint of crack resistance by 1.3 %.

Separability of the slag crust at increased temperatures in multilayer surfacing with heating by flux-cored wire PP-Np-20KhGSP is studied. It is established that introduction of 4.0–7.5 % ZrO_2 into charge of flux-cored wire PP-Np-20KhGSP increases oxidation capacity of the slag, difference in thermal expansion coefficients between the slag crust and a deposited metal within temperature range 200–600 °C, and temperature of the slag solidification, due to which separability of the slag crust at increased temperatures in surfacing using this wire and flux AN-348A is improved.

Two compositions of flux-cored wire PP-Np-20KhGSP were developed on the basis of the results of carried out investigations: for open arc surfacing and surfacing using flux AN-348A. Flux-cored wire PP-Np-20KhGSP is included into TUU 28.7.05416923.066–2002: Flux-Cored Surfacing Wires, developed in the PWI Department.

Experimental-commercial test of developed flux-cored wire PP-Np-20KhGSP in surfacing of crane wheels showed that their wear resistance increased 1.5–2 times in comparison with serial wheels of steel 65G. Economic effect from using flux-cored wire PP-Np-20KhGSP for surfacing wheels of one bridge crane is 3150 UAH / year.

PATENTS IN THE FIELD OF WELDING PRODUCTION*

Plasmatron characterized by the fact that on rear part of the electrode a cone surface with an angle smaller and equal to the angle of friction is located, over which the electrode is hermetically connected with a metal sleeve, which envelops it, whereby the end surface of the said sleeve rests via dielectric bushing upon resilient dielectric bushing. Other peculiar features are also described. Patent 73138. V.V. Protsiv [6].

Installation for butt resistance welding of tubular envelope with a plug characterized by the fact that the welding chamber contains a sleeve-like housing with a central hole in the bottom attached to the guide housing of the main clamp coaxially to its channel; the collet of an auxiliary clamp is located in the middle of the sleeve-like housing, and its drive contains a stop element, which may travel along the housing axis on the side of its open end and contact with the additional clamp collet. Other peculiar features are also described. Patent 47847. N.N. Belash, N.A. Lavrentiev, V.S. Krasnorutsky (NSC «Kharkov Physical-Technical Institute») [6].

Device for magnetic-pulse treatment of metals characterized by the fact that the first thyristor is connected by anode to the pole of the first battery of capacitors, and by cathode to one of the inductor lead-outs, the other lead-out of which is connected with minus of the last battery of capacitors, the rest thyristors being connected by anode with plus and by cathode with minus between respective batteries of capacitors. Patent 73184. A.S. Pismenny, I.V. Pentegov, E.P. Stemkovsky et al. (PWI) [6].

Composition of electrode coating characterized by the fact that into composition of the coating slag of ferrochromium production is additionally introduced as a hardener with the following ratio of components, wt.%: 50--53 marble; 12--15 fluorite; 7–9 quartz sand; 3–5 ferromanganese; 3--5 ferrosilicon; 8--12 ferrotitanium; 1–1.5 slag of ferrochromium production. Patent 7550. S.V. Bondarev, V.D. Kassov (Donbass State Machine-Building Academy) [6].

Tilter of heavy-weight metal structures characterized by the fact that the tilter frame is made in the form of a closed contour with a free opening, contours of which correspond to contours of the item perimeter in its stable position, an item being able to freely move through the contour opening and the clamps being symmetrically installed relative the frame contour planes and being able to function as clamps proper and support assemblies. Patent 7259. A.I. Zhelem, V.P. Ermakov [6].

Method of diffusion-reactive bonding of metals and alloys, in which assembled parts are heated up to the temperature that exceeds temperature of eutectics formation between the base metal and the depressant-metal, characterized by the fact that parts are connected with a fixed, close to zero, connection clearance, and the depressant-metal is placed immediately near this clearance. Patent 73308. V.S. Nesmikh, K.A. Yushchenko, T.N. Kushnaryova (Int. Ass. «Interm») [6].

Torch for gas-shielded electric arc surfacing characterized by the fact that greater part of the current-carrying tip is located in a water-cooled annular cavity, its axial channel being filled over its length with centering bushings from a refractory composite material, which form axial hole for movement of a wire electrode. Other peculiar features are also described. Patent 7718. N.B. Klejno, A.V. Andyuk, D.E. Zherebchevsky («Kant» Ltd.) [7].

Flux-cored wire for underwater welding of low-carbon and low-alloy steels characterized by the fact that the core additionally contains ferrotitanium and ferroboron with the following ratio of components, wt.%: 25--35 rutile concentrate; 15--25 hematite; 5--15 ferromanganese; 3--7 nickel; 5--15 ferrotitanium; 0.2--1.1 ferroboron; 0.7--1.3 potassium bichromate; the rest is iron powder. Patent 7914. S.Yu. Maksimov, V.S. But, A.A. Radzievskaya et al. (Ukrtransgaz Company, PWI) [7].

Composition of coating for protecting surface against sticking of molten metal spatters characterized by the fact that it contains lignin and manganese slime with the following ratio of components, wt.%: 8--10 chalk; 12--15 lignin; 17--21 manganese slime; the rest is water. Patent 8107. V.V. Chigarev, S.V. Malygina (Donbass State Machine-Building Academy) [7].

Method of manufacturing electrode for arc welding characterized by the fact that ferroalloys are remolten and refined together with titanium waste by electroslag method and introduced into composition of the coating in the form of a complex ferroalloy powder. Patent 7650. V.S. Popov, I.M. Belonik, S.P. Berezhnoj (Zaporozhie NTU) [7].

Method of rolled sheet cold cladding characterized by the fact that cold cladding is performed using metal powder, which is located in the process of rolling between the roll and a rolled sheet component with lower coefficient of friction. Patent 68900. E.V. Bajkov, A.G. Manshilin («Doniks» Ltd. with foreign investments) [8].

Method of connecting liners with housing of micro-assemblies (microcircuits) characterized by the fact that compensator-lead-outs are introduced into the structure, which are located between the housing and a suspension. Patent 8837. V.P. Rajzman, V.V. Strelbitsky [8].

Electrode for resistance spot welding characterized by the fact that at the end of the electrode a thread is made and it is equipped with an external ring made of insulation and heat-resistant material. Patent 8832. A.G. Kuzmenko,

*The information about patents published in bulletins of Ukraine «Industrial ownership» for 2006 is presented (in square brackets the bulletin No. is indicated).

V.V. Gorvat, V.V. Gorvat (Khmelnitsky National University) [8].

Double-layer welding package for manufacturing bimetal sheets characterized by the fact that slots and deformation compensators are made in the main slab material on two mutually perpendicular sides, whereby slot in cross-section is made in the form of a triangle, and deformation compensator has in the base smaller cross-section than in the upper part. Patent 8874. A.V. Popov, B.A. Popov, O.N. Litvinov et al. («Latimeriya» Company, Leasing Company «Active» Ltd.) [8].

Method of producing clad steel characterized by the fact that as an intermediate layer double-layer sheet of at least 2–3 mm thickness from structural steel and from ferronickel alloy 00H18MTYu is used, whereby thickness of the latter is assumed equal to 0.1–0.2 mm. Patent 8885. A.V. Popov, B.A. Popov, O.N. Litvinov et al. (ditto) [8].

Forming device for electroslag cladding and melting characterized by the fact that it additionally contains at least one sensor of the molten metal pool level with a dipstick in its center mounted into the slider and located at a distance from its edge not less than the value of clearance between the dipstick and the slider, whereby center of the first sensor is located at the slide front edge level, for which purpose a boss is made on the slide. Patent 8871. A.V. Popov, B.A. Popov, O.N. Litvinov et al. (ditto) [8].

Device for manufacturing heterogeneous casts characterized by the fact that a frame for movement of a carriage with a billet is additionally equipped with two hinged supports symmetrically arranged relative vertical axis of travel of consumable electrodes. Other peculiar features are also described. Patent 8922. A.V. Popov, B.A. Popov, O.N. Litvinov et al. (ditto) [8].

Method of manufacturing high-alloy welding wire characterized by the fact that over perimeter of an ingot or a bloom from high-alloy steel technological layer of low-alloy steel is deposited, the thickness of a deposited layer being assumed equal 1–5 % of the ingot thickness. Patent 8928. A.V. Popov, B.A. Popov, O.N. Litvinov et al. (ditto) [8].

Method of manufacturing protection guard of railway car trucks includes manufacturing of two elements — a guard and a plate — from metals having heterogeneous chemical composition and different mechanical properties, and connection of the elements by means of spot electric welding performed in pulsed mode of current supply to the electrodes. Patent 8935. A.I. Rudometkin, N.I. Bataev (Plant «Artyompolisvarka» Ltd.) [8].

Machine for press welding of pipes with magneticaly impelled arc heating characterized by the fact that its upset hydraulic cylinders are made as double-acting cylinders with one side source. Patent 73809. S.I. Kuchuk-Yatsenko, V.G. Krivenko, V.S. Kachinsky et al. (PWI RC for Pressure Welding) [9].

Method of arc wide-layer surfacing characterized by the fact that time of arc movement from one edge of a strap to another is divided into the periods, which are composed of three assigned time intervals, during which the surface being surfaced is sequentially heated and molten by an electrode strap while the arc remains motionless, then the surfaced area is cooled and the arc is moved to the adjacent area. Patent 9158. R.N. Ryzhov, A.L. Zimovchenko (NTUU «KPI») [9].

Head for wide-layer surfacing using lateral magnetic fields characterized by the fact that its electric magnets, which can be supplied with power independently, are components of a multipole electromagnetic system and contain rod cylindrical cores. Other peculiar features are also described. Patent 91608. A.L. Zimovchenko, R.N. Ryzhov (ditto) [9].

EQUIPMENT AND TECHNOLOGY FOR MANUFACTURE OF FLUX-CORED WIRES

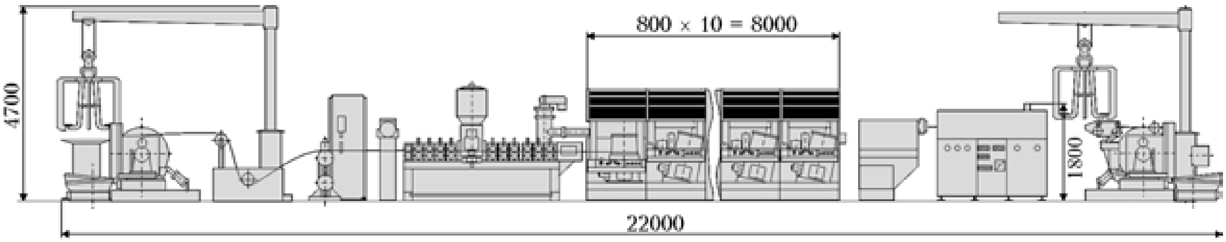

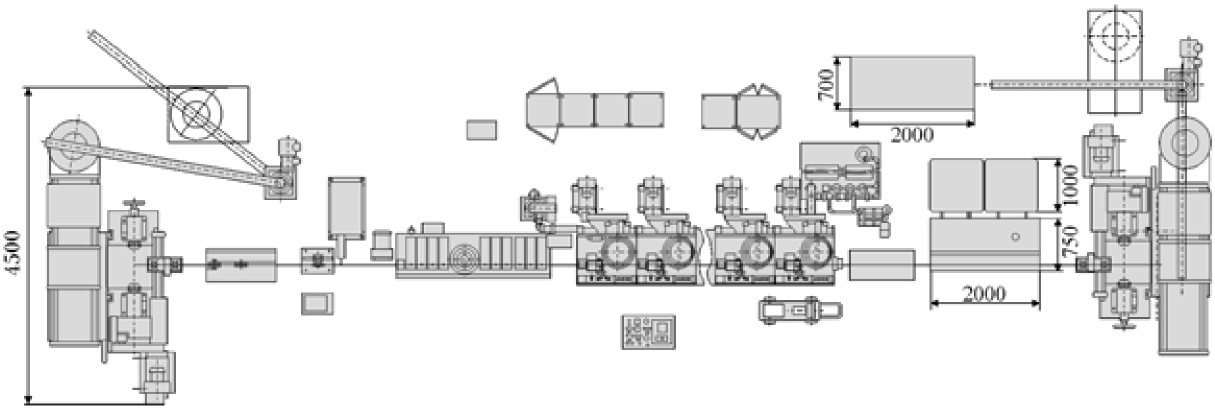

Mean productivity of line is up to 1000 t / year
Diameter of wires: from 1.2 up to 3.6 mm

Complex of machines, devices and instruments for all production stages of manufacture of wires from cold-rolled strip with powder fillers: shaping of wire strip, dosing of powder mixture, drawing and treatment of a ready wire.

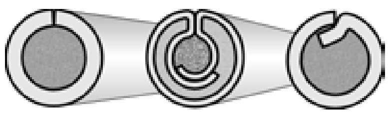

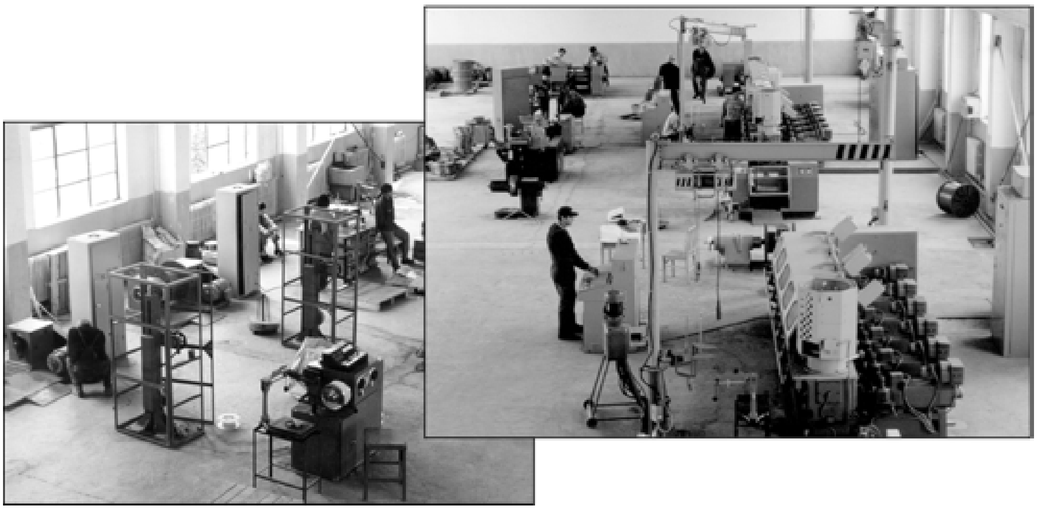

Advantages of production line: high productivity; versatility; automation of control; high quality of products.

Licenses: France, Germany, USA, Japan, Bulgaria, Hungary, Argentine, Czech Republic, Slovenia, China.

Prof. Pokhodnya I.K.
E-mail: pokhod@paton.kiev.ua